BAŞKENT UNIVERSITY
INSTITUTE OF SCIENCE
DEPARTMENT OF MOLECULAR BIOLOGY AND GENETICS
MASTER OF SCIENCE IN MOLECULAR BIOLOGY AND GENETICS

TRANSCRIPTOMIC RESPONSES TO SEVERE BORON TOXICITY IN ROOTS OF *ARABIDOPSIS THALIANA* AT SINGLE-CELL LEVEL

BY

BUĞRA CAN

MASTER OF SCIENCE THESIS

ANKARA - 2025

BAŞKENT UNIVERSITY
INSTITUTE OF SCIENCE
DEPARTMENT OF MOLECULAR BIOLOGY AND GENETICS
MASTER OF SCIENCE IN MOLECULAR BIOLOGY AND GENETICS

TRANSCRIPTOMIC RESPONSES TO SEVERE BORON TOXICITY IN ROOTS OF *ARABIDOPSIS THALIANA* AT SINGLE-CELL LEVEL

BY

BUĞRA CAN

MASTER OF SCIENCE THESIS

ADVISOR

ASSOC. PROF. DR. CEYHUN KAYIHAN

ANKARA - 2025

BAŞKENT UNIVERSITY
INSTITUTE OF SCIENCE

This study, which was prepared by Buğra Can, for the program of Master of Science with Thesis (English), has been approved in partial fulfillment of the requirements for the degree of Master of Science in Molecular Biology and Genetics Department by the following committee.

Date of Thesis Defense: 07/05/2024

Thesis Title: Transcriptomic Responses to Severe Boron Toxicity in Roots of *Arabidopsis Thaliana* at Single-Cell Level

Examining Committee Members	**Signature**
Prof. Dr. Füsun EYİDOĞAN, Başkent University	…..……
Assoc. Prof. Dr. Ceyhun KAYIHAN, Başkent University	…..……
Asst. Prof. Dr. Emre AKSOY, Middle East Technical University	…..……

APPROVAL

Prof. Dr. Dilek ÇÖKELİLER SERDAROĞLU
Director, Institute of Science
Date : … / … / ….……

BAŞKENT UNIVERSITY
INSTITUTE OF SCIENCE
YÜKSEK LİSANS TEZ ÇALIŞMASI ORİJİNALLİK RAPORU

Date: ../../….

Öğrencinin Adı, Soyadı: Buğra Can

Öğrencinin Numarası: 22120291

Anabilim Dalı: Moleküler Biyoloji ve Genetik Anabilim Dalı

Programı: Moleküler Biyoloji ve Genetik Tezli Yüksek Lisans (İngilizce)

Danışmanın Unvanı/Adı, Soyadı: Doç. Dr. Ceyhun KAYIHAN

Tez Başlığı: Transcriptomic Responses to Severe Boron Toxicity in Roots of *Arabidopsis Thaliana* at Single-Cell Level

Yukarıda başlığı belirtilen Yüksek Lisans tez çalışmamın; Giriş, Ana Bölümler ve Sonuç Bölümünden oluşan, toplam 57 sayfalık kısmına ilişkin, 17/06/2025 tarihinde şahsım/tez danışmanım tarafından Turnitin adlı intihal tespit programından aşağıda belirtilen filtrelemeler uygulanarak alınmış olan orijinallik raporuna göre, tezimin benzerlik oranı %11'dir. Uygulanan filtrelemeler:

1. Kaynakça hariç

2. Alıntılar hariç

3. Beş (5) kelimeden daha az örtüşme içeren metin kısımları hariç

"Başkent Üniversitesi Enstitüleri Tez Çalışması Orijinallik Raporu Alınması ve Kullanılması Usul ve Esaslarını" inceledim ve bu uygulama esaslarında belirtilen azami benzerlik oranlarına tez çalışmamın herhangi bir intihal içermediğini; aksinin tespit edileceği muhtemel durumda doğabilecek her türlü hukuki sorumluluğu kabul ettiğimi ve yukarıda vermiş olduğum bilgilerin doğru olduğunu beyan ederim.

Öğrenci İmzası: …….

ONAY

Öğrenci Danışmanı

Assoc. Prof. Dr. Ceyhun KAYIHAN

Tarih: 17 / 06 / 2025

……..

ACKNOWLEDGEMENTS

I would like to express my heartfelt gratitude to my thesis advisor, Assoc. Prof. Dr. Ceyhun KAYIHAN, for his continuous support, expert guidance, and invaluable contributions throughout every stage of my thesis. His dedication, patience and encouragement have played a crucial role in the successful completion of this work.

I would also like to thank my lab mates, especially Halis Batuhan ÜNAL and Oğuzhan YAPRAK, for their hard work, collaboration, and technical support. I am equally grateful to all my other lab colleagues for creating a motivating and friendly environment that contributed significantly to both my academic and personal growth during this process.

ABSTRACT

Buğra CAN

TRANSCRIPTOMIC RESPONSES TO SEVERE BORON TOXICITY IN ROOTS OF *ARABIDOPSIS THALIANA* AT SINGLE-CELL LEVEL

Başkent University Institute of Science

Molecular Biology and Genetics

2025

Boron (B) is an essential plant micronutrient vital plant cell. It is vital for cell wall formation and cell membrane integrity. Boron's concentration levels have a narrow range on the plant cells. Deficiency of boron cause negative impact such as plant growth arrest and disruption of developmental processes. It is essential for cell wall formation stability by forming boron-bridge structure and insufficient boron on the cell causes fragile tissue formation, resulting as death of plant. Excess Boron aligning with parallel reasons toxic due to impaired growth and significant yield losses on crops especially in arid regions with boron-rich soil. Cellular mechanisms to tolerate boron balance in the plant cell, especially for severe boron treatment, remain poorly understood.

In this study, severe boron treated (3mM and 5mM) *Arabidopsis thaliana* root cells have been investigated at single-cell level in order to reveal how plant tolerance mechanisms perform. Single-cell RNA sequencing (scRNA-seq) using 10x Genomics platform has been applied to Control (col-0) 3mM (3B) and 5mM (5B) treated groups of cells. Transcriptomes resulting from this methodology have been analyzed with Seurat R package to cluster and identify cells based on their transcriptome profiles using differential gene expression (DGE) analysis. Then, Gene Ontology (GO) and Kyoto Encyclopedia of Genes and Genomes (KEGG) pathway enrichment analysis have been applied to reveal cellular mechanisms that have been impacted.

This Approach identified 16 clusters in *Arabidopsis thaliana* root cells with annotation of major cell types of columella, cortex, endodermis, and the epidermal/root cap. Under the influence of severe boron toxicity, transcriptional responses have been highly cell type specific. Columella cells upregulated ATP-dependent detoxification pathways to pump out high level of boron from the cytoplasm, cortex cells undergo broad metabolic reprogramming to remodel cell-wall for sequestering or neutralizing boron and epidermis together with root cap, which are outer cell layers, demonstrated high expression levels of ribosome biogenesis genes to produce border-like cells shed as a boron loaded tissues and export.

The outermost cells layer consisting of epidermis and root cap demonstrated largest

transcriptomic shifts with 5mM B treatment, which provides this layer is the first defense line against toxic boron treatment. The distinct yet coordinated responses demonstrate that each root cell type utilizes specialized strategies to handle severe boron toxicity. Our single-cell approach helps us to understand new insights into the mechanisms of plant stress adaptation to severe levels of boron stress environment, bringing out the value of cell-type-resolved transcriptomics in explaining stress responses of *Arabidopsis thaliana* root cells against severe boron toxic environments.

KEYWORDS: Boron Toxicity, Single Cell RNA Sequencing, *Arabidopsis thaliana*

This thesis was supported by TUBİTAK (project number 121Z029).

ÖZET

Buğra CAN

***ARABİDOPSİS THALİANA* KÖKLERİNDE ŞİDDETLİ BOR TOKSİSİTESİNE KARŞI TEK HÜCRE DÜZEYİNDE TRANSKRİPTOMİK YANITLAR**

Başkent Üniversitesi Fen Bilimleri Enstitüsü

Moleküler Biyoloji ve Genetik Anabilim Dalı

2025

Bor (B), bitki hücreleri için hayati öneme sahip temel bir bitki mikro besin elementidir. Hücre duvarı oluşumu ve hücre zarı bütünlüğü için gereklidir. Borun bitki hücrelerindeki konsantrasyon seviyesi dar bir aralıkta tutulmalıdır. Bor eksikliği, bitki büyümesinin durması ve gelişim süreçlerinin bozulması gibi olumsuz etkilere yol açar. Hücre duvarının kararlılığı için bor-köprü yapısı oluşturarak gerekli olan bor, hücrede yetersiz kaldığında kırılgan doku oluşumuna ve sonunda bitkinin ölümüne neden olur. Aşırı bor ise, benzer şekilde, büyümenin bozulması ve özellikle bor bakımından zengin topraklara sahip kurak bölgelerde önemli ürün kayıpları nedeniyle toksiktir. Bitki hücresinde bor dengesini tolere etmeye yönelik hücresel mekanizmalar, özellikle yüksek düzeyde bor uygulamalarında, hâlâ tam olarak anlaşılmamıştır.

Bu çalışmada, yüksek düzeyde borka maruz bırakılmış (3 mM ve 5 mM) *Arabidopsis thaliana* kök hücreleri tek hücre düzeyinde incelenerek, bitkinin tolerans mekanizmalarının nasıl işlediği ortaya konulmuştur. Bu amaçla, Kontrol (col-0), 3 mM (3B) ve 5 mM (5B) ile muamele edilmiş hücre gruplarına 10x Genomics platformu kullanılarak tek hücreli RNA dizileme (scRNA-seq) uygulanmıştır. Bu yöntemle elde edilen transkriptomlar, hücreleri transkriptom profillerine göre kümelemek ve tanımlamak amacıyla Seurat R paketi ile analiz edilmiştir. Daha sonra, etkilenen hücresel mekanizmaları ortaya koymak için Gen Ontolojisi (GO) ve Kyoto Gen ve Genom Ansiklopedisi (KEGG) yol zenginleştirme analizleri yapılmıştır.

Bu yaklaşım, *Arabidopsis thaliana* kök hücrelerinde kolumella, korteks, endodermis ve epidermis/kök şapkası gibi ana hücre tiplerinin anotasyonu ile 16 küme tanımlamıştır. Şiddetli bor toksisitesinin etkisi altında, transkripsiyonel yanıtlar oldukça hücre tipi spesifik olmuştur. Kolumella hücreleri, sitoplazmadaki yüksek bor düzeyini dışarı atmak için ATP-bağımlı detoksifikasyon yollarını yukarı regüle etmiştir. Korteks hücreleri, boru tutmak veya etkisizleştirmek için hücre duvarını yeniden yapılandırmaya yönelik geniş çaplı metabolik yeniden programlamadan geçmiştir. Epidermis ve kök şapkası ise, dış hücre katmanları olarak, sınır benzeri hücrelerin üretimi ve bor yüklü doku olarak dökülmesi için ribozom biyogenezi genlerinde yüksek düzeyde ekspresyon göstermiştir.

Epidermis ve kök şapkasından oluşan en dış hücre katmanı, 5 mM bor uygulamasında en büyük transkriptomik değişimleri göstermiş ve bu katmanın toksik bor tedavisine karşı ilk savunma hattı olduğunu ortaya koymuştur. Bu belirgin fakat koordineli tepkiler, her bir kök hücre tipinin şiddetli bor toksisitesine karşı özelleşmiş stratejiler kullandığını göstermektedir. Tek hücreli yaklaşımımız, *Arabidopsis thaliana* kök hücrelerinin şiddetli bor toksisitesine karşı verdiği stres yanıtlarını hücre tipi bazında anlamamıza olanak sağlayarak, bitkilerin çevresel streslere adaptasyon mekanizmalarına dair yeni bakış açıları kazandırmaktadır.

ANAHTAR KELİMELER: Bor Toksisitesi, Tek Hücre RNA Dizileme, *Arabidopsis thaliana*

Bu proje, TUBİTAK tarafından (121Z029 no'lu proje) desteklenmiştir.

CONTENTS

Page

ACKNOWLEDGEMENTS i

ABSTRACT ii

ÖZET iv

CONTENTS vi

LIST OF TABLES viii

LIST OF FIGURES ix

LIST OF SYMBOLS AND ABBREVIATIONS xii

1. INTRODUCTION 1

2. LITERATURE 3

2.1. Boron as an Essential Element in Plants 3

2.2. Boron Deficiency vs. Toxicity. Mechanisms and Symptoms 5

2.2.1. Boron Deficiency 5

2.2.2. Boron Toxicity 6

2.3. Transcriptomic Responses to Boron Toxicity 8

2.4. *Arabidopsis thaliana* as a Model for Boron Stress Studies 10

2.5. Single-Cell RNA Sequencing (scRNA-seq) in Plant Research 12

2.6. Functional Enrichment Analysis (GO/KEGG) for Transcriptomic Data 15

2.7. Aim and Scope of the Thesis 17

3. MATERIALS AND METHODS 19

3.1. Plant Growth and Boron Toxicity Treatments 19

3.2. Protoplast Isolation and Cell Counting 20

3.3. Single-Cell Library Preparation and Sequencing 22

3.4. Data Analysis 26

4. RESULTS 29

4.1. Single-Cell Transcriptome Profiling and Clustering of Root Cells Under Boron Stress 29

4.2. Identification of Root Cell Types and Cluster Relationships 30

4.3. Cell Population Distribution Under Control and Boron Treatment Conditions . 35

4.4. Cell Type–Specific Transcriptomic Responses to Severe Boron Toxicity..... 38

4.5. GO and KEGG 39

5. DISCUSSION 58

6. CONCLUSION..... 64

REFERENCES 65

APPENDICES

APPENDIX 1: Gene Markers for Identification of Root Cells

APPENDIX 2: Marker Gene List and Respective Root Cell Region

LIST OF TABLES

Page

Table 3.1. Formula for Cell Viability calculation 22

Table 3.2. Mastermix protocol for GEM generation 22

Table 3.3. GEM beads RT incubation protocol 23

Table 3.4. Clean-up mixture protocol for Dynabeads for Reverse transcribed samples 23

Table 3.5. Protocol for Elution Solution I 24

Table 3.6. Protocol of cDNA Amplification Reaction Mixture 24

Table 3.7. cDNA Amplification PCR procedure protocol 25

Table 4.1. Number of significantly upregulated genes (DEGs) in each root cell type cluster 39

LIST OF FIGURES

Page

Figure 2.1. Borate Cross-Linking of Rhamnogalacturonan II (RG-II) in Plant Cell Walls..... 4

Figure 2.2. Effects of Excess Boron on Arabidopsis thaliana at the Cellular and Physiological Level..... 7

Figure 3.1. Workflow representation of experimental setup 19

Figure 3.2. Demonstration of Control (left), 3mM B treated (middle) and 5mM B treated (right) Arabidopsis thaliana plants 20

Figure 3.3. 10 Genomics single-cell-RNA-Sequencing library preparation. A. Template wells for loading for Partitioning oil, Gel Beads and mastermix + Sample. B. Cell enzyme participation and partitioning oil formation shown in GEMs for 10x Barcoded Gel Beads 22

Figure 4.1. PC_1 and PC_2 with graph of 15 clusters have been shown in the first part in the figure. The second part of the figure represents the plot of showing the standard deviation of principal components (PCs). The first ~15 PCs encompass the majority of variance, as indicated by the inflection point around PC15. 29

Figure 4.2. UMAP demonstration of all sequenced root cells colored by non-defined cluster (Louvain algorithm). Sixteen clusters (0–15) are labeled, showing distinct groupings of transcriptionally similar cells..... 30

Figure 4.3. Representation of expression of genes that is known as marker genes for the Arabidopsis thaliana root cells. Identified clusters shown as; A. Quiscent Center + Columella cluster, B. Atrichoblast cluster, C. Metaphloem cluster, D. Protoxylem cluster, E. Lateral Root Cap cluster, F. Cortex cluster, G. Phloem cluster, H. Endodermis cluster, I. Metaxylem cluster, J. Columella cluster, K. Trichoblast cluster, L. Stele cluster 32

Figure 4.4. UMAP projection with clusters colored by their annotated cell type identity. 35

Figure 4.5. UMAP projection of representation of all cell groups, not specified in cell types, colored by Control group, 3 mM Boron and 5 mM Boron Treatment conditions. ... 36

Figure 4.6. Column graph representation of cell count yield per cluster. Cell types that are identified shown with colors and cluster numbers shown in the x-axis of the graph as 15. Cell count represented as y-axis as yield. 37

Figure 4.7. Columella cells GO analysis schema for Biological Process under 5mM Boron toxicity 40

Figure 4.8. Columella cells GO analysis schema for Cellular compone"nt under 5mM Boron toxicity 40

Figure 4.9. Columella cells GO analysis schema for Molecular Function under 5mM Boron toxicity 41

Figure 4.10. Cortex cells GO analysis schema for Biological Process under 3mM Boron toxicity 42

Figure 4.11. Cortex cells GO analysis schema for Cellular Component under 3mM Boron toxicity 43

Figure 4.12. Cortex cells GO analysis schema for Molecular Function under 3mM Boron toxicity 44

Figure 4.13. Cortex cells GO analysis schema for Biological Process under 5mM Boron toxicity 44

Figure 4.14. Cortex cells GO analysis schema for Molecular Function under 5mM Boron toxicity 45

Figure 4.15. Lateral Root Cap/Epidermis/Quiescent Center/Columella GO analysis schema for Biological Process under 3mM Boron toxicity 45

Figure 4.16. Lateral Root Cap/Epidermis/Quiescent Center/Columella GO analysis schema for Cellular Component under 3mM Boron toxicity 46

Figure 4.17. Lateral Root Cap/Epidermis/Quiescent Center/Columella GO analysis schema for Molecular Function under 3mM Boron toxicity 47

Figure 4.18. Lateral Root Cap/Epidermis/Quiescent Center/Columella GO analysis schema for Biological Process under 5mM Boron toxicity 48

Figure 4.19. Lateral Root Cap/Epidermis/Quiescent Center/Columella GO analysis schema for Cellular Component under 5mM Boron toxicity 48

Figure 4.20. Lateral Root Cap/Epidermis/Quiescent Center/Columella GO analysis scheme for Molecular Function under 5mM Boron toxicity 49

Figure 4.21. Stele GO analysis schema for Biological Process under 3mM Boron toxicity 49

Figure 4.22. Stele GO analysis schema for Cellular Component under 3mM Boron toxicity 50

Figure 4.23. Stele GO analysis schema for Molecular Function under 3mM Boron toxicity 51

Figure 4.24. Stele GO analysis schema for Biological Process under 5mM Boron toxicity 51

Figure 4.25. Stele GO analysis schema for Cellular Component under 5mM Boron toxicity 52

Figure 4.26. Stele GO analysis schema for Molecular Function under 5mM Boron toxicity 52

Figure 4.27. Trichoblast GO analysis schema for Biological Process under 5mM Boron toxicity 53

Figure 4.28. Columella KEGG analysis schema under 5mM Boron toxicity 53

Figure 4.29. Cortex KEGG analysis schema under 3mM Boron toxicity 54

Figure 4.30. Cortex KEGG analysis schema under 5mM Boron toxicity 54

Figure 4.31. Lateral Root Cap/Epidermis/Quiescent Center/Columella KEGG analysis schema under 3mM Boron toxicity 55

Figure 4.32. Lateral Root Cap/Epidermis/Quiescent Center/Columella KEGG analysis schema

under 5mM Boron toxicity 55
Figure 4.33. Stele KEGG analysis schema under 3mM Boron toxicity 55
Figure 4.34. Steel KEGG analysis schema under 5mM Boron toxicity 56
Figure 4.35. Trichoblast KEGG analysis schema under 5mM Boron toxicity 56
Figure 4.36. Cortex cells GO analysis schema for Cellular Component under 5mM Boron toxicity 57

LIST OF SYMBOLS AND ABBREVIATIONS

ATP	Adenosine triphosphate
3B	3 mM boric acid treatment group
5B	5 mM boric acid treatment group
B	boron
BP	biological process
C	control group
CC	cellular component
GDH	glutamate dehydrogenase
GO	gene ontology
GSH	glutathione
GST	glutathione S-transferase
KEGG	kyoto encyclopedia of genes and genomes
kg	kilogram
LD	linkage disequilibrium
MF	molecular function
mM	millimolar
NAD	nicotinamide adenine dinucleotide
NADP	nicotinamide adenine dinucleotide phosphate
ng	nanogram
PCA	principial component analysis
scRNA-seq	single cell RNA sequencing
TF	Transcription factor

1. INTRODUCTION

Boron is a crucial micronutrient for higher plants, necessary in minimal quantities for their normal growth and development. It stabilizes molecules with cis-diol groups and maintains the cell wall via boron-bridge and membrane integrity. Range between boron deficiency and toxicity for plant cells is extremely narrow. Insufficient boron causes developmental setbacks while excess boron is toxic for biology of the plant. Toxicity of boron is a significant agricultural problem for productivity and yield loss of the plants in semi-arid regions where the soil contains high levels of boron. Tolerance to boron varies in different plants; one boron concentration of soil may be harmless to one species but toxic to other. This variability points out how important it is to understand mechanism of boron tolerance mechanisms in the plant cells.

Excess levels of boron at the root of plant causes stress to whole plant biology. Grown plants in this type of environment show similar characteristic symptoms such as decreased root elongation and leaf tip chlorosis which later progresses to necrosis of the tips. At molecular level, excess boron triggers broad metabolic disruptions and shifts. Oxidative stress damages the cell membrane structure and plant cells tolerate this by activating antioxidant defense pathways. Understanding these molecular changes in the plant cells is crucial for future studies and preventing yield loss in crops.

Advances in transcriptomics have provided powerful tools to understand mechanisms and signals at a molecular level. Genome wide expression studies such as microarrays and bulk RNA-sequencing identified various boron responsive genes and pathways for plants. In previous studies, under mild boron stress (1mM and 2mM) revealed cell wall remodeling, signaling of stress mechanisms and detoxification in cell types in the root of *Arabidopsis thaliana*. However, approaches like bulk RNA sequencing provide us average gene expression across all cell types, it masks important cell-type specific responses under excessive boron stress. Roots of plants consist functionally distinct cell layers such as epidermis, cortex, endodermis and stele. Each cell type may activate different tolerance mechanisms and show different transcriptomics under severe boron toxicity. Therefore, a finer resolution approach such as single cell RNA sequencing (scRNA-seq) required to reveal how individual cell types within root cells contribute to tolerance mechanism of plant cells.

Modern scRNA-sequencing is a transformative method to resolve transcriptomic changes at single cell level. This methodology provides a high-resolution view of transcriptome of each cell.

In recent years, scRNA-seq studies have been done in *Arabidopsis thaliana* plant in order to understand cell-type gene expression patterns. These studies show how bulk transcriptomes may differ in cell-type specific studies. This type of approach is relevant for severe boron toxicity in *Arabidopsis thaliana* to understand which cell-types change gene expression, activates signals pathways for their strategy to tolerate excessive boron in root tissues.

In order to address gap of understanding how *Arabidopsis thaliana* shifts its mechanisms to tolerate severe toxic boron, this study presents scRNA-seq analysis to investigate transcriptomic responses in root cells. We used control, 3mM and 5mM boron treated groups and applied scRNA-seq methodology to reveal transcriptomics and as further investigation, Gene ontology (GO) and Kyoto Encyclopedia of Genes and Genomes (KEGG) gene enrichments have been applied. *Arabidopsis thaliana* is chosen as a model organism due to its well-characterized root anatomy and genetics, short life cycle, ability to undergo self-pollination, minimal requirement of growth and small size.

Ultimately, this thesis presents first comprehensive single cell level transcriptome under severe boron stress in *Arabidopsis thaliana*. Insights gained from analysis shed light on cellular strategies of boron tolerance in root cells of *Arabidopsis thaliana* root cells

2. LITERATURE

2.1. Boron as an Essential Element in Plants

Boron is a nonmetallic element bonded with oxygen in nature, found in rocks, soils and water as borax or boric acid (H_3BO_3) [47]. French chemist Joseph-Louis Gay Lussac, Louis-Jacques Thénard and British chemist Sir Humphry Davy heated the boron oxide with potassium metal and isolated the boron in 1808 [65]. It is the 5th element found in periodic table counts as a semi-metal. It has 1 missing valence electron which makes it attracted to making bonds with oxygen. Ionization energy level of Boron is high which results high likely to make covalent bonding rather than metallic bonding. It is an essential element for plants in development, growth stages and metabolic pathways [28]. This element is also used in drug development and isotopes of it in nuclear fission processes [75].

Boron is an essential micronutrient for higher plants and required in small amounts for normal growth and development for plants [42, 37]. One of Boron's key roles is in the structural integrity of plant cell walls. boron cross-links the pectic polysaccharide rhamnogalacturonan II (RG-II) by forming borate di-ester bridges between two RG-II chains to make stable structural integrity through Boron bridging. This cross-linking is crucial for maintaining cell wall stability and elasticity [48]. Under the condition of Boron deficiency, weakened cell walls and growth defects occurs [37, 66].

Boron is absorbed from soil from roots, transported to shoots with xylem. Boron homeostasis, uptake xylem loading and efflux of boron relies on transporters. It was known as passive diffusion transfer in the past but researches shown that it relies on transporters [76]. Two major transporter protein plays crucial role on this regulation. *NIPs* (Nodulin-26 like intrinsic proteins) are boric acid channels that facilitate boron entry into cells and *BOR* transporters that are export boron out from the cell [77]. These transporters regulates boron uptake in optimum levels. Key transporters in regulation of boron are *NIP5;1*, *BOR1* and *BOR4*. *NIP5;1* is a boric acid channel for uptake under limited Boron levels. They are aquaporin-like channel proteins which selectively import boric acid into root cells. *NIP5;1* strongly expressed in outer cell layer of root cells in root cap, epidermis, and also endodermis [78]. *BOR1* is a xylem loading exporter transporter. It is active under low boron levels and downregulated high boron environment. It plays crucial role moving boron into xylem for translocation of boron into shoots of plant. It is mainly expressed in inner root tissues such as endodermis and pericycle cells. It is localized on stele-facing side of the root cells which is opposite site of *NIP5;1* transporter [78]. It is basically

exporting boron into xylem when boron is entered the cell. *BOR4* is a high boron tolerance exporter transporter. It is paralog of *BOR1* and its function is to export excessive boron from plant tissue to soil under excess boron. It is upregulated when boron levels are high. It is mainly found in root epidermis, endodermis and root tip cells such as columella [78]. *BOR4* transporter polar localized toward to soil side of root cells which is opposite site of *BOR1* and the same side with *NIP5;1* transporter. Its function is to pump out the excess boron [78].

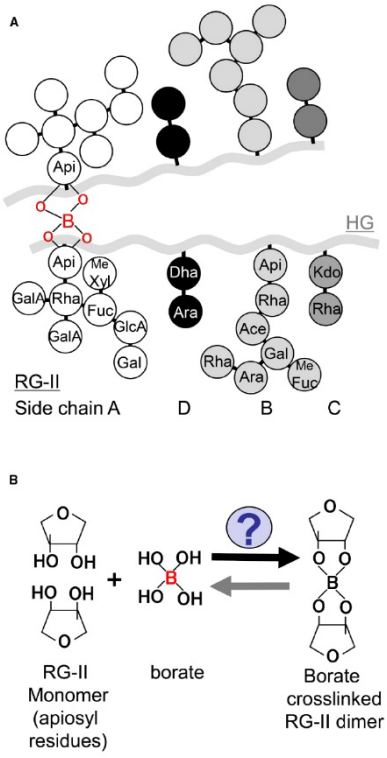

Figure 2.1. Borate Cross-Linking of Rhamnogalacturonan II (RG-II) in Plant Cell Walls [21]

This figure represents the structure and mechanism of borate cross-linking of rhamnogalacturonan II (RG-II) which is a complex pectic polysaccharide found in plant primary cell walls. **Panel A** shows the RG-II structure composed of various side chains (A–D) attached to homogalacturonan (HG) backbone. Side Chain A is particularly significant, as it comprises apiosyl residues that can establish borate diester linkages. **Panel B** demonstrates the molecular mechanism by showing how two RG-II monomers are cross-linked with borate to form borate ester bridge. This structure stabilizes the dimeric RG-II complex. This cross-linking is essential for maintaining cell wall integrity, porosity, and mechanical strength in higher plants.

Boron is also involved in maintaining membrane function and integrity in plant cells. Early studies showed that boron affects membrane potential and proton extrusion [4]. It can also

form complexes with small molecules like S-adenosylmethionine and diadenosine phosphates [52], suggesting potential roles in metabolic regulation. Together, these findings represent that boron is not merely a structural nutrient but also influences a wide range of cellular functions. However, the range between boron necessity and toxicity is exceptionally narrow in plants. Both boron deficiency and boron toxicity lead to significant impact of plant growth which makes boron nutrition in the plant cell in balance [42, 5]. Understanding boron element's roles and the plant responses, whether its deficiency or extensivity is therefore critical for both fundamental plant biology and agricultural management.

2.2. Boron Deficiency vs. Toxicity. Mechanisms and Symptoms

2.2.1. Boron Deficiency

Deficiency of Boron is well known for its negative impact which results pausing the plant's growth and disrupt developmental processes. Primary effect deficiency of boron is the failure of cell elongation and the death of meristematic growing points in the plant. This is because rapidly reproducing cells require boron to form stable cell walls. Boron insufficiency will prevent cell walls forming boron-bridges, resulting in fragility, instability, and vulnerability on the wall structure which leads to leakage.

Symptoms of boron deficiency often include tissue fragility, empty or necrotic stem cores in severe cases and floral infertility resulting in decreased seed production [18, 14]. Boron deficiency at the cellular level affects cell membrane integrity and triggers an oxidative burst, a rapid production of reactive oxygen species (ROS). For example, cultured rose cells under B deficiency showed increased phenolic leakage and a burst of ROS which resulted as loss of cell viability [18].

Ethylene signaling likely mediates certain root responses to boron deficiency, potentially serving as a stress signal for affected cell wall formation [23]. To cope with low B levels, plants activate high-affinity boron transport systems. Due to limited boron levels, boric acid channels (NIP aquaporins) and borate exporters (BOR transporters) are upregulated to scavenge and redistribute boron more efficiently in the cell [5]. In *Arabidopsis thaliana*, for instance, the boric acid channel NIP5;1 is induced in roots during B starvation to enhance uptake of boron while the BOR1 transporter is upregulated to facilitate xylem loading of boron for delivery to shoots. These adjustments help mitigate boron deficiency by prioritizing boron flow to young tissues. Despite these responses, prolonged B deficiency ultimately arrests growth of the plant. First

impacts occur in actively growing tissues such as root tips and shoot apices, which arrests development and may die off without adequate boron [67, 11]. In summary, boron deficiency primarily affects processes at the growing points, cell wall synthesis, cell division, and membrane function resulting in stunted, fragile growth and death of meristems.

2.2.2. Boron Toxicity

Conversely, an overabundance of boron in soil or water can be as harmful to plants. Boron toxicity is a widespread issue in semi-arid regions. Environmental processes such as volcanic disruptions and groundwater streams may transfer high levels of boron to the soil, leading to its accumulation and subsequent uptake of excessive boron by plants through the roots [5]. Notable cases are documented in parts of Türkiye, Australia, the western United States, and other arid areas with boron-rich parent material or irrigation water [14, 5]. Plants that are grown in boron-toxic soils show characteristic symptoms such as. reduced root elongation, yellowing of leaf tips that progresses to necrosis, and general growth suppression. Older leaves typically show toxicity symptoms. First, developing dry, brown lesions at the tips and edges because boron is mobile in the xylem stream and accumulates in transpiring leaves [14].

Excess boron in crops such as wheat and barley leads to significant yield losses, with fewer tillers and grain set, largely due to damage in the foliage [69, 36]. Boron toxicity triggers oxidative stress and broad significant metabolic disruption at both physiological and molecular levels. High B exposure leads to excessive ROS production, leading to lipid peroxidation and cell membrane damage [31, 67]. Plants activate antioxidant defenses and other stress-response pathways to reduce oxidative injury. For example, *Arabidopsis thaliana* seedlings that are exposed to toxic concentrations of boron accumulate elevated levels of flavonoids, anthocyanins, and proline. These are the compounds that are associated with antioxidative and osmo-protective functions. [17]. In the study indicated that toxic concentrations of B (3 mM) resulted in visible chlorosis in *Arabidopsis thaliana*, along with an increase in anthocyanin levels, likely serving as a protective mechanism against reactive oxygen species [17]. The activities and expression of antioxidant enzymes such as superoxide dismutase (SOD) and ascorbate peroxidase changes in response to excess boron, indicating the plant's attempts to detoxify reactive oxygen species (ROS) [17, 33].

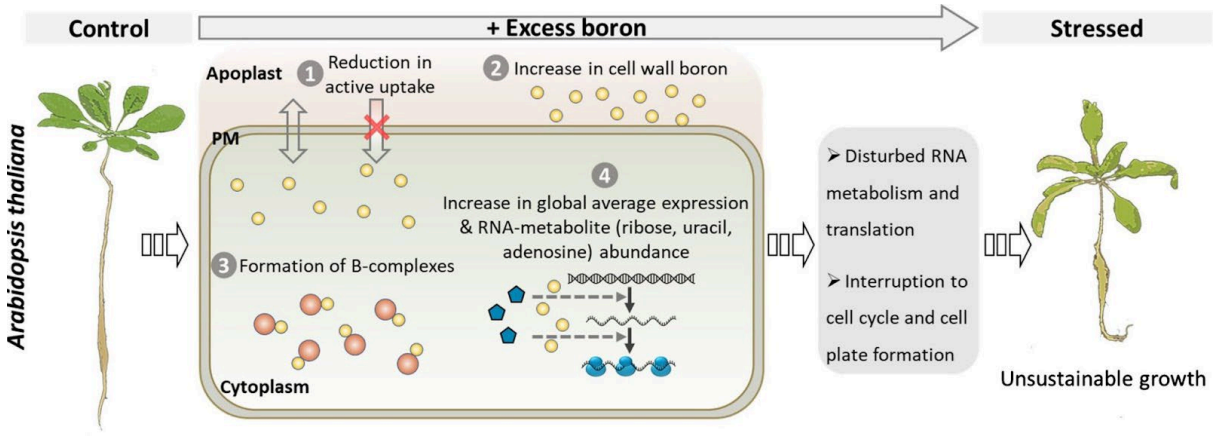

Figure 2.2. Effects of Excess Boron on *Arabidopsis thaliana* at the Cellular and Physiological Level [67]

Figure represents an overview of the physiological and molecular effects of excess boron levels in *Arabidopsis thaliana* cells. Control shows a healthy plant under normal boron conditions. Under Excess levels of Boron, several cellular formation changes occur. Downregulation of Active uptake of boron through the plasma membrane (PM) to prevent toxic accumulation of boron. Boron concentration increases in the apoplast and cell wall which indicates enhanced sequestration. Formation of boron complexes (B-complexes) occurs in the cytoplasm to diminish B-level accumulation in the cell. Increased expression of global transcript levels and elevated abundance of RNA-related metabolites such as ribose, uracil, and adenosine occur. These molecular shifts due to toxic level of B ultimately lead to stressed growth conditions which are characterized by disruption of RNA metabolism and protein translation. Interruption of cell cycle progression and cell plate formation. These result in visible growth defects and morphological abnormalities with unsustainable growth under boron stress.

Boron toxicity interferes with nutrient balance as well. Recent research showed that excess B affects sulfur metabolism which notably inducing the expression of sulfate transporters in *Arabidopsis thaliana* roots [32]. Excessive binding with cis-hydroxyl groups such as ribose may disrupt the RNA structure, damage cell wall and plasma membrane through disruption of RGII and GIPCs complex systems. Metabolic pathways are negatively affected by the accumulation of boron. The amino acid Cys and the antioxidant Glutathione (GSH) are synthesized through a process that requires the element sulfur (S). The deficiency of sulfur and elevated levels of boron in the environment leads to the activation of SULTR transporters, increasing sulfur uptake to produce more GSH. GSH is also participates in the synthesis of phytochelatins (PCs) which forms complexes with excessive boron which facilitates its conjugation to the vacuole with sulfate [32]. Consequence of this process induces cellular stress, leading to metabolic pathway instability and imbalance of biochemical entities that containing ribose, ATP, and NADH in the cell [48]. This indicates that elevated boron levels may cause sulfate or other nutrients to become unevenly distributed or less available in cell which may trigger the plant to upregulation of sulfur uptake and assimilation pathways [32].

Another consequence of boron toxicity is altered hormone signaling and gene regulation. Transcriptomic analyses have revealed that even moderate boron toxicity (for instance 1–2 mM in *Arabidopsis thaliana*) can trigger stress hormone pathways. Genes related to ethylene and jasmonate signaling are differentially expressed under boron stress [33]. Ethylene-response factors and jasmonate-regulated genes typically show higher expression, which supports the roles of these hormones in mediating stress and senescence responses. In addition, boron-toxic conditions can induce the synthesis of polyphenolic compounds, such as lignin or suberin, as plants attempt to immobilize or compartmentalize excess boron in cell walls or vacuoles [67]. At the anatomical level, boron-toxic plants may have thicker cell walls due to elevated boron bridging or callose deposition, while root growth is inhibited as meristem activity diminishes [53].

To avoid boron overaccumulation, plants apply exclusion mechanisms. specialized transporters such as BOR4 in *Arabidopsis thaliana* become highly expressed under high levels of boron, pumping borate out of root cells to prevent toxic buildup in the symplast [45, 32]. By reducing boron loading into the xylem and actively transferring it at the root-soil interface, tolerant plants can protect sensitive tissues on the plant [69]. Despite these defenses, severe boron toxicity overwhelms plant homeostasis, causing significant oxidative damage, inhibition of photosynthesis, and eventual cell death in leaves and roots. In summary, boron toxicity elicits a complex stress response in plants. it causes oxidative stress, disturbs nutrients and hormone balances, and damages cellular structures such as cell walls. However, plants counteract these effects via antioxidant production, stress signaling, and boron exclusion mechanisms.

2.3. Transcriptomic Responses to Boron Toxicity

Understanding how plants respond to boron toxicity at the gene expression level has been a major focus of research in recent years. High-throughput transcriptomic studies (microarrays and RNA sequencing) allow researchers to capture global changes in gene expression under stress and have been applied to boron stress in several plant species. Recent studies reveal that boron toxicity triggers a wide array of genetic responses that reflect the physiological changes discussed above. In *Arabidopsis thaliana*, one of the first transcriptome-level studies of B toxicity revealed numerous genes related to antioxidant defense and secondary metabolism upregulated under excess levels of boron [17]. Genes involved in the anthocyanin biosynthesis pathway and various ROS-scavenging enzymes showed higher levels of expression under B-toxic conditions, aligning with the observed accumulation of anthocyanin and the activation of

antioxidant defenses [17].

The study by Kayıhan et al. (2019) indicated that *Arabidopsis thaliana* exposed to toxic doses of boron activates glutathione-S-transferases and other elements of the GSH-dependent detoxification pathways. This indicates that, GSH-based antioxidant processes are highly critical for mechanisms of boron stress tolerance [33]. The high expression of genes responsible for GSH production and recycling under toxic boron conditions correlates with increased GSH levels, which serve to mitigate oxidative damage.

Transcriptomic analysis has also shown how boron toxicity affects hormone signaling at the gene level. In a study of moderate boron stress in *Arabidopsis thaliana*, Kayıhan *et al.* (2019) identified differential regulation of numerous microRNAs and their target genes, implicating hormonal pathways like jasmonic acid (JA) and ethylene in the boron response in cell. Specifically, certain microRNAs that regulate JA/ethylene-related transcription factors were significantly altered under B toxicity [34]. This suggests boron stress can reprogram gene expression through microRNA-mediated circuits, ultimately modulating hormone signaling networks that influences stress elevation and growth suppression. This hormonal crosstalk could clarify events like premature death or growth suppression under excess Boron levels, since JA and ethylene are known to mediate stress responses and developmental constraints

Transcriptomic studies in crop species, in addition to *Arabidopsis thaliana*, have been crucial for determining boron toxicity tolerance. In wheat (Triticum aestivum), known for its sensitivity to elevated boron concentrations, comparative transcript profiling demonstrated genotype-specific responses. Kayıhan *et al.* (2017) examined boron-toxic conditions in roots and leaves of two wheat variants (one tolerant, one sensitive) and found that the tolerant variant showed a stronger impact of stress-response genes than the sensitive variant [10]. Genes involved in cell wall reinforcement, heat shock proteins, and transporters were upregulated to a greater extent in the tolerant wheat variant. Which suggests that these pathways contribute to boron tolerance in cereal crops. Interestingly, that study indicated that boron toxicity influenced the expression of genes related to cell wall structure, such as extensins and pectin-modifying enzymes, in wheat [10]. This supports the claim that tolerant plants could improve or alter their cell walls to mitigate excess boron effects and safeguard the cell interior. Similarly, transcriptome analyses in other species such as barley and citrus have demonstrated the activity of boron toxicity-responsive genes, including those involved in sulfate transport, sugar alcohol metabolism, and stress signaling proteins [24, 43]. These cross-species studies collectively indicate that although specific

genes may vary among species, the general principles of boron toxicity response for antioxidant activity, cell wall modification, transporter regulation, and hormone signaling are conserved across plant taxa.

A significant recent advance study is the integration of multi-omics to study boron stress. Wang et al. (2021) carried out a cross-species multi-omics analysis that integrated transcriptomics, metabolomics, and proteomics in plants demonstrating differing levels of boron tolerance. Boron-tolerant plants utilize a dual strategy to manage excess boron. (1) sequestering boron in the cell wall to prevent cytosolic toxicity, and (2) upregulating an array of stress response genes to mitigate damage from the toxic environment [67]. In tolerant genotypes, transcripts that encoding cell wall pectin synthesis and binding were highly abundant, supporting enhanced boron immobilization in the apoplast, while genes associated with general stress tolerance (chaperones, antioxidants, and detoxification enzymes) were expressed at higher basal levels [67]. This multi-omics perspective strengthens the importance of cell wall and antioxidant mechanisms in boron tolerance and shows how transcriptomics contributes to a deep understanding of the plant stress response.

Most recently, researchers have begun to explore boron stress responses at even finer resolution. Until now, nearly all transcriptomic studies for boron toxicity have used whole organs or large tissue samples, which mask cell-type-specific responses. There is increasing acknowledgment that various cell types in a plant may detect and react to boron stress differently. A study by Kayıhan et al. (2023) demonstrated that roots and shoots demonstrate different transcriptional responses to excess boron, with *Arabidopsis thaliana* roots triggering specific sulfate transporter genes in reaction to boron toxicity [32]. Within a single organ such as the root, significant cellular heterogeneity exists. For example, the outer epidermis and inner vascular cells may encounter varying boron concentrations and stresses at the cellular level. This has resulted in the concept of profiling transcriptomic alterations at the single-cell level in response to boron stress. A recent study by Yılmaz et al. (2023) reported preliminary findings regarding single-cell transcriptome alterations in *Arabidopsis thaliana* roots under mild (1mM and 2mM) boron toxicity. The results indicate that each root cell type activates a distinct genetic program in response to a boron-toxic environment. This thesis builds upon this emerging approach, moving from bulk-tissue analyses to single-cell level. Investigating transcriptomic responses to severe boron toxicity in the roots of *Arabidopsis thaliana* at the single-cell level [70].

2.4. *Arabidopsis thaliana* as a Model for Boron Stress Studies

Arabidopsis thaliana plant has many aspects in advance to be used as a model organism. It is a member of the Brassicaceae (mustard) family and has relativeness with crop plants. It has long served as a model organism in plant biology and functional genomics [39]. This small plant offers numerous advantages, including a short life cycle. It gives us a life cycle as approximately 6 weeks from seed to seed. It also consists of high seed production efficiency, a compact diploid genome, and capability for genetic modifications [50]. Over decades of research, *Arabidopsis thaliana* has been used to analyze fundamental processes in plants, earning its title as the "Drosophila of plant biology." The entire genome of *Arabidopsis thaliana* has been sequenced early 2000s. This is the first plant genome to be completed, which greatly accelerated studies of genes and their functions [64]. *Arabidopsis thaliana* plant serves as an optimal system for investigating gene function in studies, supported by extensive community resources as well. For instance, well-annotated gene databases and T-DNA insertion mutant libraries are some resources that are easily accessible [13]. *Arabidopsis thaliana* serves as the key model organism for investigating mineral nutrition and stress responses in plant cells, particularly in relation to boron deficiency and toxicity like this study. Many of the molecular systems in plant boron homeostasis were first identified and characterized in *Arabidopsis thaliana*. For example, the BOR family transporters that mediate boron export were discovered using *Arabidopsis thaliana* mutants. For example, *bor1* mutants helped reveal the role of BOR1 in xylem loading under low B levels, whereas overexpression of *BOR4* was found to play role on boron tolerance by excluding excess boron from roots [45]. Likewise, *Arabidopsis thaliana* studies unrevealed NIP5;1 as a boric acid channel that required for Boron uptake when external B is less found in environment [62]. The wealth of genetic mutants and reporter lines in *Arabidopsis thaliana* allows researchers to observe how altering these boron-related genes impacts the plant, under controlled conditions [20].

Arabidopsis thaliana is particularly useful for transcriptomic studies of stress because its small size and simple architecture enables uniform treatment applications and sampling. Its primary root is organized in tissue layers such as epidermis, cortex, endodermis, pericycle, vasculature that are largely consistent, and also its cellular composition is well-mapped [7, 51] This means that gene expression patterns can often be assigned to specific cell types or tissues, especially with modern methods like fluorescent reporters or single-cell sequencing. Prior findings from *Arabidopsis thaliana* under boron stress underscore its value as a model organism. As mentioned, *Arabidopsis thaliana* transcriptomic studies have shown general strategies of boron toxicity responses such as antioxidant gene induction, hormone signaling changes and

more [17, 34]. *Arabidopsis thaliana* mutants have long served as a valuable model organism in elucidating the molecular mechanisms underlying boron (B) tolerance. Studies specifically have used loss-of- function mutants to verify the functional relevance of genes encoding boron transporters and channels. For example, Takano et al. (2006) showed that disruption of the BOR1 gene, which codes for an efflux-type boron transporter in charge of xylem loading of boron, causes hypersensitivity to low boron conditions. That means affecting growth and development, especially in the shoot meristem. Under both shortage and excess of boron, Kayıhan et al. (2023) provided more evidence. Loss of function in aquaporin-like channels involved in boron transportation across membranes enhances vulnerability to boron toxicity. These findings help to understand the critical role of tightly regulated boron homeostasis for normal plant development and illustrate how *Arabidopsis thaliana* genetic mutants enable precise analysis of how individual genes contribute to abiotic stress tolerance mechanisms. [62, 32].

Furthermore, *Arabidopsis thaliana* can serve as a model organism for advanced methodologies such as live-cell imaging and single-cell omics, which are more challenging to implement in larger crop species. The features of *Arabidopsis thaliana* make it a perfect model organism for investigating single-cell-specific responses to boron toxicity. This thesis utilizes *Arabidopsis thaliana*, a model organism with a comprehensive knowledge base and established tools, to ensure that findings regarding boron stress responses are effectively framed and functionally validated within existing literature.

2.5. Single-Cell RNA Sequencing (scRNA-seq) in Plant Research

Traditional RNA sequencing of bulk tissue provides an average gene expression profile over millions of cells; however, it masks the differences between individual cell types. Single-cell RNA sequencing (scRNA-seq) is a revolutionary methodology that overcomes this limitation by profiling transcriptomes at the resolution of single cell level. Firstly, this methodology used in animal systems in the early 2010s, scRNA-seq method has since been adapted to and used on plants and is transforming our understanding of cellular heterogeneity [27]. Core principle of scRNA-seq is isolating single cells from a tissue, capturing each cell's mRNA, and sequencing cDNA libraries. This approach allows us to keep the information which cell and transcript came from. The usual workflow of scRNA-seq begins with the tissue dissociation.

In the plants this often requires enzymatic digestion of the cell wall to yield protoplasts (or alternatively isolation of nuclei for single-nucleus RNA-seq). Individual cells (or nuclei) are then

segregated – either into microfluidic droplets or microwells – and barcoded such that transcripts from each cell receive a unique molecular tag [27]. After reverse transcription and amplification processes, sequencing has been performed.

Bioinformatics pipelines then helped us to separate the reads by cell barcode and quantify gene expression per cell. For high-throughput single-cell transcriptomic profiling, the Chromium platform developed by 10X Genomics has been used on this thesis and it also may count as a standard technology due to its robust microfluidics system that enables efficient encapsulation and barcoding of thousands of cells within nanoliter-scale droplets [73]. The resulting data analyzed using Seurat R package, which is a great tool for data normalization, dimensionality reduction, clustering, and identification of cell-type–specific expression patterns [25]. The resulting data then represented in low-dimensional spaces such as UMAP plots to visualize clusters of cells with similar expression profiles. Each cluster ideally corresponds to a distinct cell type or condition, which can be identified by known marker genes. In *Arabidopsis thaliana* root, for example, scRNA-seq method allows us to get cluster cells into groups representing epidermal cells, cortex cells, endodermis, root cap, meristematic cells, and more, each with characteristic gene expression profiles. [16]. First single-cell atlas of the *Arabidopsis thaliana* root identified around 15 distinct cell clusters corresponding to all major root tissues and developmental stages on study of Denyer et al. (2019) demonstrating that scRNA-seq can express the anatomy of an organ purely to transcriptomic data.

Applying scRNA-seq to stress conditions allows researchers to see how each cell type in a tissue responds to the stress, which genes are activated or repressed specifically in that cell type, and how cell-to-cell signaling networks may be bound together. This level of detail is extremely valuable for complex stresses like nutrient toxicity such as Boron, where effects are localized and cell specific. In recent years, scRNA-seq has been successfully used in plant stress studies.

One of the example studies is the single-cell transcriptomic analysis of pea (*Pisum sativum*) shoot apices under boron deficiency by Chen *et al.* (2023). In that study, they identified up to 15 cell clusters in the pea shoot. It also found that different cell types, such as mesophyll cells, guard cells, and stem cells in the shoot meristem, demonstrated distinct responses to low boron conditions. For instance, boron deficiency led to strong down-regulation of photosynthesis genes specifically in mesophyll cells, while genes controlling stomatal development were down-regulated in guard cells. That correlates with observed reductions in stomatal density under B deficiency [12]. These findings highlight how scRNA-seq can identify which cellular processes

are impacted, information that bulk tissue analysis can't reveal due to the total outcome of the results masks the cell specific information. Similarly, in the context of boron toxicity, one would expect that cell types in the root that accumulate boron (like the epidermal cells at the root tip or the lateral root cap) might activate different protective genes compared to inner cells that experience less Boron intake. Until recently, no study mapped the single-cell transcriptomic analysis of plants under mild boron toxicity at 1-2mM level. This gap filled by study of Yılmaz *et al.* (2023), that applied scRNA-seq to *Arabidopsis thaliana* roots treated with mild toxic boron levels for 1mM and 2mM. Preliminary results from the study indicated that *Arabidopsis thaliana* root cells could be clustered into about six major types (including quiescent center, endodermis, cortex, columella, trichoblast/root-hair cells, and root cap), and that boron toxicity caused unique gene expression changes in each cluster. From the study, columella (central root cap) cells showed the greatest number of upregulated genes under moderate Boron toxic environment at 1 mM boron, whereas under more severe B stress 2 mM boron many stress-responsive genes mainly upregulated in root cap and endodermal cells [70]. These findings point out that different root regions may have specialized roles in high-boron conditions. The outermost root cap cells perhaps act as a sacrificial barrier by absorbing and reacting to excess boron, and inner cells like the endodermis mounting defense responses as a second layer of protection. In the same study, scRNA-seq facilitated the identification of enriched pathways in specific cell types. For example, genes related to glutathione (GSH) metabolism were significantly enriched among the boron-upregulated genes in columella cells, indicating a localized activation of GSH-mediated detoxification in these cells [70]. This level of understanding demonstrates the power of single-cell approaches. Moreover, single-cell data can reveal complex cell subpopulations or stress-induced cell states with higher levels of Boron Toxicity 3mM and 5mM – for example, a subset of cortex cells expressing high levels of a transporter could be discovered, which might be important for adaptation and further cellular pathways.

Despite its promise and advanced technique, single-cell transcriptomics in plants comes with technical challenges as well. Most importantly, the requirement to separate intact cells from hard tissues without affecting the transcriptome of the cells. The protoplasting step (removing cell walls) can itself induce osmotic and oxidative stress in cells. Protocols have been established to minimize artifactual stress responses during isolation on this study [27].

Control studies and the alignment of identified cell types with established markers demonstrate that scRNA-seq results in reproducible outcomes consistent with existing biological literature [16, 27]. This is shown by the fact that precise execution of the technique gives reliable

outcomes. In this thesis, we adopt these cutting-edge single-cell methods to interrogate the high levels (3mM and 5mM) of boron toxicity response in *Arabidopsis thaliana* roots. By capturing transcriptomic snapshots of thousands of individual root cells under control and high boron conditions, we aim to map out which genes each cell type expressed up-regulated in response to boron stress. This approach gives us the opportunity to address questions like. Which cell type in the root is most sensitive to excess boron? Do different tissues activate different defense pathways in severe conditions, for example does the epidermis induce one set of genes while the cortex induces another? How do cell-to-cell signaling genes, such as peptide hormones or transporters, coordinate a whole-organ response to toxic boron levels? Single-cell RNA-seq provides the data to answer these questions comprehensively. Overall, single-cell transcriptomics represents a transformative tool for plant biology, and its application to the severe levels of boron toxicity problem stands to deliver novel insights into plant stress adaptation that were previously not found in literature.

2.6. Functional Enrichment Analysis (GO/KEGG) for Transcriptomic Data

Large scale transcriptomic experiments, both bulk and single cell, generally produce extensive lists of differentially expressed genes (DEGs) in response to specific conditions, such as severe boron toxicity in this study. Functional enrichment analysis helps in understanding gene lists by identifying the statistical over-representation of specific gene categories or pathways [61, 71]. Two of the most commonly used resources for enrichment analysis are the Gene Ontology (GO) and the Kyoto Encyclopedia of Genes and Genomes (KEGG) pathway database.

Gene Ontology (GO) offers a systematic vocabulary that categorizes gene functions into three domains. Biological Process, Molecular Function, and Cellular Component. This framework enables researchers to identify the biological processes or functions most impacted within their gene sets [2, 22]. KEGG provides a curated collection of metabolic and signaling pathways, enabling the mapping of differentially expressed genes onto established biochemical pathways and regulatory modules [30].

GO/KEGG enrichment analysis involves taking a list of upregulated or downregulated genes in a specific condition and assessing which annotations are overrepresented compared to what would be expected by chance. For example, if numerous upregulated genes are categorized under "response to oxidative stress," GO analysis will identify that term as significantly enriched, highlighting a critical aspect of the condition's impact, such as boron toxicity.

Enrichment analysis is valuable for identifying overall trends in transcriptomic data for Boron stress studies. Boron toxicity and deficiency impact multiple physiological processes. GO/KEGG analysis helps to highlight which processes are most affected at the gene level. One of the latest examples comes from a recent transcriptome study of boron deficiency in *Acacia* plants.

GO enrichment analysis of Boron-deficiency-responsive genes in *Acacia* showed over-representation of oxidoreductase activity and cell wall organization [11]. This indicates that under even low boron conditions, *Acacia* ramps up processes associated with oxidation-reduction, just like as part of dealing with stress or altered metabolism and modifies cell wall components as defense mechanism. That concludes that fit with known deficiency effects. Likewise, in this single-cell analysis of *Arabidopsis thaliana* under high level of boron toxicity, after identifying DEGs in each cell cluster, performing of GO/KEGG enrichment done to understand the functional themes. As noted, one outcome was that columella cells under high B had an enrichment of genes in the GSH metabolic process [70] demonstrates GSH-based detoxification plays a role as a major pathway in those cells. Another cell type from the study showed enrichment of genes in "carbon metabolism" pathways, pointing out that at changes in primary metabolism under mild boron stress conditions [70]. These enriched categories from GO/KEGG guide our interpretation by linking gene expression changes to broader biological functions. Rather than discussing dozens of individual genes, it can be said that boron toxicity triggers antioxidant pathways (e.g., glutathione and flavonoid biosynthesis) and alters primary metabolic and cell wall pathways, with specific nuances in different cell types. KEGG pathway analysis complements GO by placing the DEGs on pathway maps. As an example, highlighting the *phenylpropanoid biosynthesis* pathway, if multiple enzymes in that pathway are induced, which would suggest increased synthesis of phenolic compounds like lignin or anthocyanins.

Another advantage of enrichment analysis is uncovering less obvious effects of the treatment on the cells. In an earlier bulk RNA-seq of *Arabidopsis thaliana* under B toxicity, GO analysis revealed enrichment of sulfur compound transport and homeostasis genes [32], which led to investigate and find that, sulfate transporter genes were induced by high Boron toxicity (an unexpected crosstalk between boron and sulfur nutrition). Thus, GO/KEGG can point to new hypotheses.

In this thesis, functional enrichment is applied at multiple stages, to interpret the global response of *Arabidopsis thaliana* roots to severe boron toxicity and to compare functional

themes across different root cell types. By consistently using GO and KEGG enrichment, we ensure that our analysis moves beyond gene lists to biological meaning, identifying which pathways are activated as protective mechanisms and which processes are hindered by boron stress. Such analysis is crucial for formulating a coherent picture of boron toxicity responses, ultimately lets us to discuss how the stress of severe Boron impacts *Arabidopsis thaliana* physiology in terms of enriched processes like "oxidative stress response," "cell wall modification," "hormone signaling," or specific pathways like glutathione metabolism and lignin biosynthesis. These insights from enrichment analysis will feed into the identification of key regulatory genes and the proposal of mechanisms in the concluding parts of the thesis.

2.7. Aim and Scope of the Thesis

The aim of this thesis was to understand the transcriptomic responses to severe boron toxicity in the roots of *Arabidopsis thaliana* at single-cell resolution. While previous studies have documented bulk tissue responses to boron stress and 1mM and 2mM stress level conditions [32, 24], a cell-type-specific understanding for severe toxicity has been lacking in the literature. This research seeks to fill that gap by applying single-cell RNA sequencing to 3mM and 5mM boron-stressed and unstressed *Arabidopsis thaliana* roots, thereby capturing cells to reveal how each cell type in the root contributes to the overall stress response. The questions in order to achieve this goal are. *Which root cell types are most affected by excess boron, and what gene expression changes define their response?* and *What are the key molecular pathways and regulatory mechanisms activated under high boron conditions, and how do these play a role among different cells or tissues of the root?*

To achieve these aims, *Arabidopsis thaliana* seedlings were grown under control and high level of boron toxicity conditions. Root cells were isolated and profiled with scRNA-seq using the Chromium platform from 10X Genomics, yielding an atlas of thousands of individual cells. The data were then analyzed using the Seurat R package to identify clusters corresponding to distinct root cell types and to determine differentially expressed genes due to severe boron treatment within each cluster. Functional enrichment analyses (GO and KEGG) were performed on the DEGs to pinpoint overrepresented processes and pathways. Additional computational analyses, such as cell trajectory inference and network analysis, were employed to explore changes in developmental states or gene regulatory networks under stress. These results collectively represent the first comprehensive single-cell map of *Arabidopsis thaliana* response to micronutrient toxicity in severe conditions of boron [72, 35].

In conclusion, this thesis significantly expands our understanding of how *Arabidopsis thaliana* cope with severe toxic levels of boron. It highlights the spatial dimension of stress responses, where various cell types in the root of *Arabidopsis thaliana* apply unique yet complementary protective strategies. The findings bring and point out pathways like GSH-mediated detoxification, carbohydrate metabolism adjustments, and cell wall modifications as central to the severe boron toxicity response. The thesis presents a single-cell resolution perspective, contributing to a refined model of severe boron toxicity tolerance. This model can guide crop improvement initiatives, such as the engineering of specific root cell types to enhance overall plant tolerance. This introduction presents the background and rationale for the study, addressing the significance of boron, the characteristics of boron stress, the model system of *Arabidopsis thaliana*, and the advanced methodologies employed [38, 39]. The chapters that follow will outline the experimental methodology and present the findings from the single-cell transcriptomic analysis, followed by a discussion of the implications of these results within the broader framework of *Arabidopsis thaliana* stress biology and nutrient management.

3. MATERIALS AND METHODS

3.1. Plant Growth and Boron Toxicity Treatments

In this study, Columbia 0 (Col-0) wild-type *Arabidopsis thaliana* was used as the plant material. Seeds were surface sterilized prior to sowing to prevent microbial contamination.

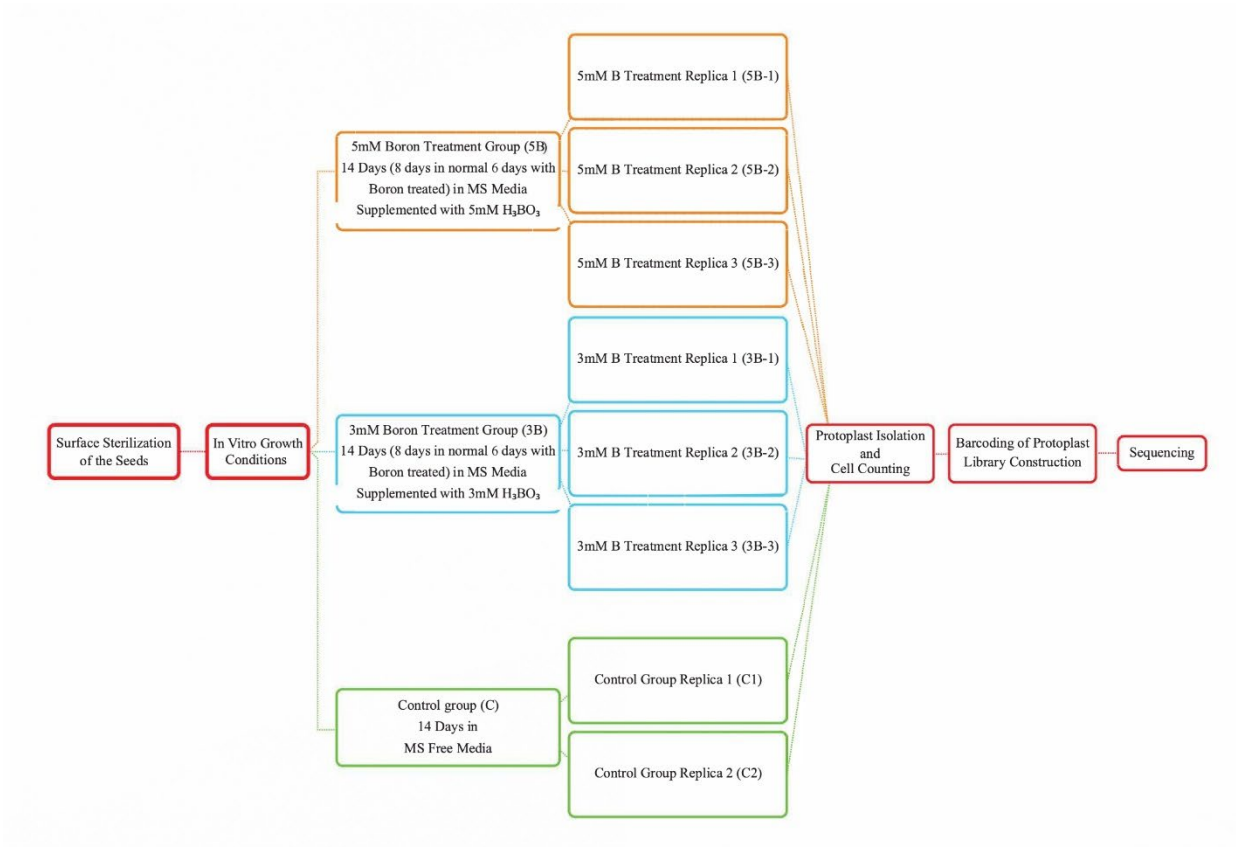

Figure 3.1. Workflow representation of experimental setup

Seeds of *Arabidopsis thaliana* were subjected to surface sterilization prior to being sown on the growing medium. The seeds have been transferred to an Eppendorf tube with 500 µl of 70% (v/v) ethanol, inverted for 2 minutes, and after ethanol has been removed. 500 µl of 2.5% (v/v) sodium hypochlorite has been added. Inverted for 10 minutes and after that NaOCl has been extracted. Subsequently, the seeds were rinsed three times for 30 seconds each time with 500 µl of distilled water.

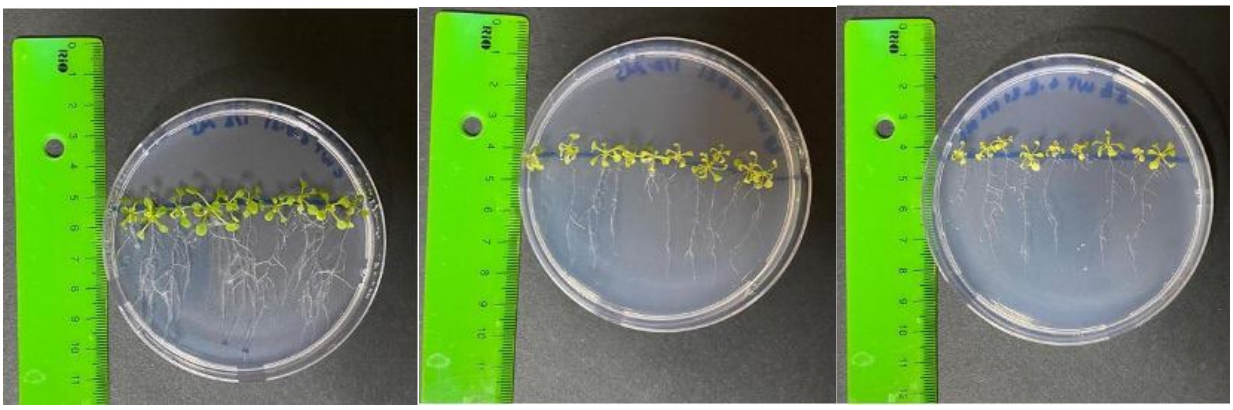

Figure 3.2. Demonstration of Control (left), 3mM B treated (middle) and 5mM B treated (right) *Arabidopsis thaliana* plants

Figure demonstrated the root elongation levels of treated groups 3mM and 5mM and control group col-0. Most left picture represents control group and mean root length observed as 3.2 cm ± 0.2. Middle picture represents 3mM B treated group and mean root length observed as 2.0 cm ± 0.2. Most right pictures represent 5mM B treated group and mean root length observed as 1.4 cm ± 0.2.

Surface-sterilized seeds were individually positioned along the line marked on the petri dishes at specified intervals. Control groups were cultivated in half-strength MS medium (Murashige and Skoog, 1962) at a pH of 5.7. Conversely, 3 mM and 5 mM boric acid treatments were selected to address B toxicity. The 3 mM boric acid treatment group (3B) and the 5 mM boric acid treatment group (5B) were cultivated in MS media supplemented with 3 mM or 5 mM boric acid, respectively. Petri dishes were initially encased in stretch film and then in aluminum foil. Following a 3-days incubation at 4°C, then samples of control group have been maintained in a growth chamber at 22 ±1°C for 14 days. Treatment group samples growth in 8 days in normal growth MS Free media and later 6 days in MS treated Media with same conditions. Afterwards, exposed to a photoperiod of 16 hours of light (200 µmol $m^{-2}s^{-1}$) and 8 hours of darkness, with %60 of humidity.

3.2. Protoplast Isolation and Cell Counting

Arabidopsis thaliana after 14 days of growth, root protoplasts were isolated from the seedlings for application of single-cell RNA seq. Approximately 20 primary roots per sample, each about 2 cm in length from the root tip upward has been collected using sterilized forceps and transferred immediately into a pre-prepared enzymatic digestion solution for isolation. The enzyme solution was formulated to aim of digesting the cell walls and release individual root cells as protoplasts.

Enzyme solution consists of 1.25% (w/v) cellulase (Onozuka R10; Yakult Honsha Co.,

Japan) [19], 0.1% (w/v) pectolyase (Sigma-Aldrich, P-3026) [59], 0.4 M mannitol, 20 mM 2-(N-morpholino)ethane sulfonic acid (MES) buffer adjusted to pH 5.7, 20 mM KCl, 10 mM $CaCl_2$, and 0.1% (w/v) bovine serum albumin (BSA). Enzyme solution creates an osmotic and enzymatic environment suitable for isolation of protoplasts [15, 68].

For each sample, 3 mL of the enzyme solution was dispensed into a sterile 60 mm Petri dish. A 70 μm nylon mesh cell strainer was placed into dish and roots were isolated in the enzyme solution beneath the strainer. The dish was incubated on an orbital shaker at ~90 rpm for 2.5 hours at room temperature. Throughout the incubation, the samples were periodically for every ~30 minutes, gently agitated by swirling or tapping the plate in order to isolate protoplast from root. The 70 μm mesh successfully separated larger root fragments while permitting the passage of released cells into the suspension below.

After enzymatic digestion, the cell suspension that containing released root protoplasts filtered through a 40 μm cell strainer into a 15 mL conical tube to remove any remaining large debris. The filtrate that enriched in single cells centrifuged at low speed (100 × *g* for 6 minutes at 22 °C) to pellet the protoplasts. The supernatant was carefully aspirated, and the protoplast pellet was gently resuspended in 500 μL of an osmotic stabilization buffer consisting of 8% (w/v) mannitol (which is osmotically balanced to prevent protoplast rupture). To further ensure a clean single-cell suspension, the resuspended protoplast solution was passed through a fine 40 μm mesh (for example, a mesh attached to a pipette tip) one more time. This step removed any remaining cell clumps and yielded a highly uniform population of single root protoplasts.

An aliquot of the resulting protoplast suspension was used to assess cell yield and viability. Trypan Blue staining was performed by mixing a small volume of protoplast suspension (e.g. 10 μL) with 0.4% (w/v) Trypan Blue dye (at roughly a 10.0.8 ratio of sample to dye). The mixture was incubated at room temperature for 1–2 minutes, then loaded onto a hemocytometer (Thoma counting chamber) and examined under a light microscope. Protoplasts that took up the blue dye were considered non-viable (dead), whereas viable protoplasts remained unstained. Live (unstained) and dead (blue) cells were counted in several fields of the hemocytometer, and the total protoplast yield (cells per μL of suspension) as well as the viability percentage were calculated. Only preparations with high yield and viability were used for subsequent single-cell library preparation.

Table 3.1. Formula for Cell Viability calculation

Cell/ml = A * SF * 10000
cell/ µl = A * SF * 10
Viability = (Alive cell number / Total cell number) * 100
A. Cell number for 16 squares, SF. Dilution Factor

3.3. Single-Cell Library Preparation and Sequencing

Single-cell cDNA libraries from root protoplasts were prepared using the 10x Genomics Chromium platform following the manufacturer's protocol for the Single Cell 3′ Gene Expression assay. For each experimental sample (control, 3B, and 5B), live protoplasts were loaded into one channel of a Chromium Next GEM microfluidic chip along with barcoded gel beads with prepared master mix on Table 3.2 and partitioning oil. Reagents from the Chromium Single Cell 3′ v3.1 kit (10x Genomics) were used for cell capture and barcoding.

Table 3.2. Mastermix protocol for GEM generation

Mastermix (Reagents were added in order listed)	**8X (10% µl)**
RT Reagent B	165.0
Template Switch Oligo	20.8
Reducing Agent B	17.3
RT Enzyme C	76.8
TOTAL	279.8

The Chromium Controller device was employed to generate Gel Bead-In-Emulsion (GEM) droplets, each ideally containing a single cell and a single barcoded gel bead.

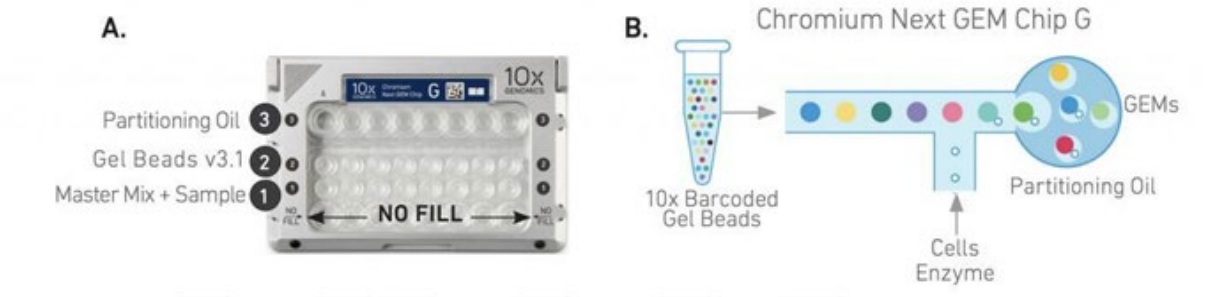

Figure 3.3. 10 Genomics single-cell-RNA-Sequencing library preparation. **A.** Template wells for loading for Partitioning oil, Gel Beads and mastermix + Sample. **B.** Cell enzyme participation and partitioning oil formation shown in GEMs for 10x Barcoded Gel Beads

Table 3.3. GEM beads RT incubation protocol

Lid Temperature	Reaction Volume	Run Time
53°C	125 µl	~55 min
Step	**Temperature**	**Time**
1	53°C	00.45.00
2	85°C	00.05.00
3	4°C	Hold

Within these nanoliter-scale GEM droplets, cells were lysed and messenger RNA (mRNA) molecules from each cell hybridized to a unique barcoded oligonucleotide primer on the gel bead. This primer contains a cell-specific barcode (to tag all transcripts from the same cell with an identical sequence), a unique molecular identifier (UMI) to label individual cDNA molecules, and a poly-dT tract to anneal to the poly(A) tails of mRNA.

After this process, GEMs that ensured uniformation and opacity in the channels, dispensed to the tube strips for 20 seconds using pipette tips to the incubation chambers with thermal cycler under circumstances of Table 3.3. Reverse transcription (RT) was carried out inside the droplets, converting mRNAs into barcoded complementary DNA (cDNA). As a result, cDNA from each cell acquired a cell-specific barcode and each transcript molecule a UMI during first-strand synthesis.

Table 3.4. Clean-up mixture protocol for Dynabeads for Reverse transcribed samples

DynabeadsCleanup Mix (Reagents were added in the order listed)	8X (10% µl)
Cleanup Buffer	1602
Dbeads MyOne SILANE	70
Reducing Agent B	44
Nuclease-free Water	44
TOTAL	1760

For clean-up procedure after RT has taken, 125 µl of recovery agent was applied to the samples and allowed to incubate for 2 minutes at room temperature, after which 125 µl of the recovery agent together with partitioning oil was gradually withdrawn. As per Table 3.4, the Dynabeads Cleanup mixture preparation completed, vortexed and 200 µl of it has been added to the sample, mixture by pipetting, and incubation has taken place at room temperature for 10 minutes. Subsequently, the mixture was re-homogenized by pipetting approximately five minutes after the initiation of the incubation to resuspend beads.

Table 3.5. Protocol for Elution Solution I

Elution Solution I (Reagents were added in the order listed)	1X (µl)	10X (µl)
Buffer EB	98	980
10% Tween 20	1	10
Reducing Agent B	1	10
TOTAL	100	1000

Elution Solution I prepared accordance to Table 3.5, then vortexed and briefly centrifuged. The solution was incubated for 10 minutes and thereafter positioned in the 10X Magnetic Separator in an elevated orientation until clarity was achieved. The supernatant was discarded. 300 µl of 80% ethanol were injected into the pellet on the magnet, and a wait of roughly 30 seconds. 200 µl of 80% ethanol poured into the pellet and allowed to sit for approximately 30 seconds. Afterwards, Ethanol was discarded. Subjected to brief centrifugation. Afterwards, positioned on the magnet at a low position. The residual ethanol was discarded and air-dried for approximately one minute. As result of this, Ethanol cleaned from the magnet. 35.5 µl of Elution Solution I swiftly added and stirred using a pipette, ensuring no bubbles were formed. Put in incubation for 2 minutes at room temperature. Solution was positioned on the magnet at a low position until it became clear.

After RT clean-up, the GEM emulsion was broken to release the barcoded cDNA from the oil phase as a result. Purified single-stranded cDNA then subjected to amplification via polymerase chain reaction (PCR) to generate sufficient quantities of cDNA for library construction. In order to prepare Amplification mixture, protocol shown in Table 3.6 has been followed. Then, PCR protocol has been carried out with following protocol on Table 3.7.

Table 3.6. Protocol of cDNA Amplification Reaction Mixture

cDNA Amplification Reaction Mix (Reagents were added in the order listed)	8X (10% µl)
Amp Mix	440
cDNA Primers	132
TOTAL	572

Table 3.7. cDNA Amplification PCR procedure protocol

Lid Temperature	Reaction Volume	Run Time
105°C	100 µl	~30-45 min
Step	**Temperature**	**Time**
1	98°C	00.03.00
2	98°C	00.00.15
3	63°C	00.00.20
4	72°C	00.01.00
5	15 cycles	
6	72°C	00.01.00
7	4°C	Hold

The procedure followed the standard 10x Genomics 3′ gene expression protocol. The amplified cDNA enzymatically fragmented to appropriate lengths and size selected. Fragmented cDNA ends were repaired and *A*-tailed, and sequencing adaptors (Illumina paired-end adapters) with sample indices were ligated. A final round of PCR enrichment has been performed to produce the indexed sequencing-ready library. Quality control (QC) of the libraries has been conducted using Qubit fluorometer in order to quantify the DNA concentration and an Agilent Bioanalyzer in order to assess fragment size distribution. These quality control confirmed that library fragments were of the expected size and that there was no significant contamination or degradation, ensuring suitability for high-throughput sequencing.

Prepared scRNA-seq libraries were then subjected to high-throughput sequencing. All libraries (for control and boron-treated samples) were sequenced on an Illumina NovaSeq 6000 platform by a commercial sequencing service (Gen Era Diagnostics A.Ş., Ankara). Sequencing was performed in paired-end mode to capture both the 3′ gene expression read and the 5′ cell barcode/UMI read for each cDNA fragment. Each sample library sequenced to a depth of approximately 100 million reads, corresponding to roughly 20,000 reads per cell for 5,000 captured cells. This sequencing depth has been chosen to ensure enough coverage of transcriptomes for even relatively low expressed genes. The raw sequencing data were output as base call (BCL) files, which were demultiplexed and converted to FASTQ format using the 10x Genomics Cell Ranger mkfastq pipeline (essentially a wrapper around Illumina's bcl2fastq). The result for each sample was a set of paired-end FASTQ files ready for downstream bioinformatic

analysis.

3.4. Data Analysis

After sequencing, the 10x Genomics Cell Ranger software and the Seurat R package have been applied to process and analyze the single-cell RNA-seq data. Sequencing reads were initially preprocessed and aligned using Cell Ranger (v3.0.0, 10x Genomics). The cellranger count pipeline has been executed for each sample to perform reference alignment and gene counting. At this step reads have been aligned to the *Arabidopsis thaliana* reference genome (TAIR10 assembly) utilizing the STAR aligner incorporated within Cell Ranger. Cell Ranger filtered low-quality reads, identified valid cell barcodes and UMIs, and then generated a gene-cell count matrix for each sample containing UMI counts.

For comparative analysis across conditions, the count matrices from all samples (control, 3 mM B, and 5 mM B) were aggregated using the cellranger aggr function This step integrated the datasets and normalized the read depth across samples, ensuring that each cell possessed a comparable average number of reads, thereby reducing potential biases arising from minor variations in sequencing depth among the libraries [1].

The aggregated digital gene expression matrix then imported into R for higher-level analysis using Seurat (v4.x) which is a highly known and useful toolkit for single-cell genomics. In Seurat, standard quality control (QC) filtering has been applied to remove low-quality cells and technical artifacts. Cells with an extremely low number of detected genes (potential empty droplets) or an excessively high number of genes/UMIs (potential doublets or multiplets) were excluded. Likewise, cells with a high percentage of mitochondrial gene reads were filtered out. This often indicates damaged or dying cells [9]. After QC filtering, a total of several thousand high-quality single cells remained for downstream analysis. The raw UMI counts for each cell were then normalized and log-transformed using Seurat's global-scaling normalization (NormalizeData function), which converts counts to a relative measure (counts per 10,000, followed by log10 transformation) to account for differences in sequencing depth per cell [60] The data were then normalized to eliminate the unwanted sources of variation.

Next, feature selection methods were performed in order to identify genes showing high cell-to-cell variance. Seurat's FindVariableFeatures method was used to detect a set of highly variable genes. These variable genes were used as input for principal component analysis (PCA).

PCA has been conducted to reduce the data dimensionality. the expression matrix transformed into a set of orthogonal principal components (PCs), each capturing a portion of the variance in gene expression. The principal components were analyzed to determine the quantity to maintain for clustering, either by identifying the "elbow" in the variance explained plot or via statistical testing. In the analysis, the first ~15 principal components were selected as they captured the majority of meaningful variance in the dataset while excluding noise.

Using the retained principal components, we performed graph-based clustering of the cells. A k-nearest neighbors' graph was constructed (via Seurat's FindNeighbors function) in the PCA space, and then the Louvain algorithm was applied (FindClusters function) to group cells into clusters based on transcriptomic similarity. The clustering resolution parameter was tuned to obtain a suitable number of clusters that balanced detail and interpretability. This unsupervised clustering yielded distinct groups of cells, each representing cells with similar expression profiles. Importantly, the data from all three conditions were analyzed together in an integrated manner, meaning that clustering was driven by overall gene expression patterns rather than pre-labeling by treatment, this allowed direct comparison of cell populations across control and severe boron treatments within the same low-dimensional space [26].

In order to visualize the clusters, a two-dimensional embedding of the cells was generated using Uniform Manifold Approximation and Projection (UMAP). The UMAP algorithm then had been applied to the principal component (PC) space to produce a scatter plot in which each point corresponds to a single cell and points had been positioned such that cells with similar expression profiles lie close together. The UMAP plots displayed cells according to their cluster identity, and by treatment group for the assessment of mixing. This allowed a visual representation of cluster separation and the intermixing of cells from different treatment conditions resulting in successful integration. Clusters identified by cell type identity rather than treatment, as cells from control, 3B, and 5B conditions mixed within the same clusters. This suggests that our clustering reflected cell-type differences rather than conditions.

Cell type identification was then carried out by examining the gene expression patterns of each cluster. For each cluster, we obtained lists of marker genes using Seurat's FindAllMarkers function, which finds genes significantly enriched in a given cluster compared to others. These cluster marker genes were compared against known *Arabidopsis thaliana* root cell-type markers reported in the literature and earlier single-cell atlases [57].

By matching the signature genes of each cluster to well-characterized markers, Clusters have been assigned to a specific root cell type or tissue layer. Through this approach, clusters have been annotated as representing major root tissues such as the root cap (including columella and lateral root cap), epidermis (trichoblasts and atrichoblasts), cortex, endodermis, and various stele cell types (pericycle, protoxylem/metaxylem, phloem). In cases where a cluster's identity that uncertain, multiple marker genes were used in combination to make an informed assignment. All primary root cell types have been found and represented among the clusters, resulting as successful capture of diverse cell populations.

Finally, to investigate the effects of severe boron toxicity at the single-cell level, we performed differential gene expression analysis (DGE) between treatment conditions within each identified cell type. In practice, this involved sub-setting the combined dataset by cluster (cell type) and comparing gene expression in cells from the boron-treated groups (3B or 5B) against cells from the control group. Using statistical testing, Genes have been identified that were significantly upregulated in boron-exposed cells for each cell type cluster. This analysis revealed the cell type–specific transcriptional responses to severe excess boron, highlighting which genes and pathways have been activated by severe boron toxicity based on cell populations. The lists of differentially expressed genes (DEGs) were later subjected to functional enrichment analyses (e.g., Gene Ontology categories and KEGG pathways) to interpret the biological processes affected by high boron in each cell type (details of these analyses are provided in the Results chapter). All data analysis steps were conducted using R (v4.x) and Python and visualization of the results performed through Seurat's plotting functions and custom scripts [57]. The combination of these computational approaches allowed a comprehensive dissection of how *Arabidopsis thaliana* root cells, at single-cell level, respond to and cope with the stress of severe boron toxicity.

4. RESULTS

4.1. Single-Cell Transcriptome Profiling and Clustering of Root Cells Under Boron Stress

To investigate cell-specific responses to boron toxicity, single-cell RNA sequencing performed on *Arabidopsis thaliana* root cells from control, 3 mM B, and 5 mM B conditions. Roots were enzymatically dissociated into protoplasts and captured using the 10x Genomics platform, yielding transcriptomes for thousands of cells. After sequencing, applied standard quality control and normalization procedures using the Seurat pipeline in R. The gene expression data from all three conditions were then combined for integrated analysis, allowing direct comparison of cell states across treatments of 3mM B and 5mM B. Principal component analysis (PCA) was used for initial dimensionality reduction, and the top principal components captured the major variance in the dataset.

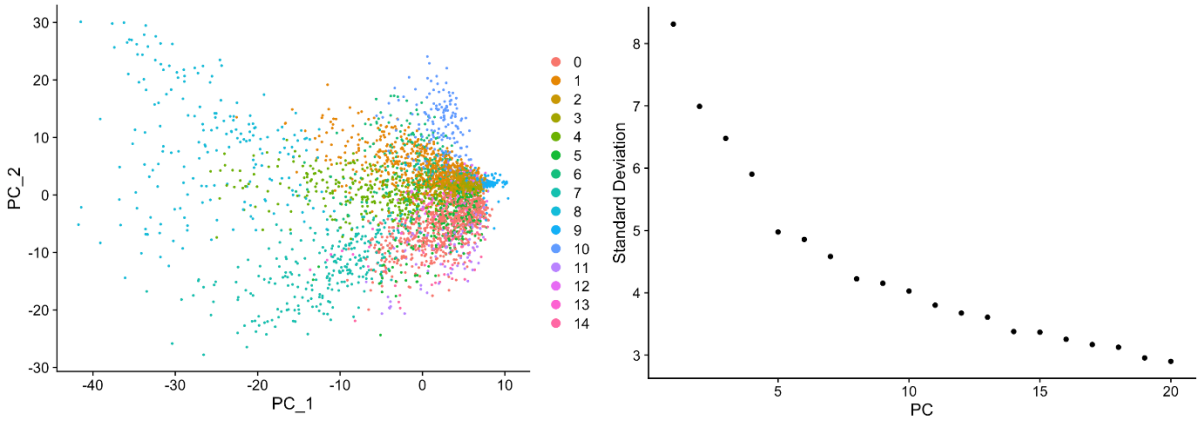

Figure 4.1. PC_1 and PC_2 with graph of 15 clusters have been shown in the first part in the figure. The second part of the figure represents the plot of showing the standard deviation of principal components (PCs). The first ~15 PCs encompass the majority of variance, as indicated by the inflection point around PC15.

First part of figure, PCA scatter plot explains how many groups based on gene expression levels of cell groups are clustered. Each group from 0-14 has significantly similar gene expression levels therefore, they are grouped together in a cluster group. The graphical representation is in scatter plot colored in order to distinguish groups. Second part of the figure, scree plot of principal components from the same dataset represents the standard deviation of each component. Variance explained by each PC and inflection point around PC15 is observed. The first 15 PCs were used since the elbow, meaningful variation data is represented until PC15 and the rest was not significant.

Based on the PCA results (as shown in Figure 4.1), the first 15 principal components for downstream clustering and visualization were retained. Next, a two-dimensional Uniform Manifold Approximation and Projection (UMAP) to visualize the cell population structure has been generated. Using the Louvain graph-based algorithm on the PCA space, **16 distinct clusters** of cells, each representing groups of cells with similar transcriptomic profiles has been identified.

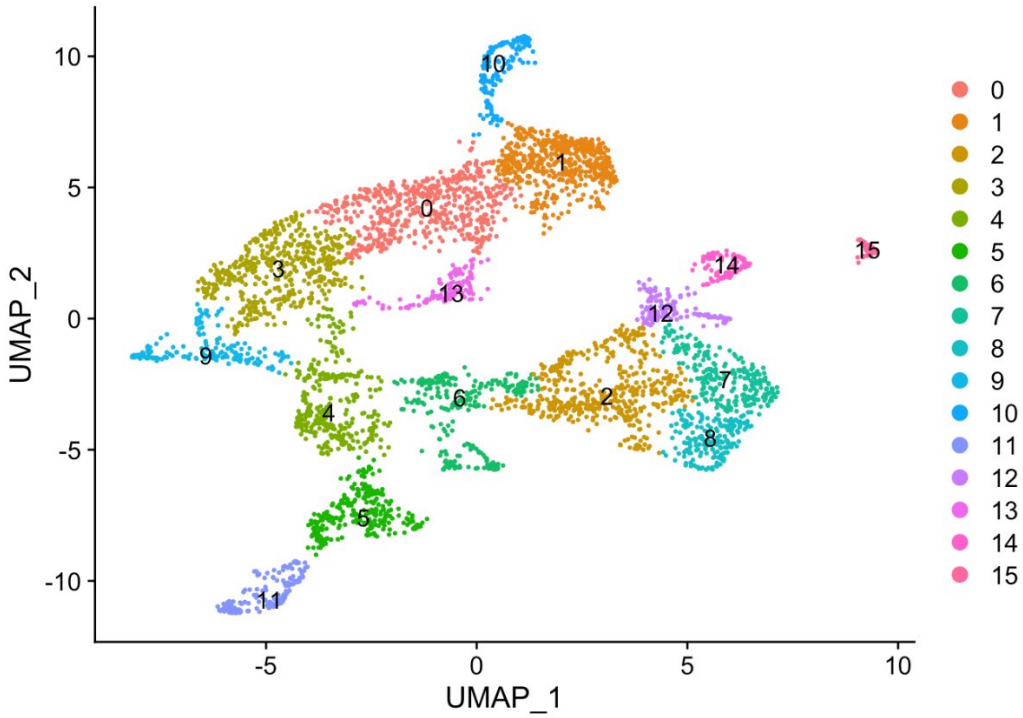

Figure 4.2. UMAP demonstration of all sequenced root cells colored by non-defined cluster (Louvain algorithm). Sixteen clusters (0–15) are labeled, showing distinct groupings of transcriptionally similar cells.

The UMAP plot (Figure 4.2) reveals well-separated clusters, indicating clear transcriptional differences between groups of cells. Notably, these clusters were derived without using treatment information, meaning cells from control and boron-treated samples not defined and mixed within the same clusters rather than forming separate treatment-specific clusters. This suggests that the primary drivers of variation in our data are cell identity (cell type) rather than treatment alone.

4.2. Identification of Root Cell Types and Cluster Relationships

To interpret the biological identity of each cluster, it has been examined the expression of well-characterized *Arabidopsis thaliana* root cell marker genes in our dataset. Afterwards, we compiled a set of known marker genes for each major root tissue (from classical cell-type studies and recent single-cell atlases of the root, e.g., Brady et al., 2007; Denyer et al., 2019) and overlaid their expression on the UMAP. Each cluster displayed a distinct marker gene signature, allowing us to assign it to a specific cell type or region of the root.

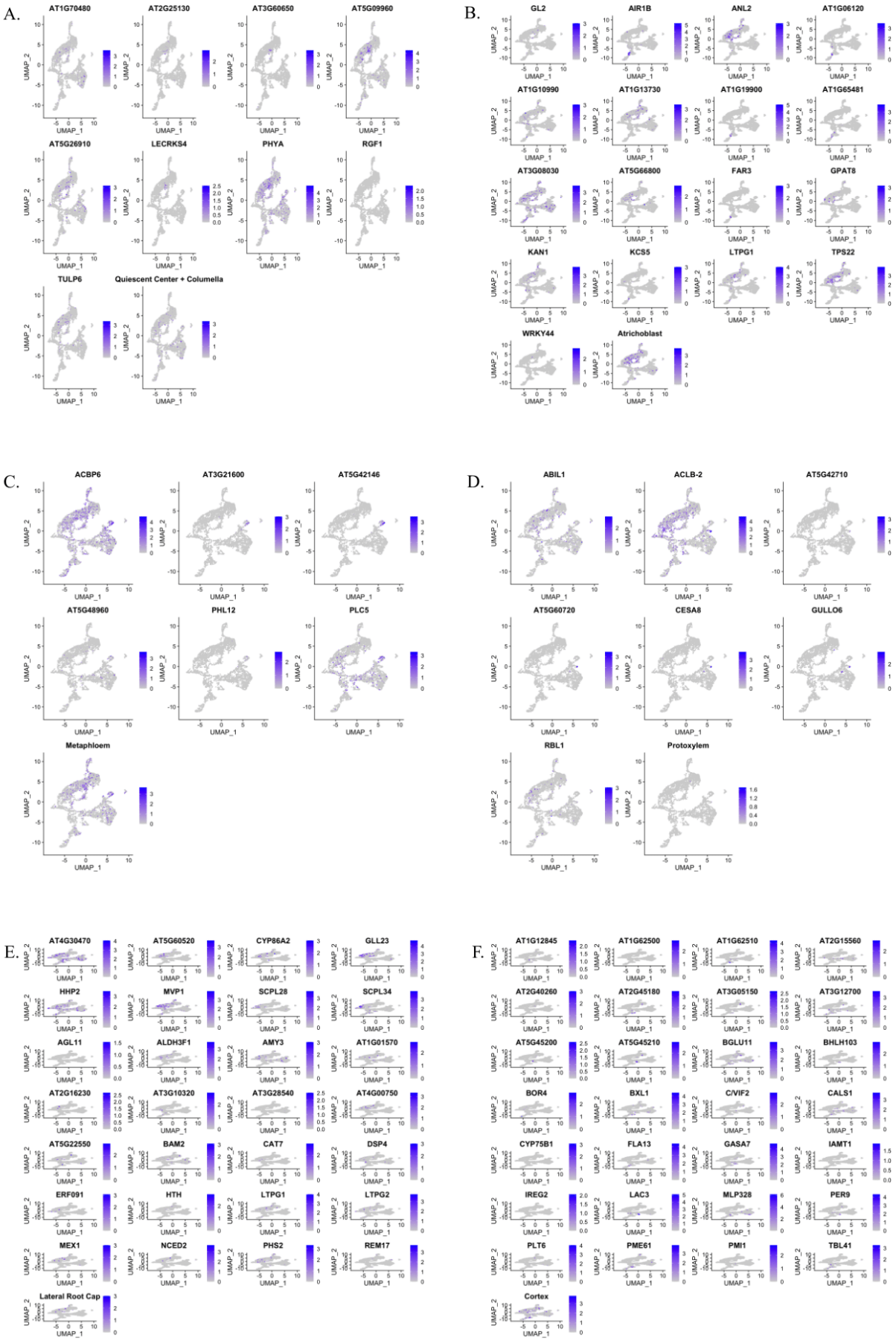
A.
AT1G70480
AT2G25130
AT3G60650
AT5G09960
AT5G26910
LECRKS4
PHYA
RGF1
TULP6
Quiescent Center + Columella
B.
GL2
AIR1B
ANL2
AT1G06120
AT1G10990
AT1G13730
AT1G19900
AT1G65481
AT3G08030
AT5G66800
FAR3
GPAT8
KAN1
KCS5
LTPG1
TPS22
WRKY44
Atrichoblast
C.
ACBP6
AT3G21600
AT5G42146
AT5G48960
PHL12
PLC5
Metaphloem
D.
ABIL1
ACLB-2
AT5G42710
AT5G60720
CESA8
GULLO6
RBL1
Protoxylem
E.
AT4G30470
AT5G60520
CYP86A2
GLL23
HHP2
MVP1
SCPL28
SCPL34
AGL11
ALDH3F1
AMY3
AT1G01570
AT2G16230
AT3G10320
AT3G28540
AT4G00750
AT5G22550
BAM2
CAT7
DSP4
ERF091
HTH
LTPG1
LTPG2
MEX1
NCED2
PHS2
REM17
Lateral Root Cap
F.
AT1G12845
AT1G62500
AT1G62510
AT2G15560
AT2G40260
AT2G45180
AT3G05150
AT3G12700
AT5G45200
AT5G45210
BGLU11
BHLH103
BOR4
BXL1
C/VIF2
CALS1
CYP75B1
FLA13
GASA7
IAMT1
IREG2
LAC3
MLP328
PER9
PLT6
PME61
PMI1
TBL41
Cortex

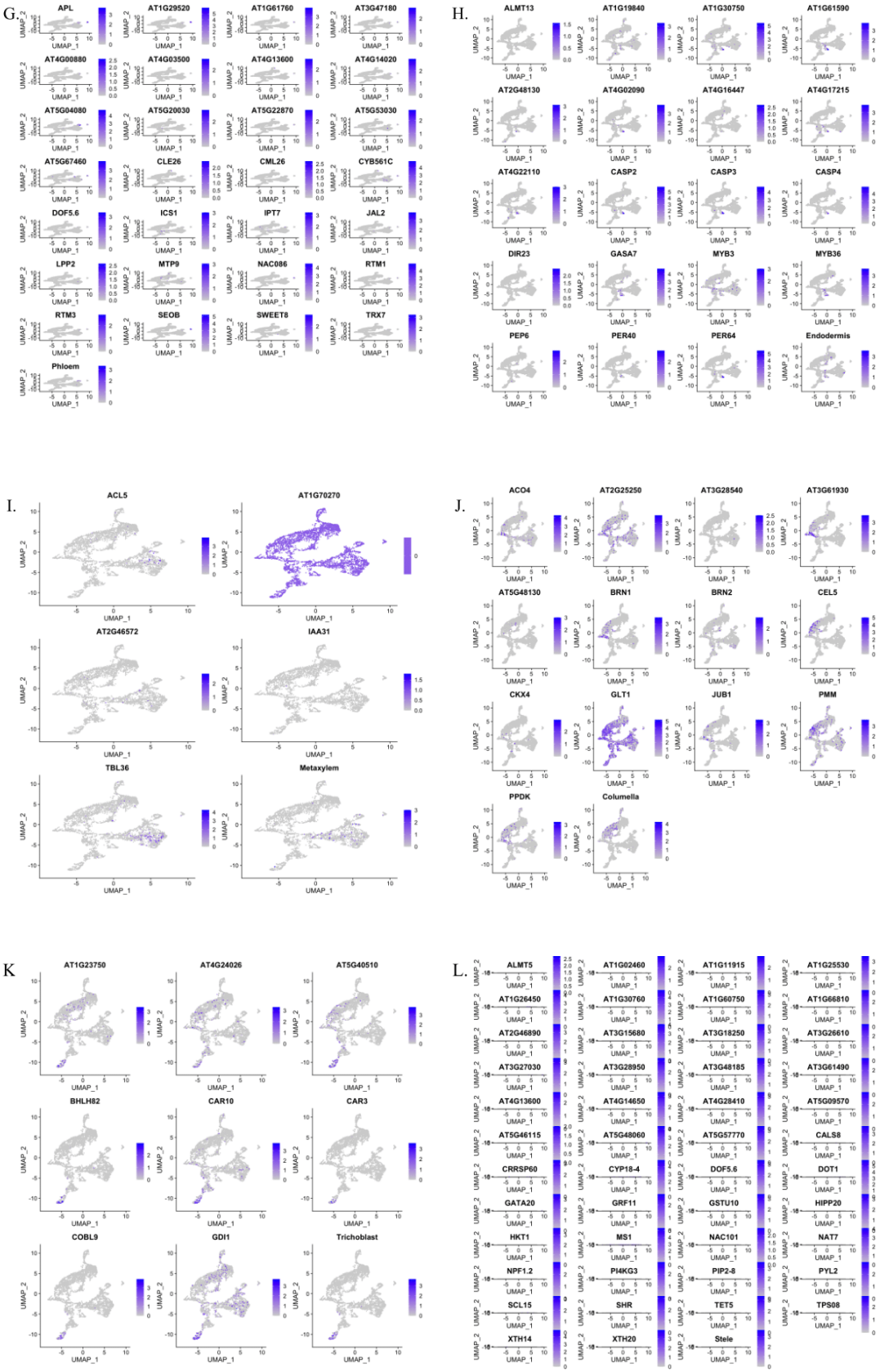

Figure 4.3. Representation of expression of genes that is known as marker genes for the *Arabidopsis thaliana* root cells. Identified clusters shown as; **A.** Quiscent Center + Columella cluster, **B.** Atrichoblast cluster, **C.** Metaphloem cluster, **D.** Protoxylem cluster, **E.** Lateral Root Cap cluster, **F.** Cortex cluster, **G.** Phloem cluster, **H.** Endodermis cluster, **I.** Metaxylem cluster, **J.** Columella cluster, **K.** Trichoblast cluster, **L.** Stele cluster

One of the clusters showed high levels of *GLABRA2* (*GL2*) expression which is a transcription factor that regulates epidermal cell fate and are required for non-hair (atrichoblast) cell differentiation in the root epidermis [44, 40].

It has been observed that one of the clusters exhibited strong expression of *ALUMINUM-ACTIVATED MALATE TRANSPORTER 13* (*ALMT13*)—a transporter whose mRNA is highly restricted to the endodermal layer and is routinely used as an endodermis marker in recent single-cell atlases [16]. The co-enrichment of *ALMT13* together with other endodermal hallmark genes such as *PER64* [54] provided independent confirmation that the cluster corresponded to the root endodermis, strengthening our cell-type assignment based on marker-gene signatures.

Metaxylem cluster – cells in this group showed strong expression of *ACAULIS 5* (*ACL5*), *AT2G46572*, and *TBL36*. *ACL5* encodes a thermospermine synthase required for later stages of vessel maturation and secondary-wall thickening [29], while *TBL36* and other *TBL* family members participate in secondary-wall acetylation [74]. Their co-expression, together shows no correlation for early protoxylem genes, marks these cells as differentiating metaxylem.

Protoxylem cluster – a neighboring group instead expressed *ABL1*, *ACLB-2*, *CESA8*, *RBL1*, and related wall-biosynthesis genes. *ABL1* and *ACLB-2* encode acyl-CoA ligases implicated in lignin monomer activation, whereas *CESA8* is a cellulose-synthase isoform specific to primary xylem fibers [63]. The presence of these early xylem factors, combined with lower *ACL5* signal, identifies this cluster as protoxylem. Taken together, the mutually exclusive expression of the metaxylem markers (*ACL5*/*TBL36*/*AT2G46572*) and protoxylem markers (*ABL1*/*ACLB-2*/*CESA8*/*RBL1*) confirms that the two adjacent clusters correspond to successive developmental stages of xylem vessel differentiation, therefore validating these clusters as xylem-associated clusters in our dataset.

The conductive phloem cluster was marked by co-expression of *ALTERED PHLOEM DEVELOPMENT* (*APL*), *SEOB*, *SWEET8*, and the cytokinin-biosynthetic gene *IPT7*, a signature combination characteristic of mature sieve elements and their companion cells [20, 6]. An adjacent cluster instead accumulated *ACBP6*, *PHL12*, and *PLC5*, matching the marker set recently reported for differentiating metaphloem strands [16], thereby confirming its identity.

Lateral root-cap cluster was defined by the concerted expression of *CYP86A2*, *LTPG1/2*, *HHT*, and *SCPL34*—genes that are highly enriched in mature lateral-root-cap cells in recent single-cell atlases [55, 56]. This marker combination identifies the cluster as lateral root cap.

The cortex has been identified expression of *β-XYLOSIDASE 1* (*BXL1*), *FLA13*, and *LACCASE 3* (*LAC3*) together with the pectin-modifying enzyme *PME61*. This marker set is consistently reported as cortex-specific in *Arabidopsis thaliana* root single-cell atlases [16, 58] confirming that the corresponding cluster group aligns with cortex region.

Trichoblast (root-hair) cluster identified by co-localized expression of *COBRA-LIKE 9* (*COBL9*), the basic helix–loop–helix factor *BHLH82*, and the trafficking regulator *GDI1*, together with root-hair membrane proteins *CAR3/10*. This marker co-expression is significant for differentiating root-hair cells based on *Arabidopsis thaliana* single-cell atlases [8, 16], confirming the cluster's identity as trichoblasts.

The stele cluster was defined by the co-expression of the stele/vascular-initial markers *SHORT-ROOT* (*SHR*), *SCL15*, and *DOF5.6*, together with solute transporters *PIP2-8* and *HKT1*, and the aluminum-activated malate channel *ALMT5*.

The columella cluster shown by co-expression of the NAC-domain regulators *BRN1*/*BRN2* together with *GLT1* and *ACO4*. This marker combination repeatedly reported as columella-specific in *Arabidopsis thaliana* root atlases [3, 16]. It confirms that the corresponding group represents the central columella root-cap cells.

Using this marker-guided approach with conjunction of published single-cell root atlases for reference [16, 55], annotated all 16 clusters with biologically meaningful identities. The clusters spanned all major regions of the *Arabidopsis thaliana* from the root and the quiescent center through the outer epidermis underlying cortex and endodermis layers, and into the central stele tissues. Notably, the quiescent center (QC) did not form a separate cluster; instead, the QC cells were found within the columella cluster, parallel with their close spatial and developmental association with columella cells. This significant identification of cell types in our single-cell data was essential for downstream analysis, as it provided the foundation for examining how each specific cell type responds to boron toxicity. Knowing the cluster identities allowed us to interpret differential gene expression under high boron conditions in the context of specific tissues, revealing cell type–specific stress responses rather than just generic changes in arbitrary clusters.

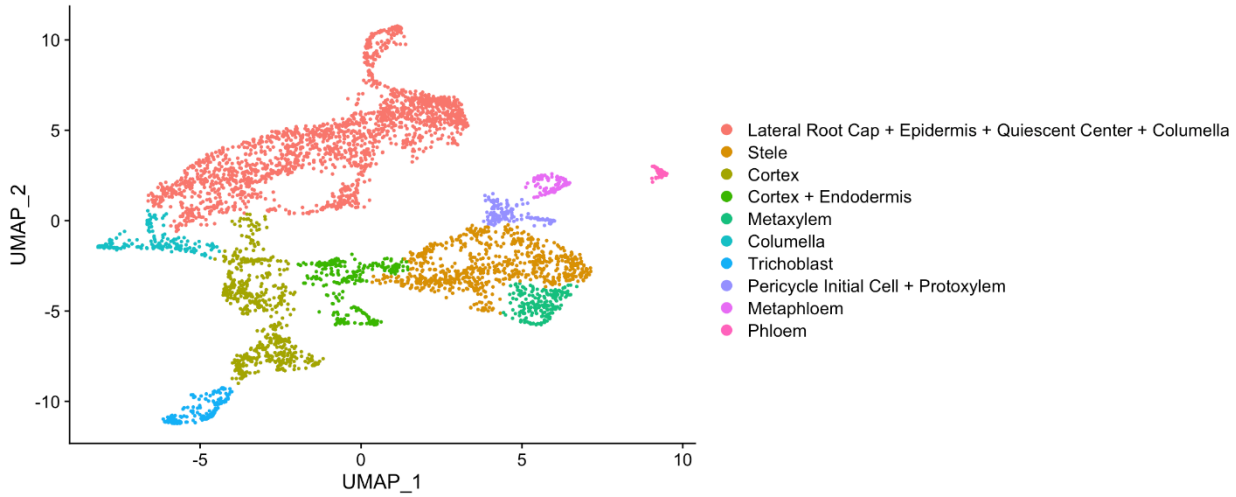

Figure 4.4. UMAP projection with clusters colored by their annotated cell type identity.

Each color corresponds to a specific root cell type or tissue (e.g., cortex, endodermis, root cap, trichoblast, xylem, phloem, etc.), confirming that the 16 transcriptional clusters represent all major root cell types. Note that the quiescent center cells are included in the root cap/columella group due to their small number and transcriptional similarity to those cells.

Overall, the clustering and marker analysis indicates that our single-cell dataset encompasses a comprehensive atlas of Arabidopsis root cell types, providing a solid foundation for comparing how each cell type responds to excess boron as shown in Figure 4.4.

4.3. Cell Population Distribution Under Control and Boron Treatment Conditions

Having defined the cell type clusters, next examined how the boron treatments affected the representation of these cell populations. It has been visualized the UMAP with cells colored by their treatment origin (control vs 3 mM B vs 5 mM B) to see if any treatment caused cells to cluster separately or altered the distribution of cells among clusters.

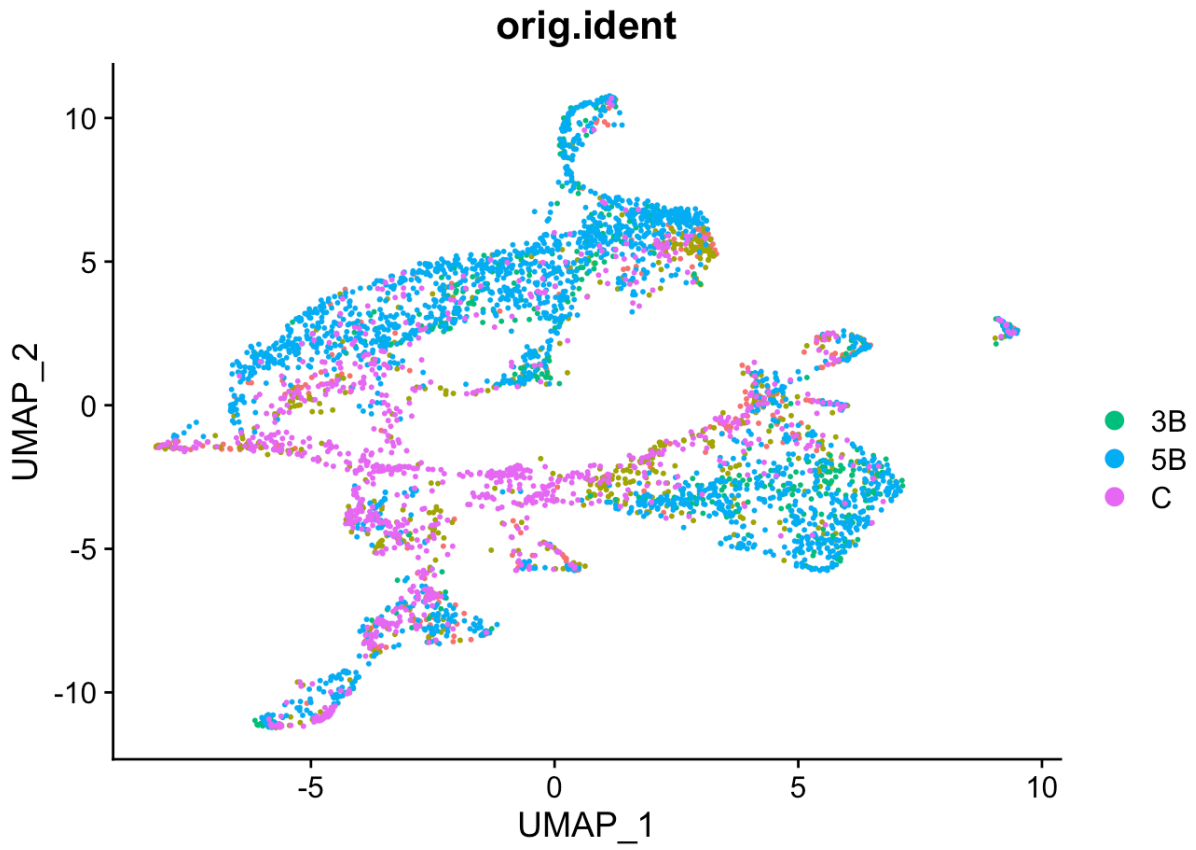

Figure 4.5. UMAP projection of representation of all cell groups, not specified in cell types, colored by Control group, 3 mM Boron and 5 mM Boron Treatment conditions.

Pink points correspond to Control (C) cells, green to 3 mM B (3B), and blue to 5 mM B (5B). Cells from all conditions are intermingled within each cluster, indicating that clusters are defined by cell type rather than treatment.

As shown in Figure 4.5, cells from the control (C, pink) and high-boron treatments (3B in green, 5B in blue) are largely overlapping on the UMAP. Every cluster contains a mixture of control and treated cells, and there are no new clusters that consist of only treated cells. This demonstrates that boron toxicity did not produce entirely novel cell states at the clustering level; instead, the stress is manifest as changes in gene expression within the established cell type clusters.

Although the overall clustering structure remained the same, it was observed subtle shifts in the proportion of cells from each condition in certain clusters. For example, the epidermal/root cap clusters contained slightly fewer 5 mM B cells relative to control, whereas some inner tissue clusters (notably the cortex and endodermis) showed a modest increase in representation by 5 mM B-treated cells. This trend suggests that under severe boron stress, outer cell layers might be more adversely affected, while inner cortical cells may persist or accumulate to a greater extent.

It is important to note that our experimental design captured snapshot cell populations after treatment, and all major cell types were still present under both 3 mM and 5 mM B conditions. Thus, high boron exposure may influence the abundance or transcriptional activity of certain cell types.

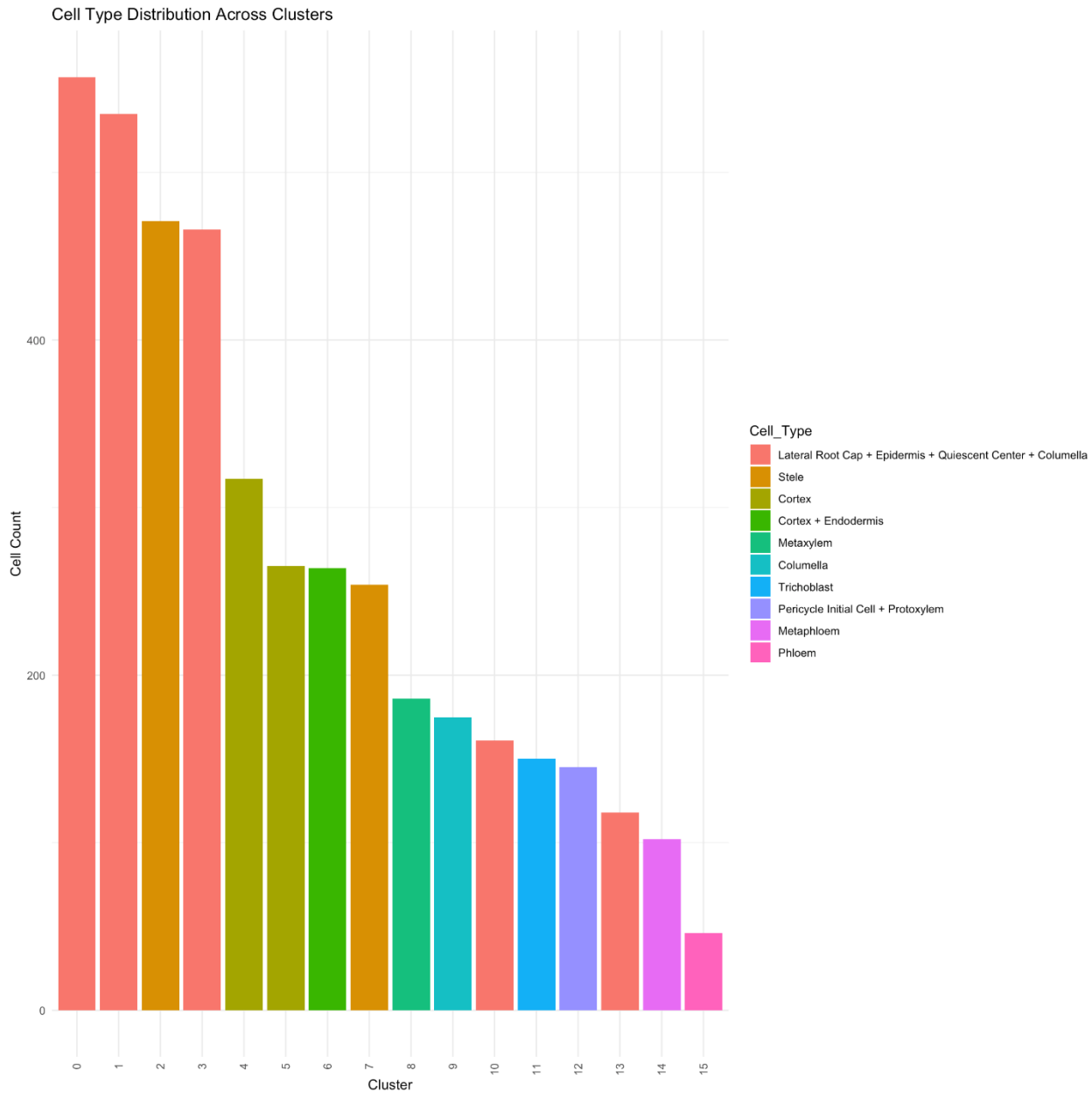

Figure 4.6. Column graph representation of cell count yield per cluster. Cell types that are identified shown with colors and cluster numbers shown in the x-axis of the graph as 15. Cell count represented as y-axis as yield.

A summary of cell yield per cluster per condition as shown in Figure 4.6 confirms that each cluster contains cells from all conditions, with only moderate differences in the fraction of cells contributed by 3B or 5B treatments compared to control. These results indicate that boron toxicity operates through transcriptional reprogramming within cells rather than wholesale loss

or gain of specific cell populations.

4.4. Cell Type–Specific Transcriptomic Responses to Severe Boron Toxicity

Next analyzed section was differential gene expression in each cluster to uncover how each cell type responds to excess boron at the molecular level. For each cluster (cell type), has been identified genes that were significantly upregulated under boron treatment conditions (3 mM or 5 mM B) compared to control. This single-cell differential expression approach allows us to pinpoint stress-responsive genes in a cell-type–resolved manner. Table 4.1 summarizes the number of upregulated genes detected in each cell type cluster at 3 mM B and at 5 mM B.

Several clear patterns emerged. At 3 mM B (moderate excess), relatively few clusters showed large transcriptional changes – notably, the root cap/lateral root cap cluster (which includes the outermost root tip cells) exhibited the strongest response with approximately 258 genes upregulated, while most other cell types had only a handful of genes induced (for instance, cortex cells had 22 genes upregulated, and root hair cells (trichoblasts) showed only 2 genes upregulated at 3 mM). By contrast, at 5 mM B (severe excess) the number of induced genes was much higher in several clusters. The cortex cluster showed the greatest response at 5 mM, with 165 genes upregulated, indicating a dramatic activation of stress responses in cortical cells under extreme boron toxicity. The columella (central root cap) cells likewise had a substantial response at 5 mM (76 upregulated genes, whereas they had essentially no significant changes at 3 mM).

Endodermis-associated cells (cortex/endodermis interface cluster) also began responding at 5 mM (28 genes upregulated at 5 mM compared to 0 at 3 mM). The root cap cluster that was strongly activated at 3 mM still showed many induced genes at 5 mM (70 genes, though fewer than at moderate stress). Interestingly, the stele cells (which include pericycle and vascular initials) had a moderate number of genes induced under both conditions (around 50 genes at 3 mM and 38 at 5 mM), suggesting the central vascular cylinder carries a response even to moderate stress and maintains it. In contrast, fully differentiated vascular tissues such as mature xylem and phloem exhibited little or no differential expression in our data. No significant upregulated genes were detected in the metaxylem, metaphloem, or phloem cluster under either 3 mM or 5 mM B. This indicates that those cells, once differentiated or do not respond transcriptionally to boron stress or the response is below our detection threshold.

Overall, these results demonstrate that different root cell types have markedly different sensitivities and response magnitudes to boron toxicity at the gene expression level. Outer cell

layers (root cap and epidermis) are activated even at moderate excess B, presumably serving as an early defense barrier, whereas inner cortical and columella cells require more extreme B stress to trigger large-scale transcriptomic changes.

Table 4.1. Number of significantly upregulated genes (DEGs) in each root cell type cluster

Clusters	Conditions	
	3B	5B
Columella	0	76
Cortex	22	165
Cortex_Endodermis	0	28
Lateral Root Cap + Epidermis + Quiescent Center + Columella	258	70
Metaphloem	0	0
Metaxylem	0	0
Phloem	0	0
Pericycle Initial Cell + Protoxylem	0	0
Stele	50	38
Trichoblast	2	18

Cell types with no detected DEGs under a condition are indicated with 0. Outer root cap/epidermal cells show a strong response at 3 mM, while cortex and columella responses dominate at 5 mM. Vascular tissues (xylem/phloem) show minimal changes. *(The cluster labeled "Lateral Root Cap + Epidermis + QC + Columella" represents the combined outer root tip region, including the quiescent center; see text. Columella cells are also partly represented in a separate cluster.)*

4.5. GO and KEGG

To further interpret these changes, carried out with Gene Ontology (GO) and Kyoto Encyclopedia of Genes and Genomes (KEGG) pathway enrichment analysis on the sets of upregulated genes for each cluster. This analysis revealed that each cell type activates distinct biological processes in response to boron stress, aligning with their functional roles in the root. Several common themes emerged across the enriched GO terms.

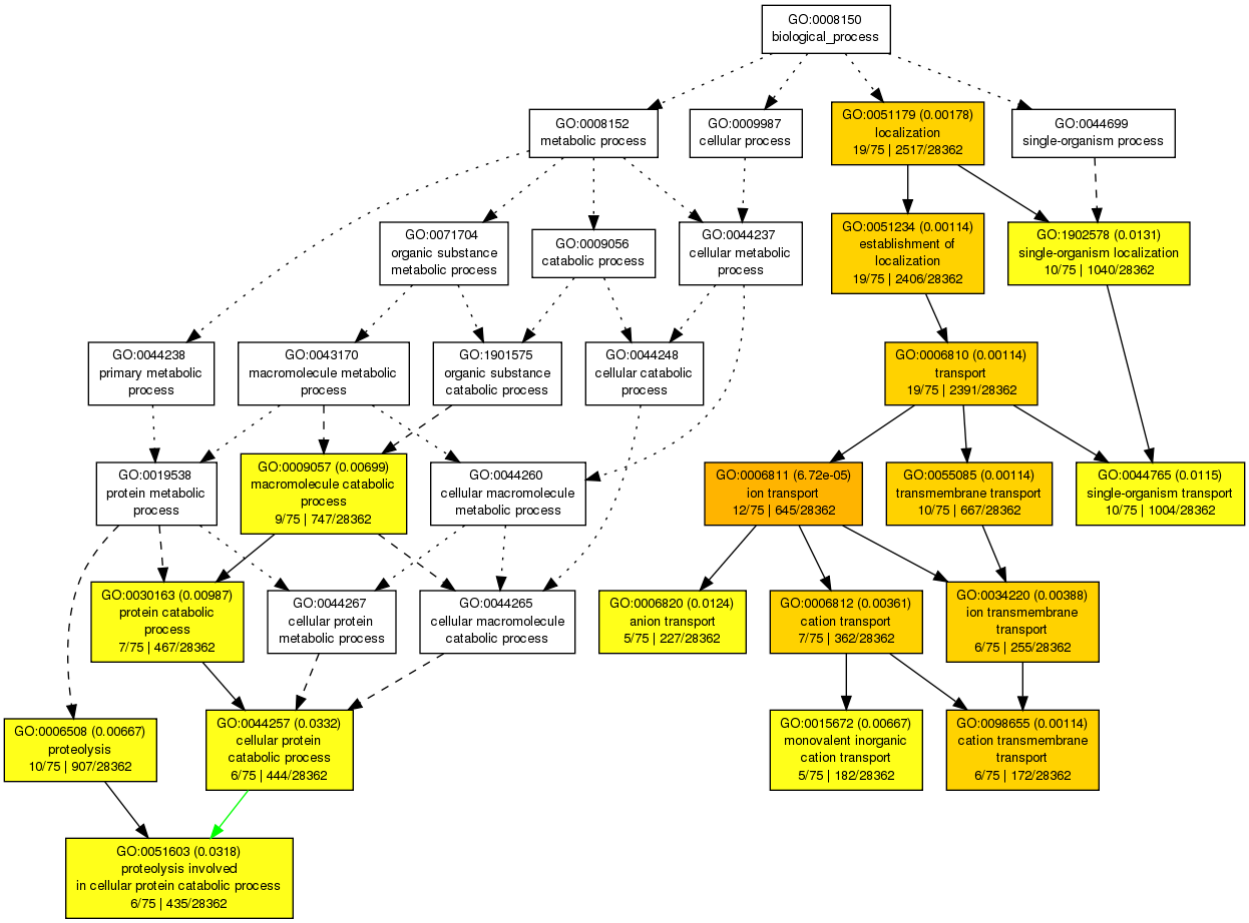

Figure 4.7. Columella cells GO analysis schema for Biological Process under 5mM Boron toxicity

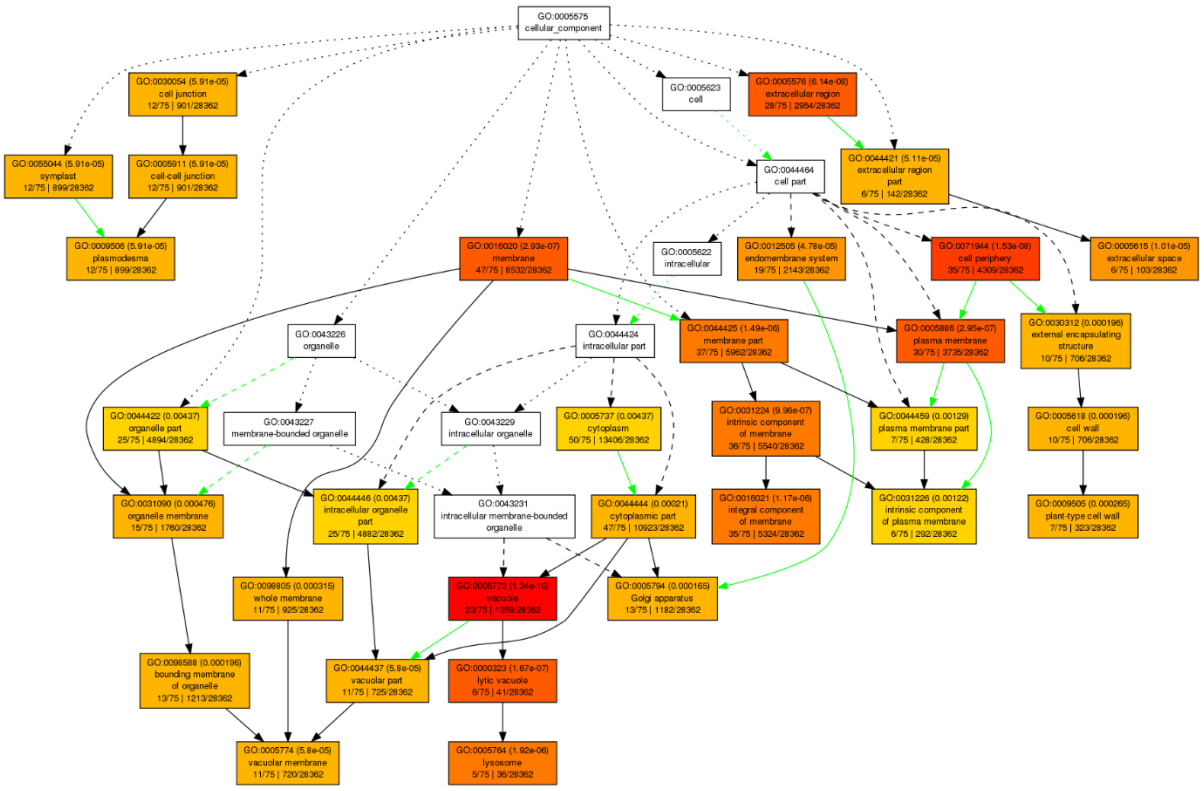

Figure 4.8. Columella cells GO analysis schema for Cellular component under 5mM Boron toxicity

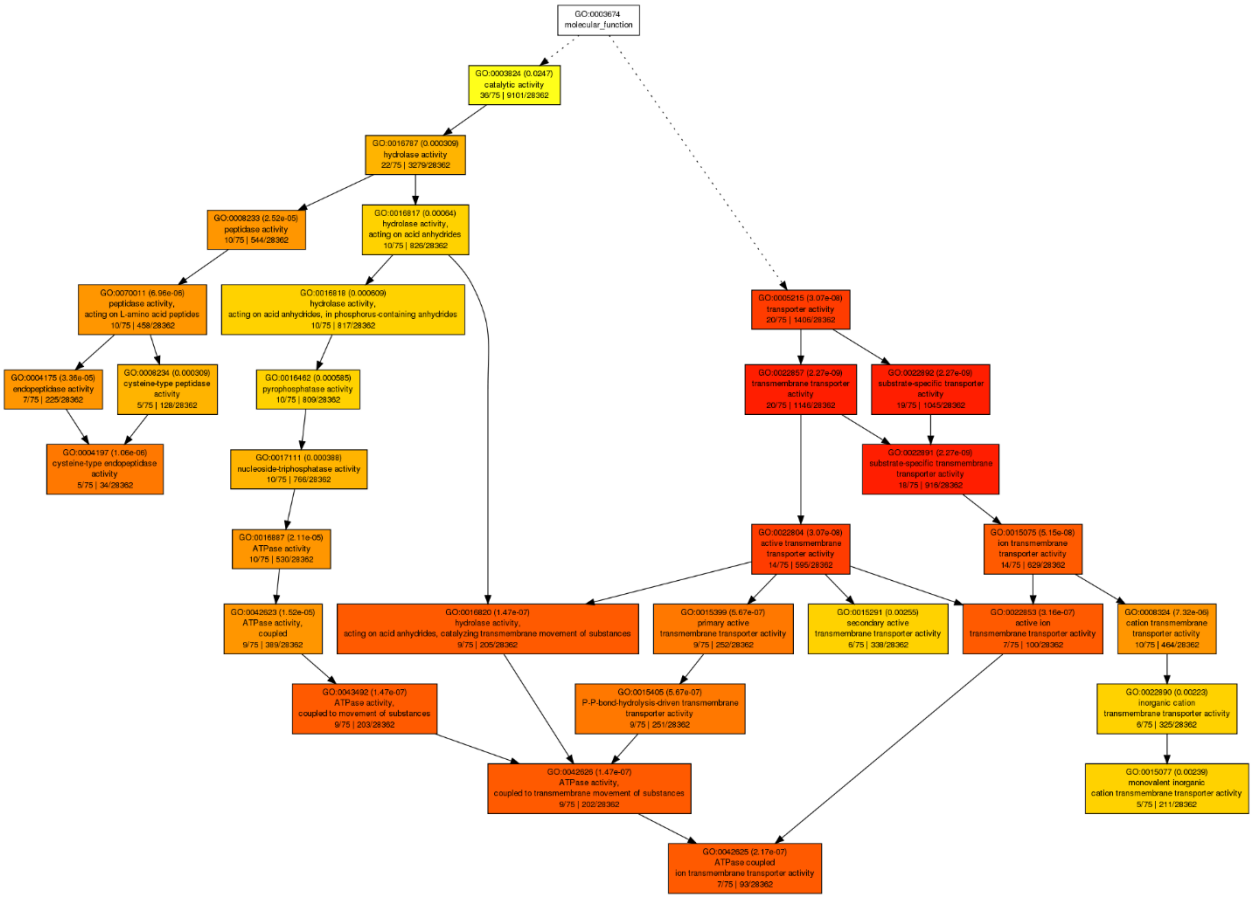

Figure 4.9. Columella cells GO analysis schema for Molecular Function under 5mM Boron toxicity

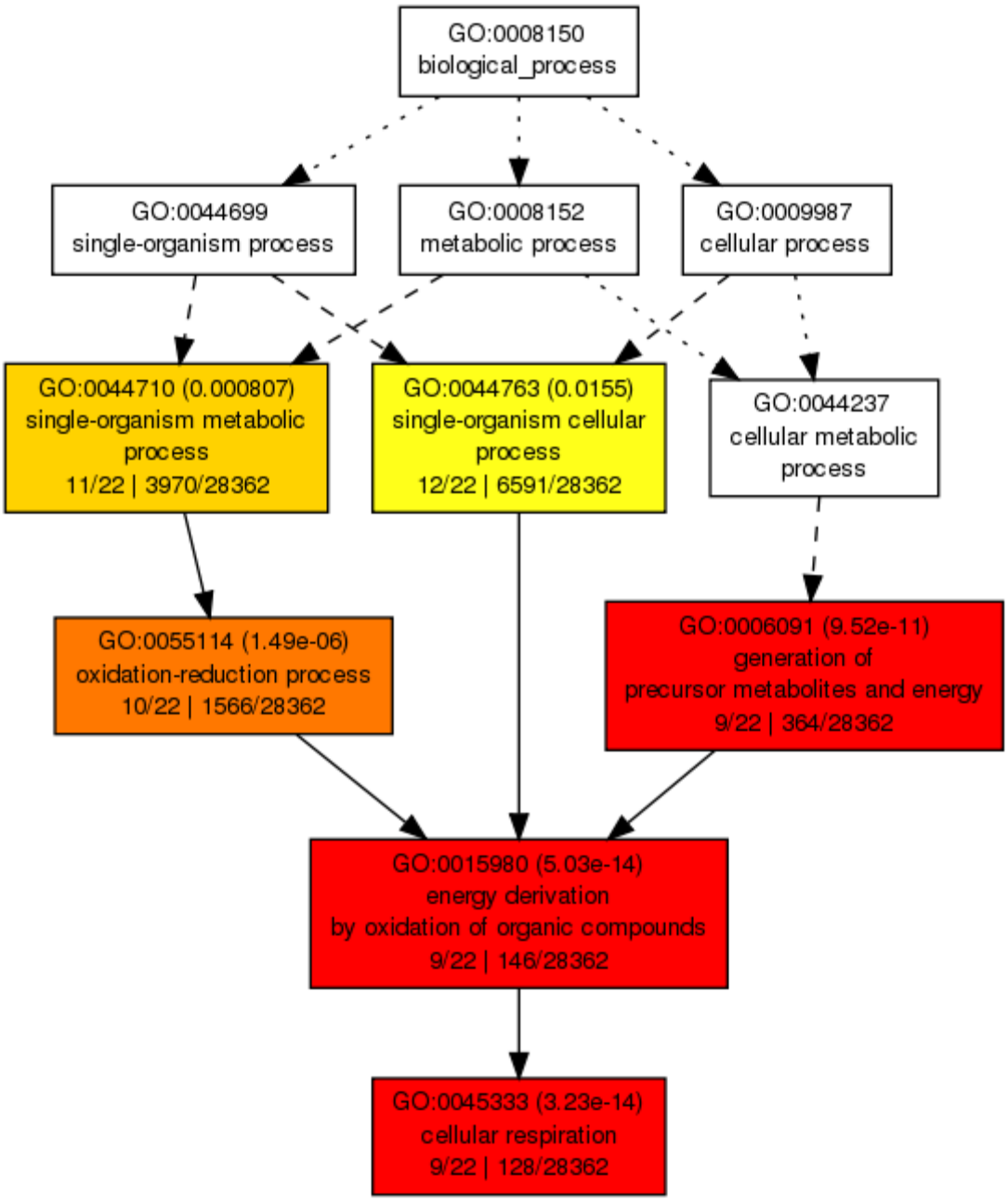

Figure 4.10. Cortex cells GO analysis schema for Biological Process under 3mM Boron toxicity

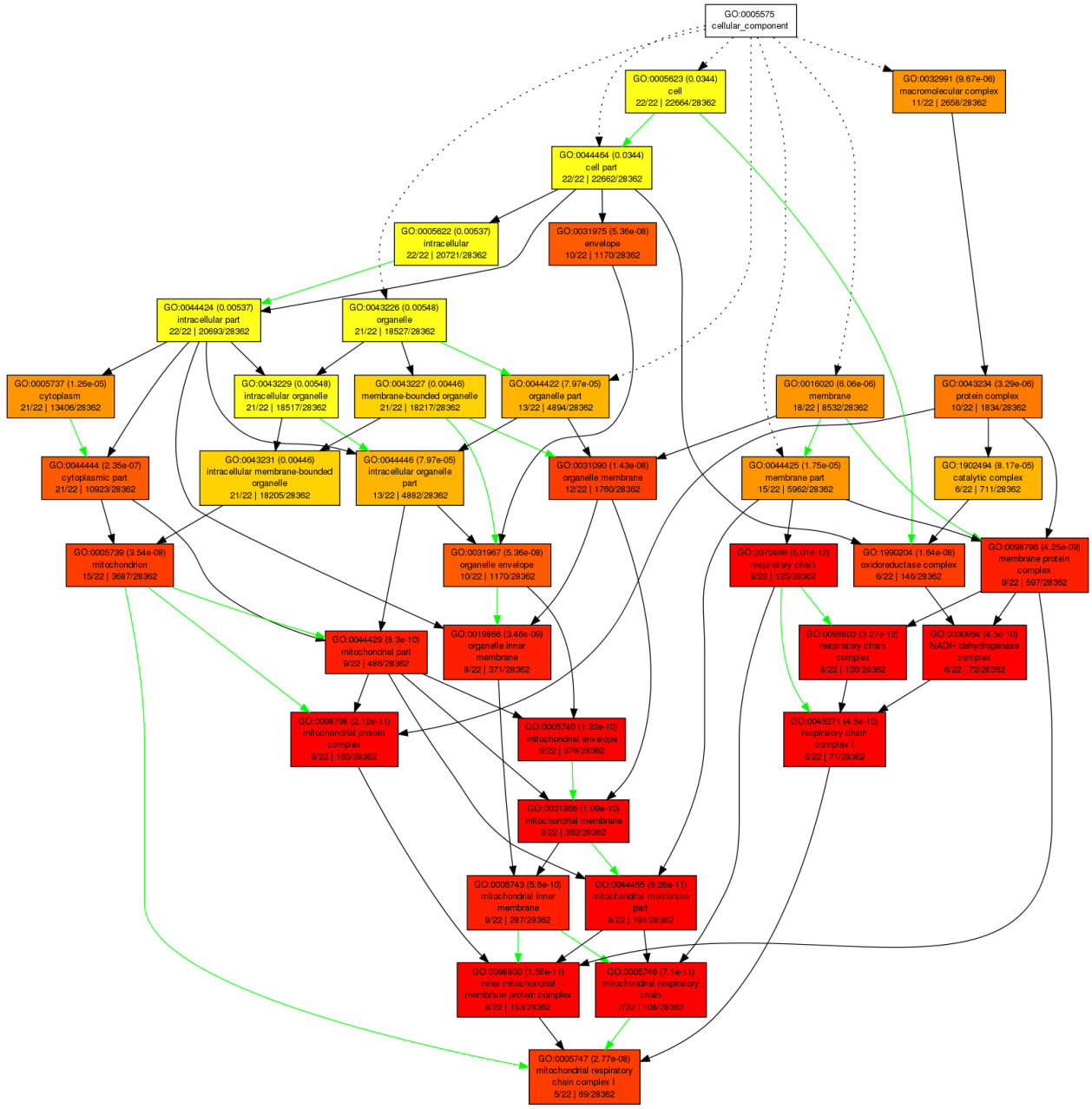

Figure 4.11. Cortex cells GO analysis schema for Cellular Component under 3mM Boron toxicity

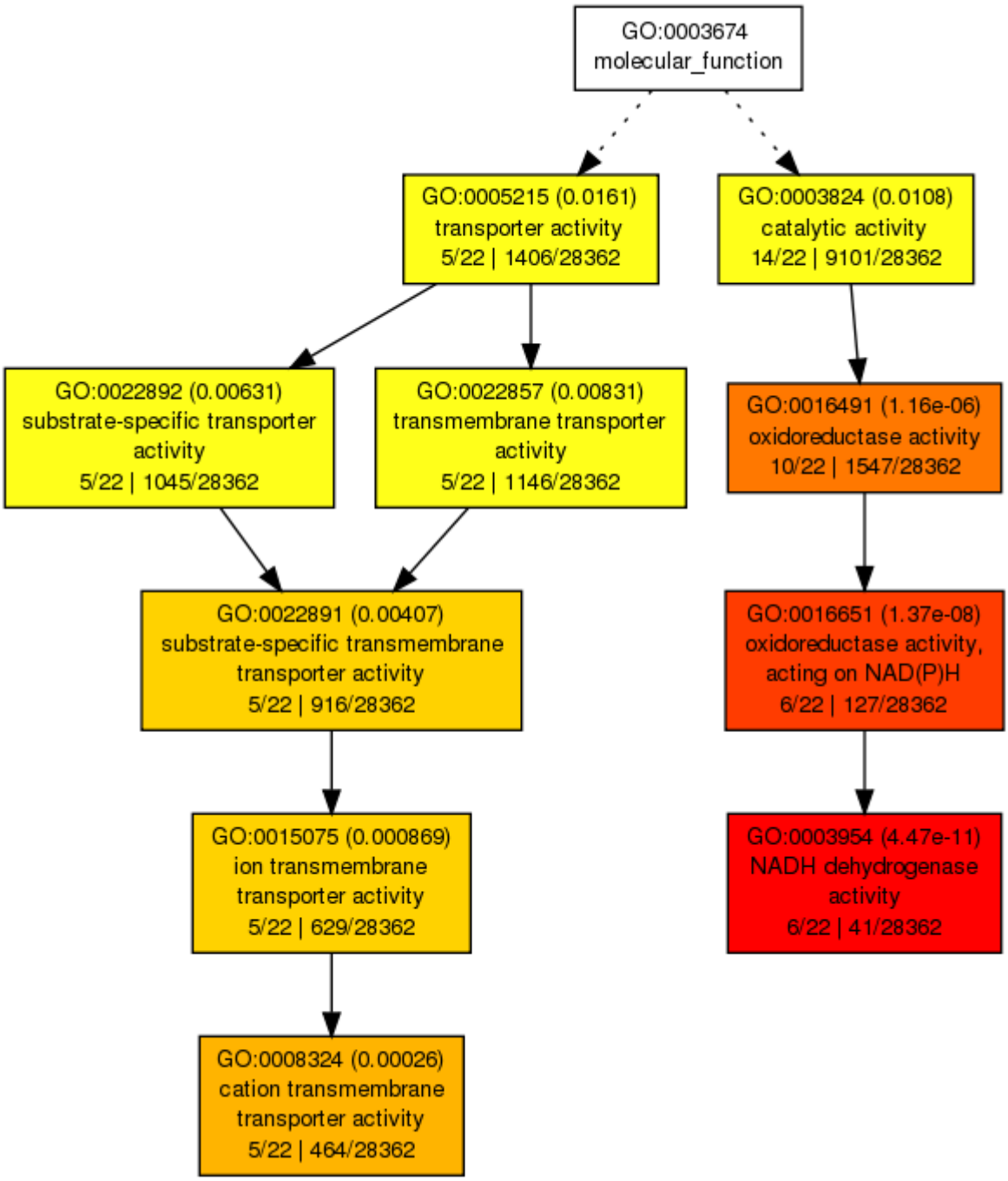

Figure 4.12. Cortex cells GO analysis schema for Molecular Function under 3mM Boron toxicity

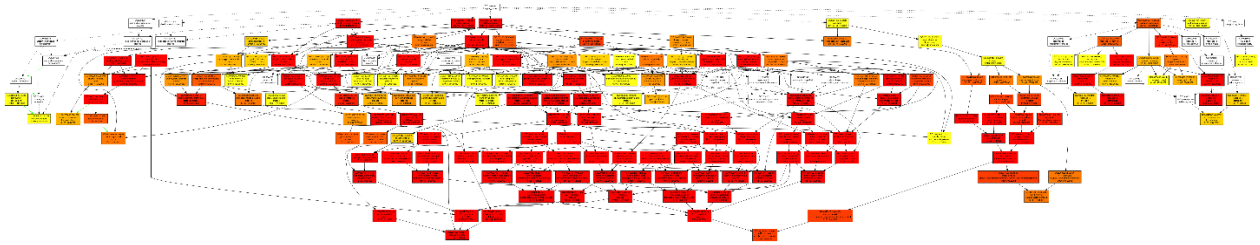

Figure 4.13. Cortex cells GO analysis schema for Biological Process under 5mM Boron toxicity

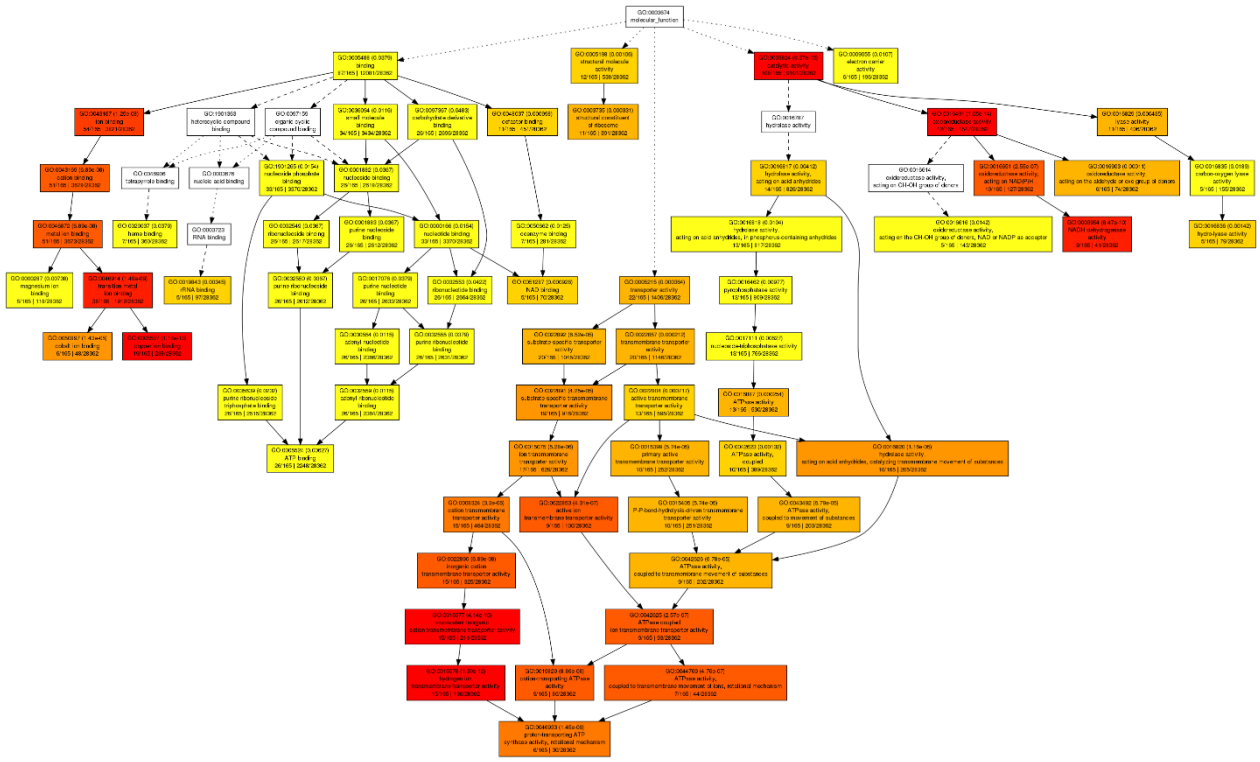

Figure 4.14. Cortex cells GO analysis schema for Molecular Function under 5mM Boron toxicity

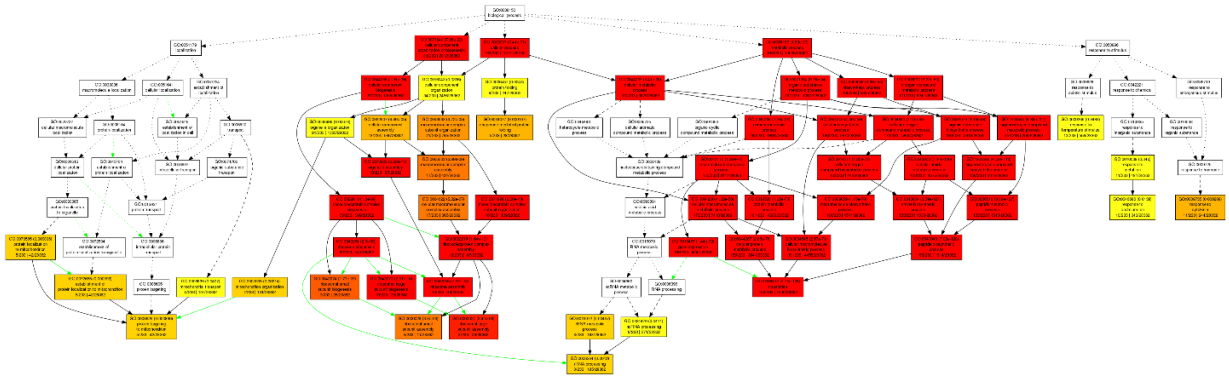

Figure 4.15. Lateral Root Cap/Epidermis/Quiescent Center/Columella GO analysis schema for Biological Process under 3mM Boron toxicity

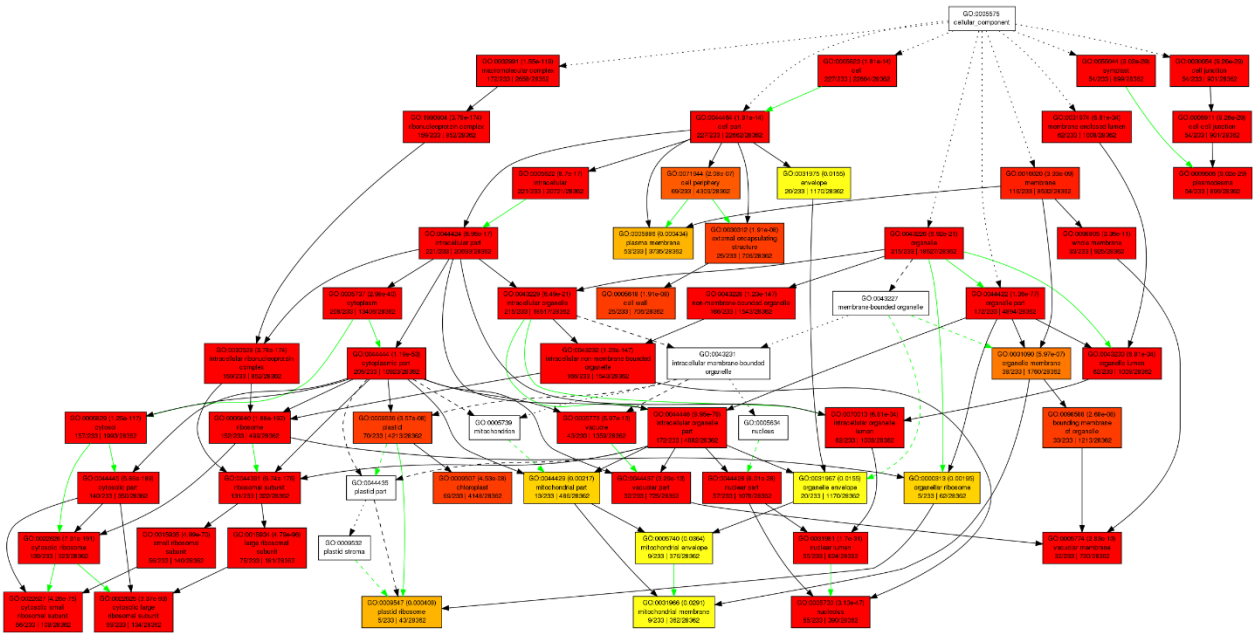

Figure 4.16. Lateral Root Cap/Epidermis/Quiescent Center/Columella GO analysis schema for Cellular Component under 3mM Boron toxicity

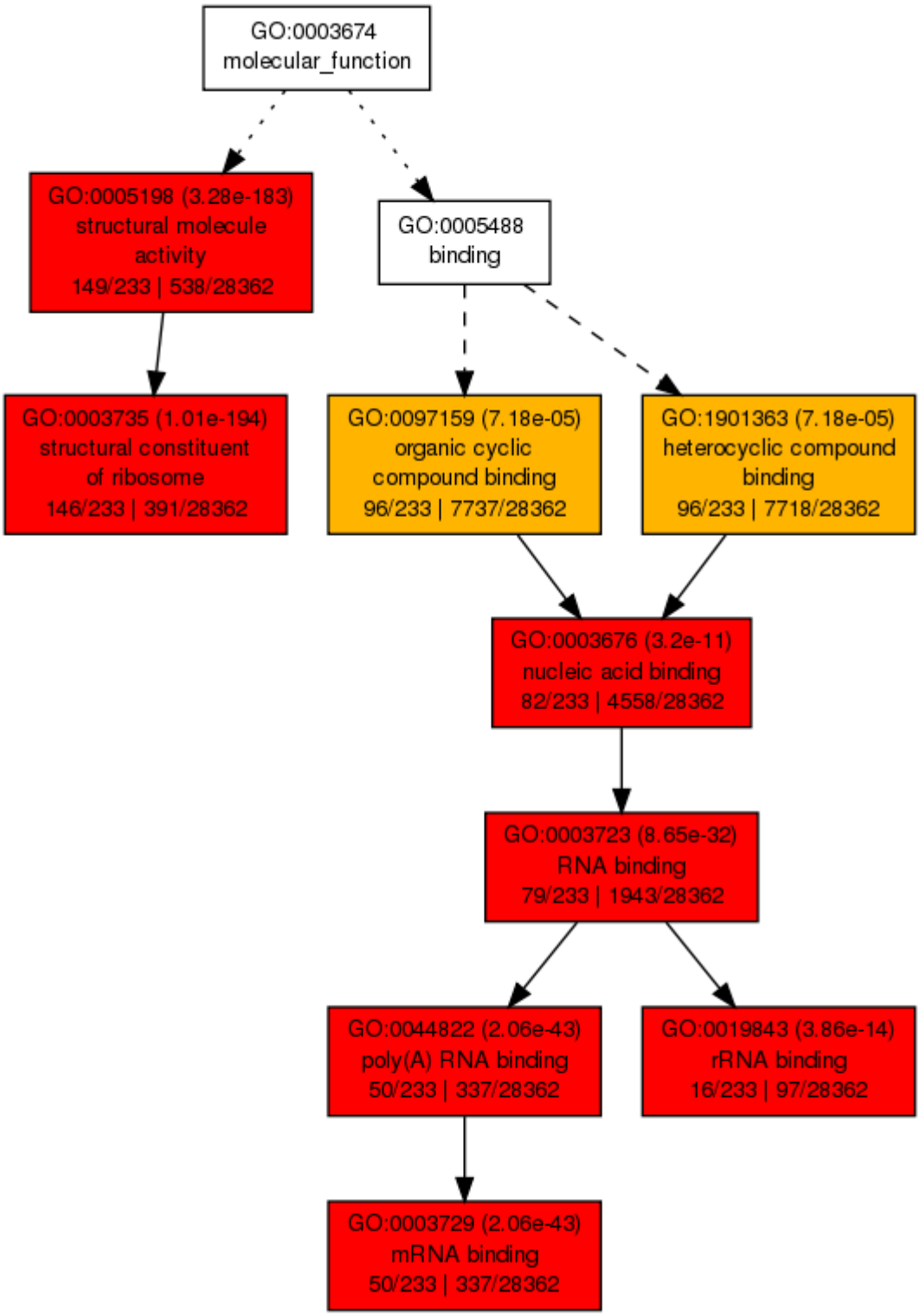

Figure 4.17. Lateral Root Cap/Epidermis/Quiescent Center/Columella GO analysis schema for Molecular Function under 3mM Boron toxicity

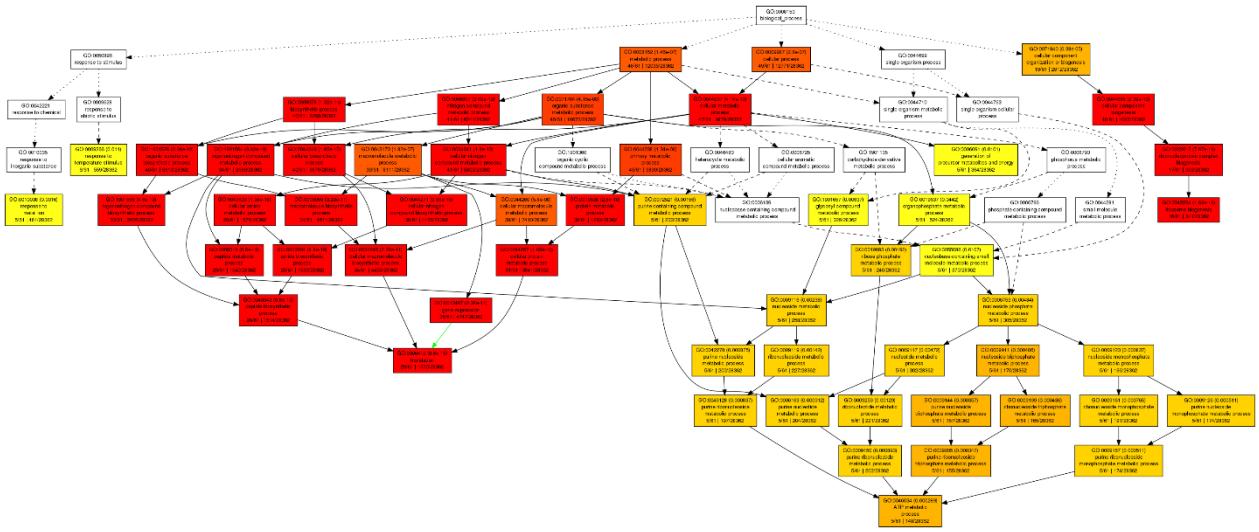

Figure 4.18. Lateral Root Cap/Epidermis/Quiescent Center/Columella GO analysis schema for Biological Process under 5mM Boron toxicity

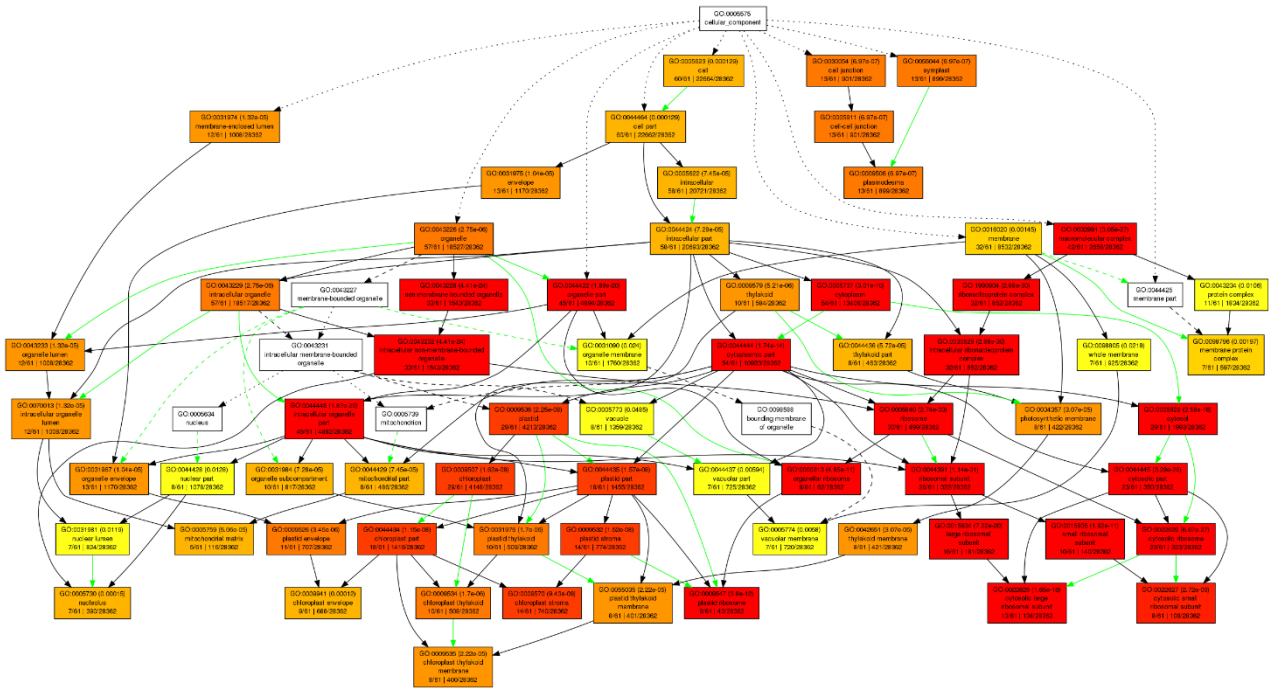

Figure 4.19. Lateral Root Cap/Epidermis/Quiescent Center/Columella GO analysis schema for Cellular Component under 5mM Boron toxicity

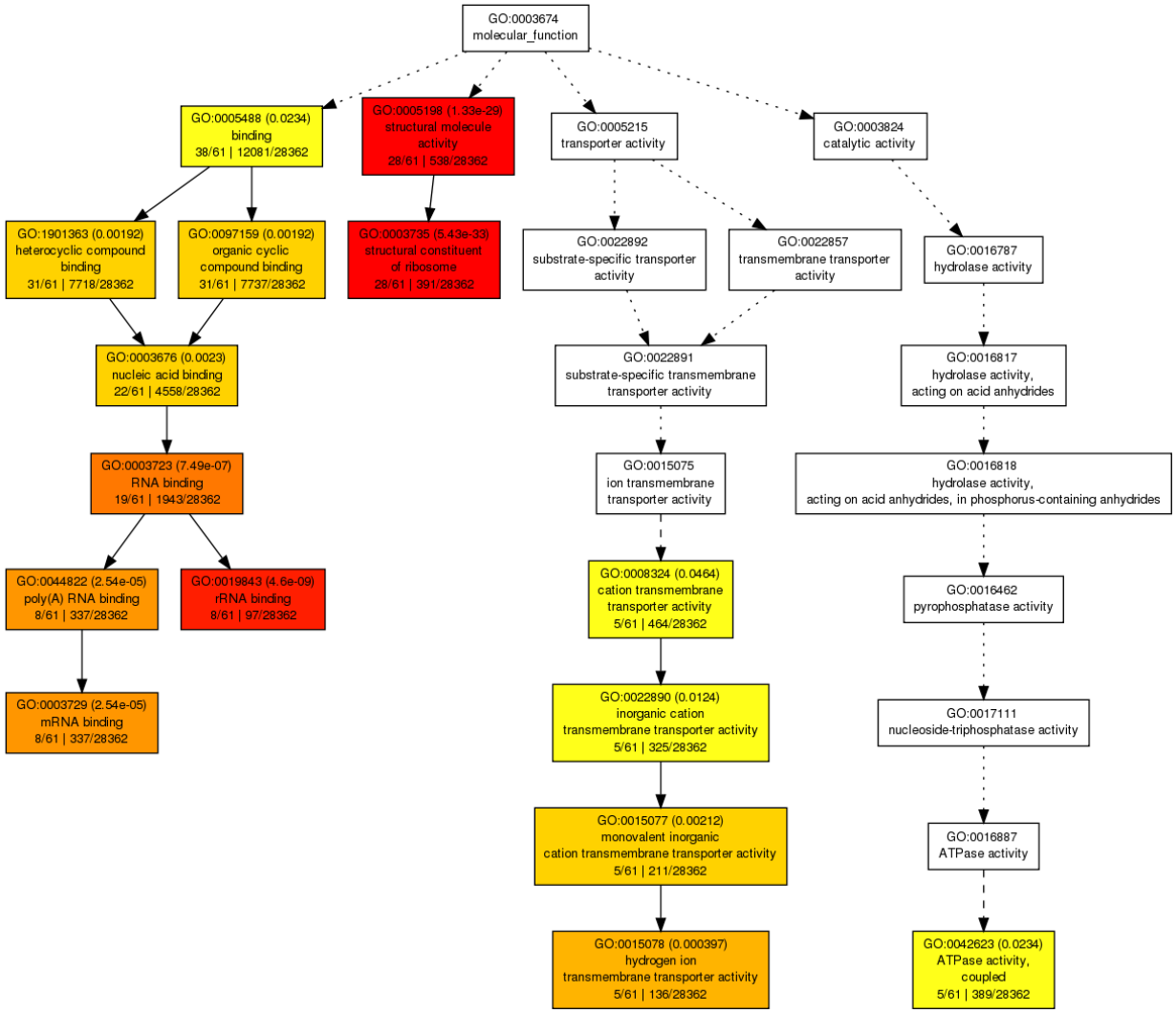

Figure 4.20. Lateral Root Cap/Epidermis/Quiescent Center/Columella GO analysis scheme for Molecular Function under 5mM Boron toxicity

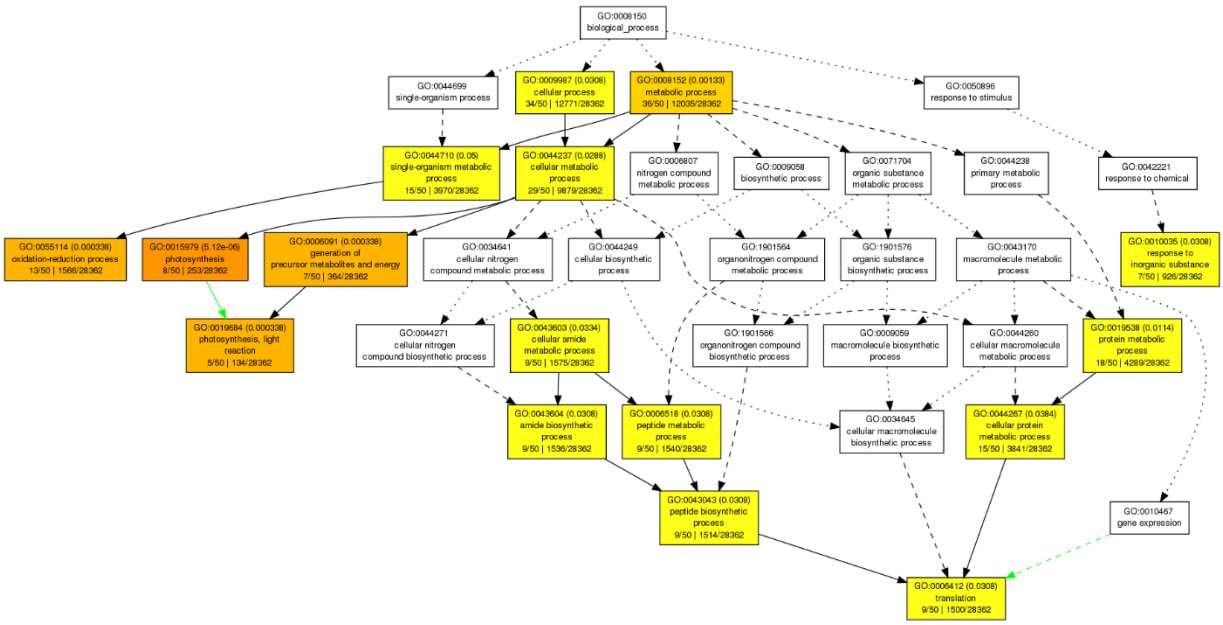

Figure 4.21. Stele GO analysis schema for Biological Process under 3mM Boron toxicity

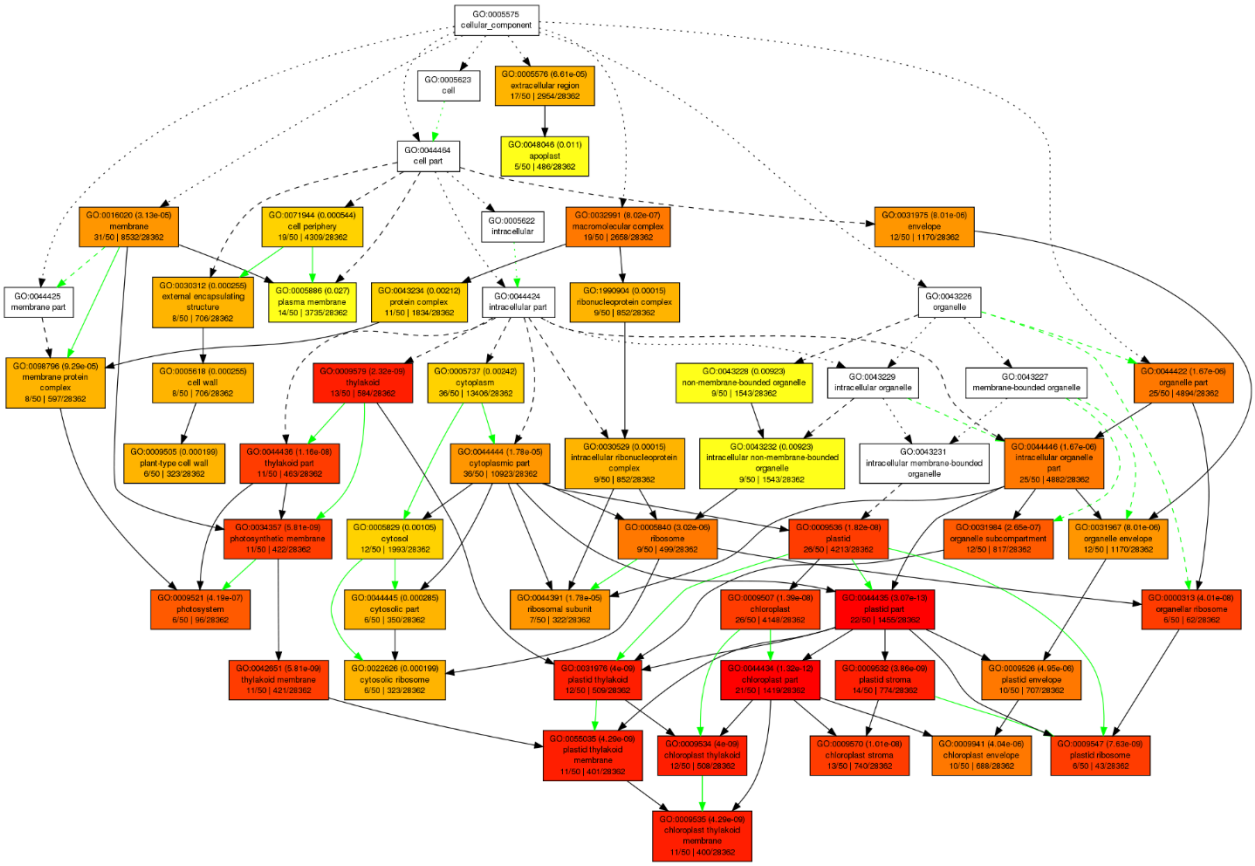

Figure 4.22. Stele GO analysis schema for Cellular Component under 3mM Boron toxicity

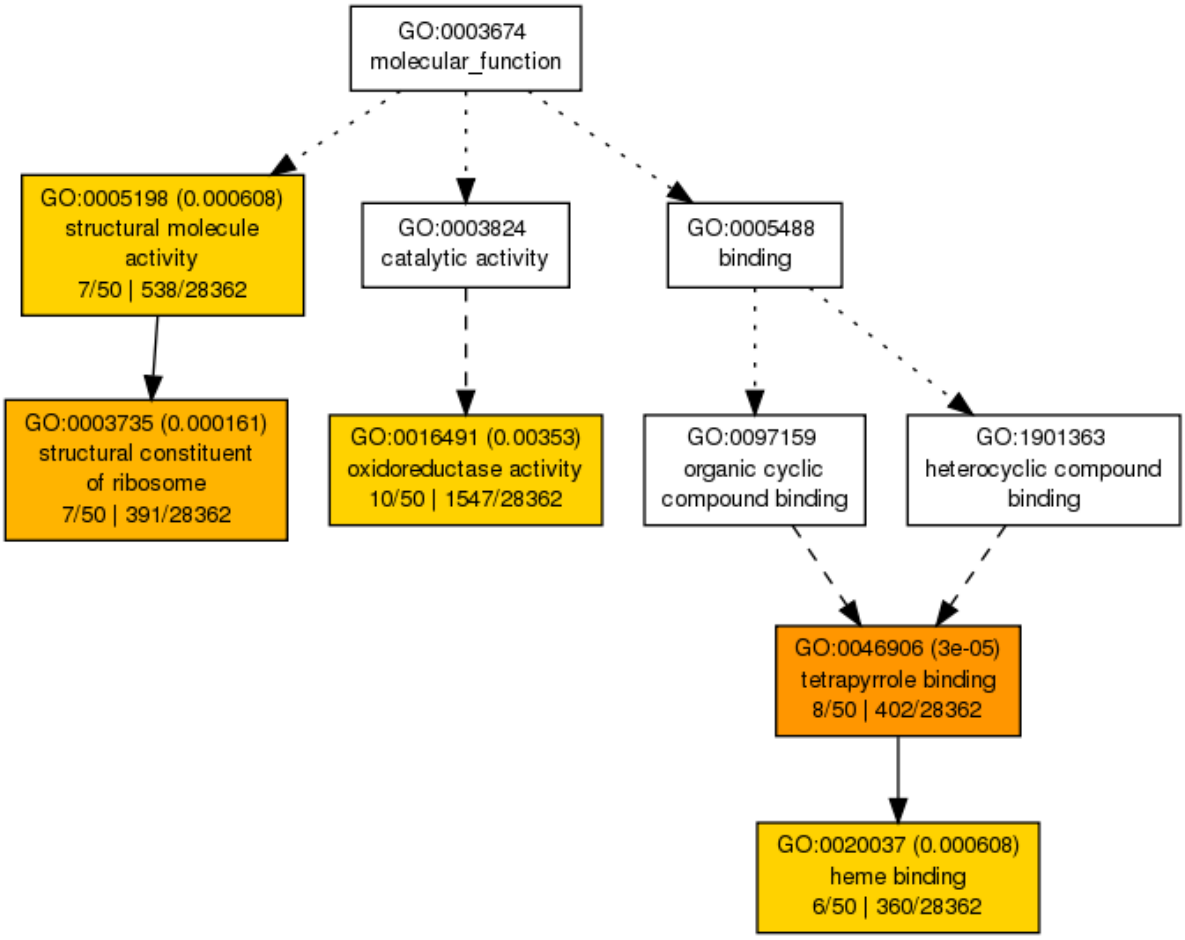

Figure 4.23. Stele GO analysis schema for Molecular Function under 3mM Boron toxicity

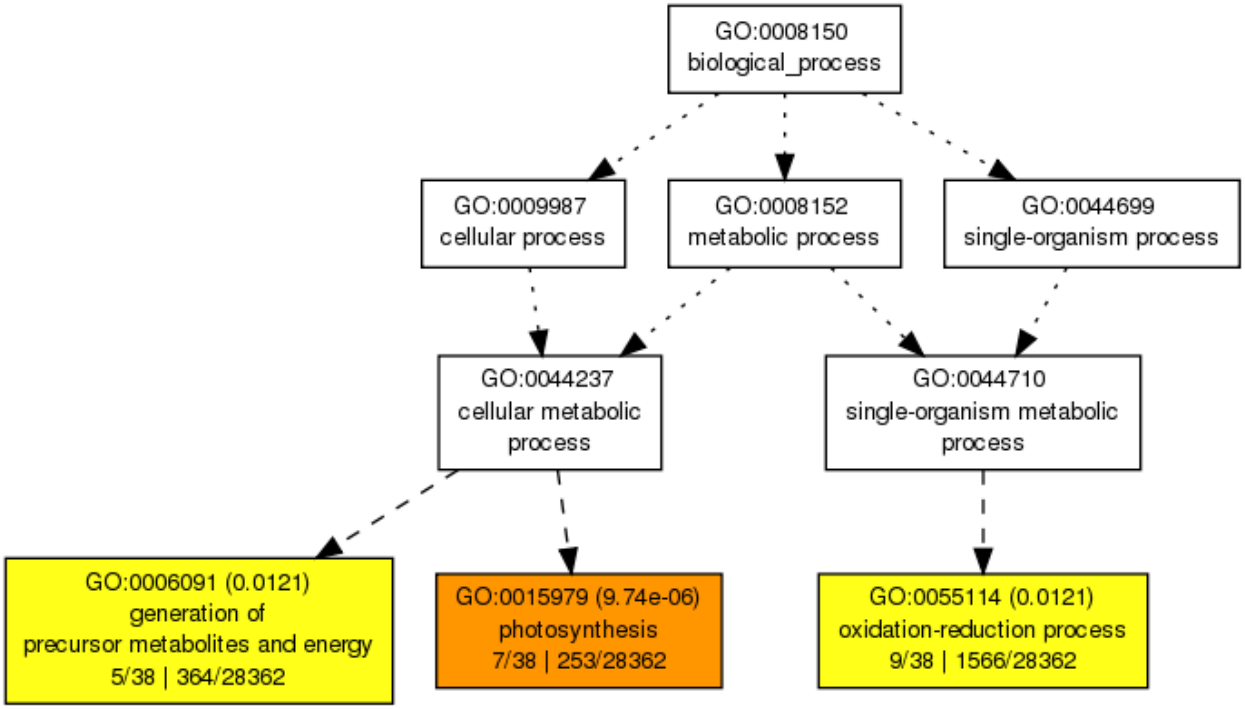

Figure 4.24. Stele GO analysis schema for Biological Process under 5mM Boron toxicity

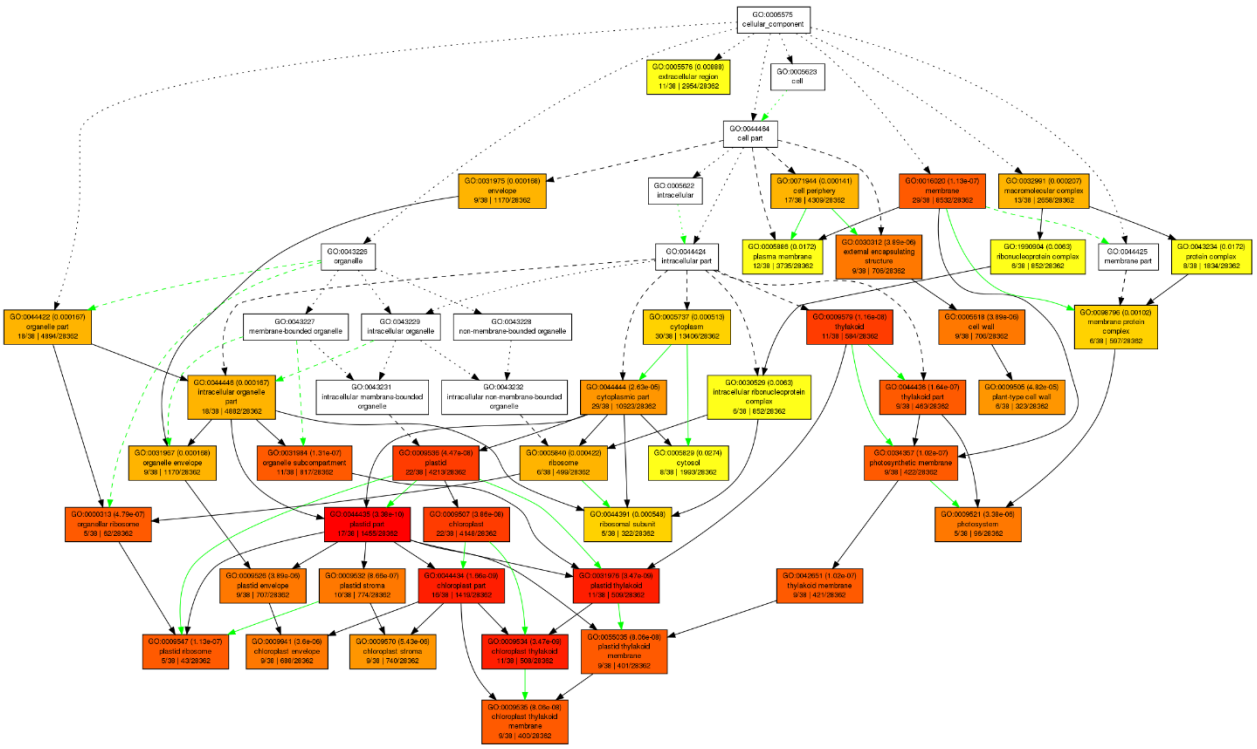

Figure 4.25. Stele GO analysis schema for Cellular Component under 5mM Boron toxicity

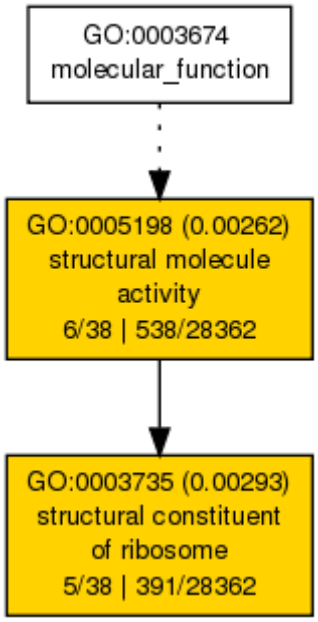

Figure 4.26. Stele GO analysis schema for Molecular Function under 5mM Boron toxicity

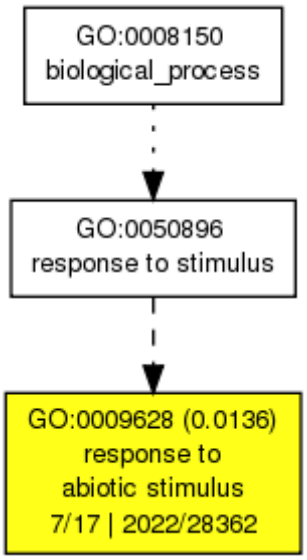

Figure 4.27. Trichoblast GO analysis schema for Biological Process under 5mM Boron toxicity

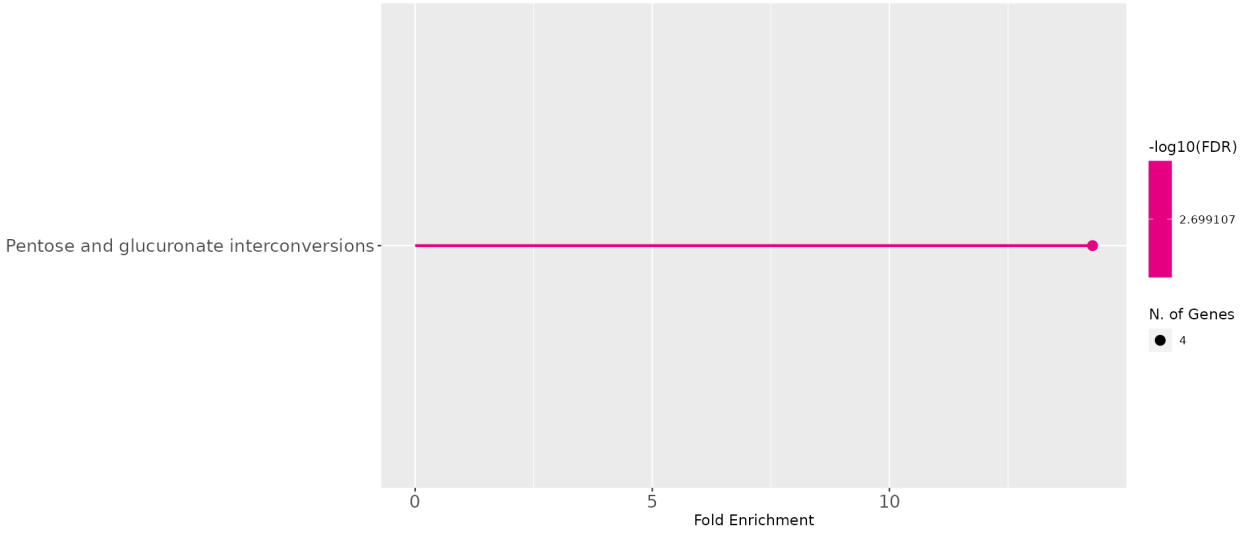

Figure 4.28. Columella KEGG analysis schema under 5mM Boron toxicity

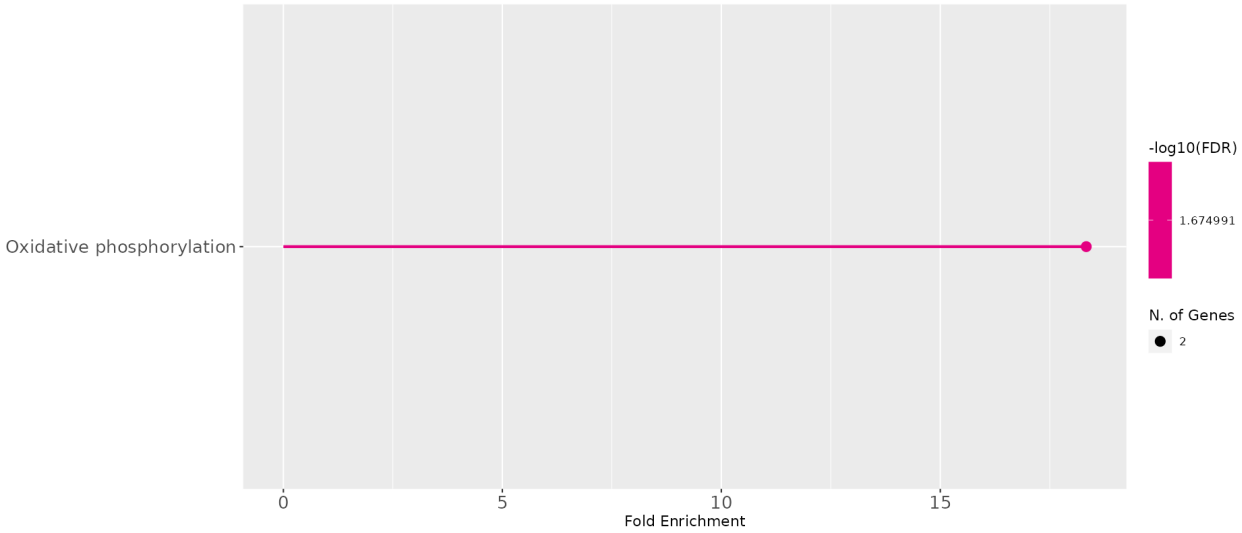

Figure 4.29. Cortex KEGG analysis schema under 3mM Boron toxicity

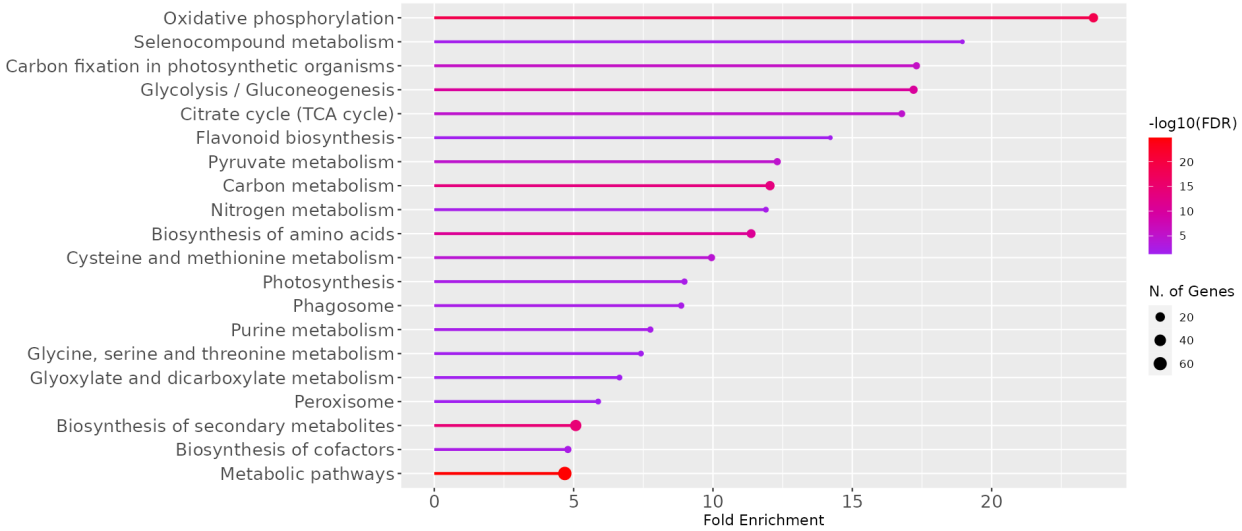

Figure 4.30. Cortex KEGG analysis schema under 5mM Boron toxicity

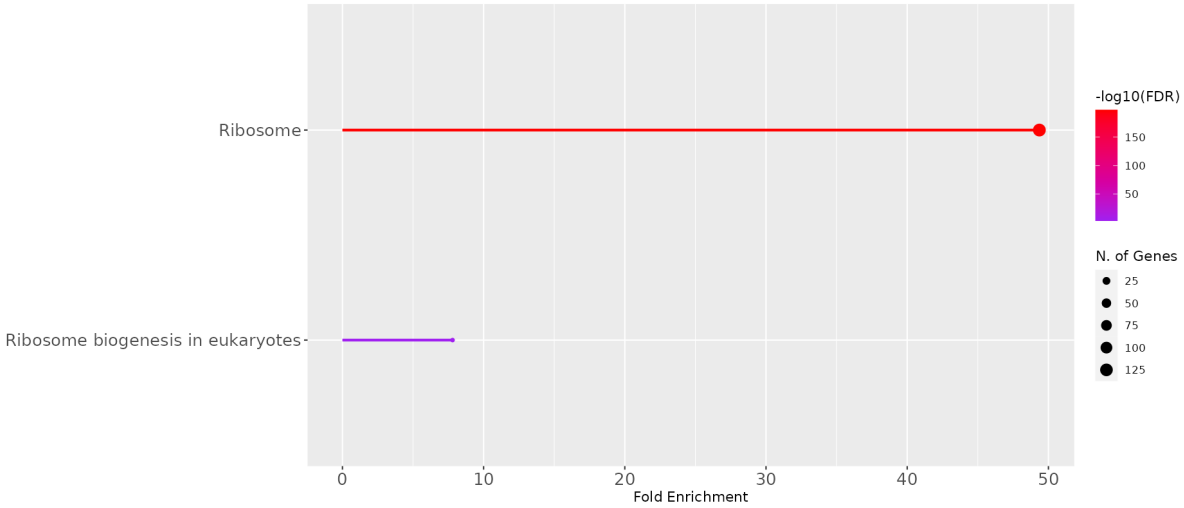

Figure 4.31. Lateral Root Cap/Epidermis/Quiescent Center/Columella KEGG analysis schema under 3mM Boron toxicity

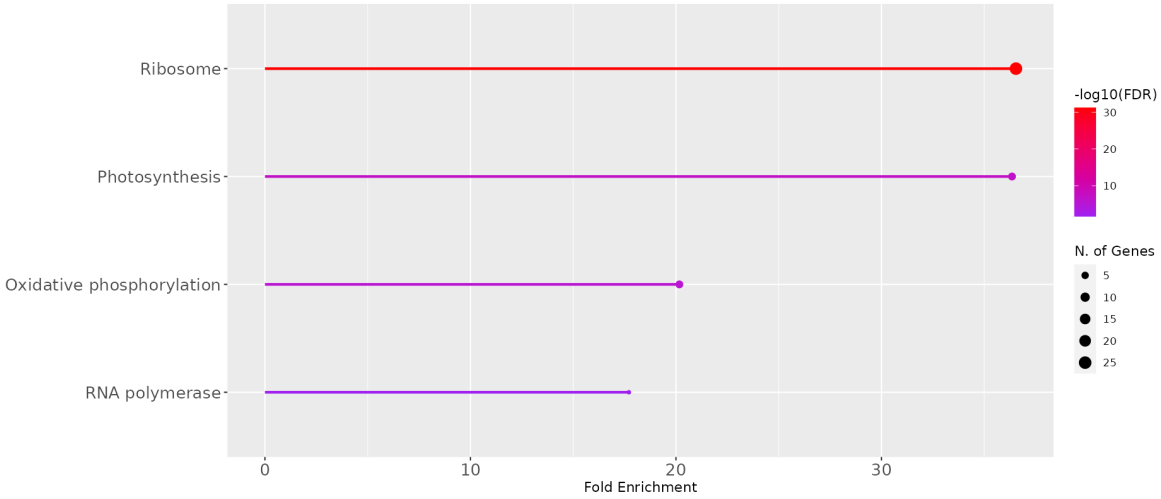

Figure 4.32. Lateral Root Cap/Epidermis/Quiescent Center/Columella KEGG analysis schema under 5mM Boron toxicity

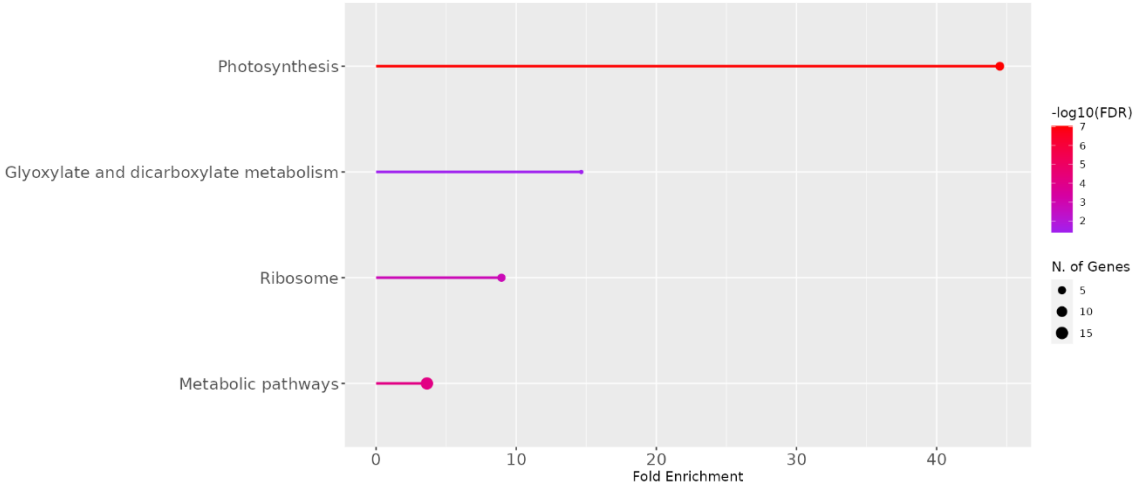

Figure 4.33. Stele KEGG analysis schema under 3mM Boron toxicity

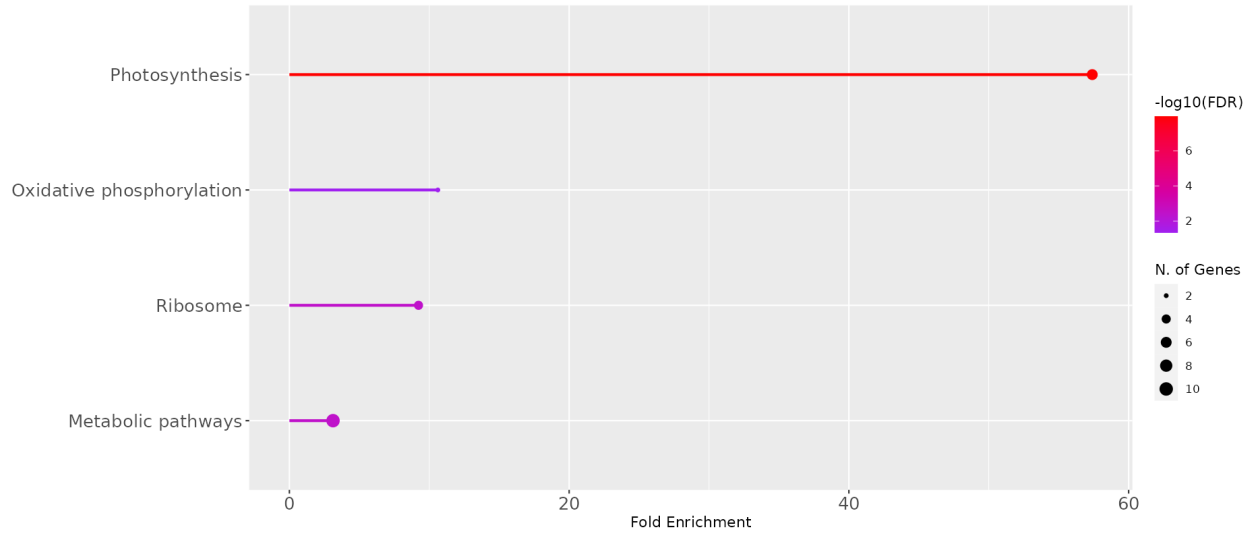

Figure 4.34. Steel KEGG analysis schema under 5mM Boron toxicity

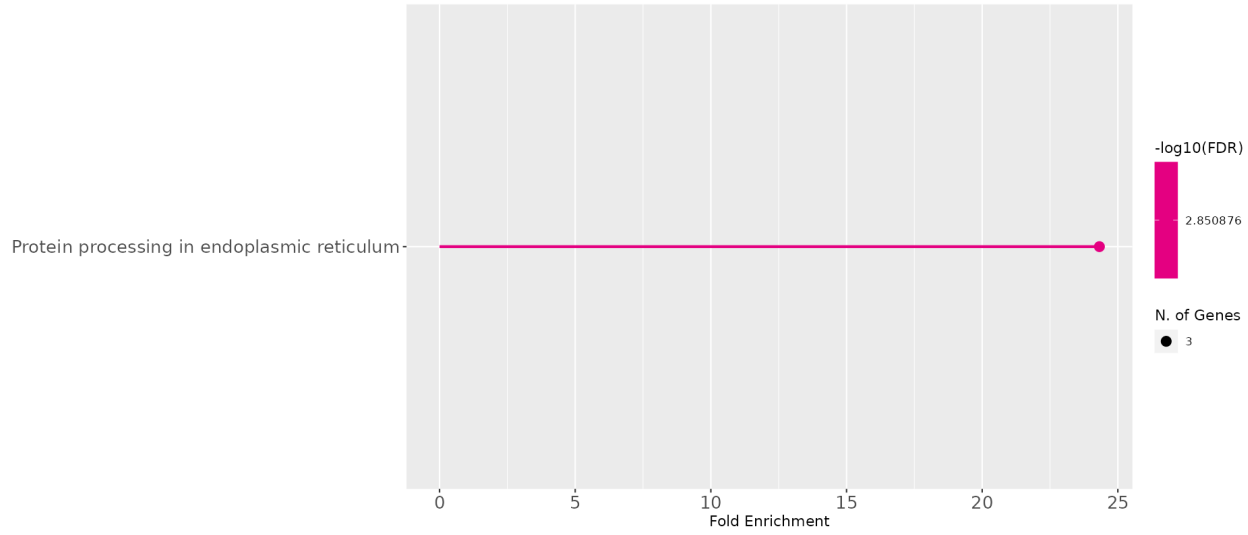

Figure 4.35. Trichoblast KEGG analysis schema under 5mM Boron toxicity

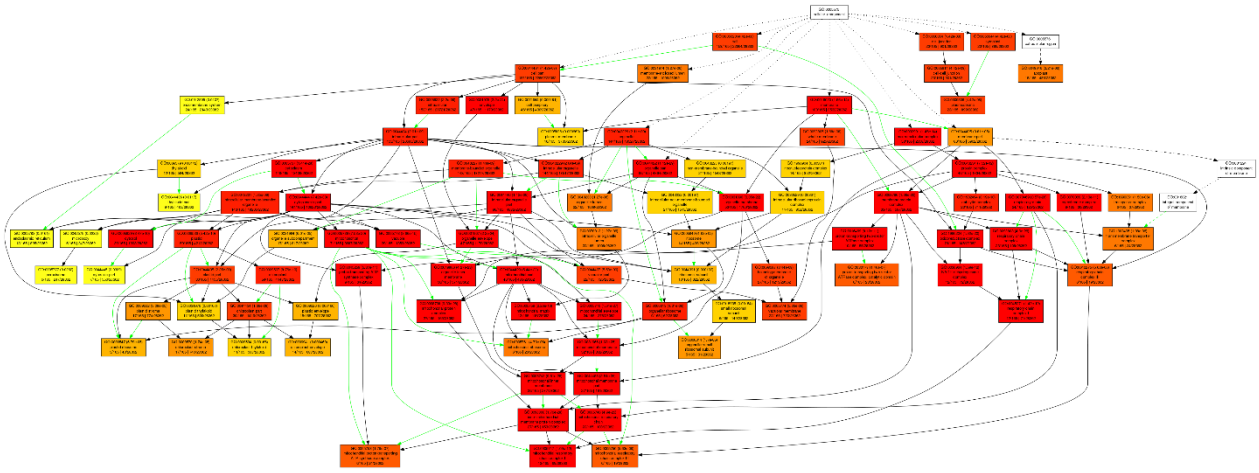

Figure 4.36. Cortex cells GO analysis schema for Cellular Component under 5mM Boron toxicity

5. DISCUSSION

Increasing boron concentration affects the root elongation levels. As seen in Figure 3.2, control groups have 3,2 cm mean root length. When the condition changes to 3mM boron treatment, it shortens to 2,0 cm. Paralell to this finding increasing the concentration to 5mM reveals 1,4 cm elongation. Which simply explains, increasing concentration levels of boron toxicity affects elongation levels of roots in *Arabidopsis thaliana*.

We chose root tissue specifically for our in-depth transcriptomic analysis. It is well-known that boron accumulates more in leaves (shoots of plant) rather than in roots. Boron is transported upward from toots through the xylem with transpiration stream with water. As the water evaporates, nutrients of Boron is not and as result, accumulation of Boron on leaves occurs [76]. Since it has low phloem mobility in many plants, meaning once it reaches a cell group such as leaves, it joins into cell-wall formation and therefore cannot be easily redistributed into other parts of the plant. Roots do not usually accumulate boron the same context as leaves since root is a transit point, where absorption occurs and loads into xylem. Toxicity symptoms appear in shoots of plants and leaves are the accumulation of where boron is accumulated. However, even though this is the situation, primary site for toxic boron studies chosen as roots rather than leaves even though leaves also respond to this stress with triggering stress responses oxidative stress pathways and more. Because, biologically, root tissue is the first frontline of boron interaction from the soil. It's also where the critical regulatory responses, boron uptake control and origin of tolerance mechanisms happened. Root is locus of the boron uptake control and early response mechanisms. It is where plants perceive excess boron in soil and prepare defenses to mitigate boron entry. In depth, roots are housing the key transporters such as *NIP5;1*, *BOR1* and *BOR4* that control boron uptake and distribution [76]. When excess boron is found in the environment, they do focus on more exporting boron and when it is insufficient, they activate these transporters more and uptake boron into cell. In other words, it is the region where molecular decision making for boron homeostasis occurs. In leaves, boron toxicity usually triggers general stress and damage responses. Therefore, since the roots are where defense mechanism starts for the whole plant and able to decide boron uptake or export, it is chosen in this thesis in order to understand tolerance mechanisms.

Single-cell Transcriptomic analysis in the study successfully revealed 16 clusters and 10 of those clusters differentiated based on differential gene expression analysis. Lateral Root cap, Epidermis, Quiescent Center and Columella cells grouped together since they revealed similar

gene expression profiles. Therefore, they identified as one group of cells. Similarly, Cortex and Endodermis grouped together as 1 cluster. Pericycle initial cell and protoxylem clusters also grouped and identified as 1 cluster. Therefore, in total 10 significant clusters have been identified and shown in Figure 4.4.

Single-cell transcriptomic analysis results show that *Arabidopsis thaliana* root cells respond cell-type specific tolerance mechanisms to severe boron toxicity. Different tissues activate different defense mechanisms. GO and KEGG analysis revealed that outer cell layers (Epidermis/Lateral Root cap/Quiescent Center/Columella) are the most affected group as Boron toxicity intensifies to (3-5 mM B). However, with milder stress (1-2 mM B) from previous study, inner tissues (Endodermis/Cortex) dominated upregulated genes number as the response against boron toxicity [70]. This phenomenon indicates a shift of stress adaptation from inner to outer cell layers as the B concentrations increase in the environment. Specifically, 3mM-5mM boron treatment revealed the highest upregulated genes in outermost cell groups (Epidermis/Lateral Root cap/Quiescent Center/Columella). This implies outermost cells plays a critical front-line tolerance defense mechanism against severe boron toxicity. Innermost cells on the other hand, act as an early stress sensor/adaptor, whereas outermost cells more dominantly take role in more severe conditions. It is proof that how single-cell level transcriptomic analysis is important since such findings wouldn't be possible to reveal with bulk tissue analysis.

GO and KEGG analysis support the previous claim. For columella cells, GO and KEGG enrichment analysis of the 5 mM-B columella cluster indicates that these root-cap cells switch from the glutathione-centered antioxidant response that has been previously reported for moderate B stress [33] to an excessive, membrane-focused detoxification strategy. The most over-represented biological-process terms are ion transport, anion/cation transport and macromolecule catabolic processes. Together with cellular-component terms such as plasma membrane and vacuolar membrane, it points that large-scale re-organization of the endomembrane system to pump borate across the cell surface or sequester it in the vacuole [45, 53] .Parallel to that, molecular-function categories are dominated by ATP-dependent primary and secondary transporters and vacuolar/lysosomal peptidases, pointing out the high energy demand of this response [41]. The significant KEGG pathway, Pentose and glucuronate interconversions, UDP-glucuronic acid for pectin and hemicellulose re-modelling, suggesting strengthening of the cell wall to not give a chance to move for excess boron in the apoplast [49, 67]. Together with all, these data show that under severe B toxicity. columella cells prioritize ATP-driven export, vacuolar sequestration and cell-wall reinforcement instead of glutathione-based accumulation in order to

prevent boron-induced damage. In addition, Columella cells upregulate a suite of genes involved in detoxification and antioxidant defense. At milder stress conditions of 1mM boron, enrichment analysis shown higher activity on “glutathione metabolism pathway” parallel with “glutathione S-transferases” and other redox-protective enzymes. All of these helps to combat reactive oxygen species (ROS) generated because of boron toxicity [70].

For cortex cells (inner cell group), GO enrichment points to a two-step defense program as external boron rises from 3 mM to 5 mM. At 3 mM B the dominant biological-process categories are “oxidation-reduction process,” “energy derivation by oxidation of organic compounds,” and “cellular respiration,” while cellular-component terms focus on the mitochondrial inner membrane and respiratory-chain complexes. Molecular-function enrichment is restricted to NAD(P)H oxidoreductases and a small set of ion-transmembrane transporters. These transporters regulates of boron uptake with *NIP5;1*, *BOR1* and *BOR4* transporters. Based on Molecular function, it can be said that *BOR4* is upregulated, *BOR1* and *NIP5;1* are downregulated to maximize pumping out excessive Boron on cortex cells [79]. These patterns points that cortex cells first cope with moderate boron excess by up-regulating mitochondrial respiration via upregulation of *NDA1, AOX1A* and redox capacity, an energy-intensive adjustment that provides ATP for borate export from *BOR4* transporter activity and helps maintain redox balance [45, 33]. KEGG analysis supports this point of view, at 3 mM B the only significant pathway is “Oxidative phosphorylation,” reflecting elevated ATP production. When the concentration reaches 5 mM B, more than a dozen KEGG pathways become enriched. Core energy routes (oxidative phosphorylation, glycolysis/gluconeogenesis, TCA cycle) shows major role, however they are joined by carbon-fixation and photosynthesis modules, suggesting that cortical plastids are also recruited to generate reducing power on the cell [67]. Parallel enrichment of flavonoid biosynthesis and other secondary-metabolite pathways matches GO evidence for phenylpropanoid-driven wall reinforcement, while peroxisome and amino-acid/sulphur pathways point to enhanced reactive-oxygen detoxification and the synthesis of glutathione precursors [41, 34]. Collectively, the data shows that cortex cells first boost mitochondrial ATP output at 3 mM B, and then, at 5 mM B, launch a broader metabolic re-programming that draws on both mitochondrial and plastid energy systems.

For Later Root Cap/Epidermis/Quiescent Centre/Columella cell group (outermost tissue), enrichment pattern goes into two distinct phases for 3mM and 5mM Boron. At 3 mM B all three GO domains show to the cytosolic translation apparatus. cellular-component terms highlight the ribosome, its large and small subunits and related ribonucleoprotein complexes; molecular-

function terms are highly pointed at “structural constituent of ribosome” and a hierarchy of RNA-binding categories; biological-process enrichment emphasizes ribosome biogenesis, protein localization to mitochondria and mitochondrial transport. KEGG mirrors this focus with “Ribosome” and “Ribosome biogenesis in eukaryotes”. Together these data indicate that, outer-layer cells initially respond to 3mM dose by expanding ribosome production and mitochondrial protein import, sustaining a high rate of stress-protein synthesis while maintaining mitochondrial energy supply [45, 33].

When the dose reaches 5 mM dose, translation remains central, but the response broadens significantly. Biological-process terms extend from ribosome assembly to large-scale macromolecule biosynthesis, gene expression and peptide biosynthesis; cellular-component enrichment goes to nucleolus, nuclear envelope, chloroplast, thylakoid, vacuolar and mitochondrial membranes. Molecular-function categories incorporate both ribosomal proteins and a new tier of cation-transporter and ATPase activities, pointing activation of energy-dependent export systems. KEGG confirms this extended program, alongside “Ribosome,” pathways for photosynthesis, oxidative phosphorylation and RNA polymerase as significant. Therefore, while outer tissues first accelerate ribosome biogenesis at 3 mM B; at 5 mM B, up-regulate plastid and mitochondrial energy machinery, general transcription and ATP-driven ion pumps which changes that collectively raise cellular energy output and export capacity needed to detoxify the higher boron load [67].

In the stele cluster the boron-response is comparatively more moderate and plastid-centered. At 3 mM B, GO biological-process terms include “photosynthesis,” “oxidation-reduction process” and “generation of precursor metabolites and energy,” while cellular-component terms focus on chloroplast, thylakoid membrane and plastid ribosome; molecular-function enrichment is limited to ribosomal structural proteins and heme-binding oxido-reductases. KEGG confirms this pattern, with “Photosynthesis,” “Glyoxylate and dicarboxylate metabolism” and “Ribosome” the as significant pathways. Photosynthesis increase in stele go and KEGG caused by plastids in stele that can engage in electron transport and redox metabolism rather than classical photosynthesis purpose. Limited protein synthesis and plastidial electron transport activity is for reducing energy consumption and securing energy in cells for housekeeping functions and driving stress mitigation processes such as antioxidant defense. Together these results indicate that stele cells counter moderate boron excess mainly by up-regulating chloroplast energy metabolism and a modest translational boost, presuming to secure ATP/NADPH for housekeeping and limited detoxification [53, 34].

Raising the dose to 5 mM B does not broaden the response greatly like outer cells instead of the same plastid signature concentrated. GO in 5mM lists only three significant biological-process nodes which are “photosynthesis,” “oxidation-reduction process” and “generation of precursor metabolites and energy”. Cellular-component enrichment remains concentrated on plastid envelope, thylakoid and plastid ribosome. KEGG likewise shows “Photosynthesis,” “Oxidative phosphorylation,” “Ribosome” and a generic “Metabolic pathways” category. Thus, even under severe stress the stele mainly boosts both photosynthetic and respiratory electron-transport chains, rather than launching the large-scale wall-fortification or transporter programs seen in outer tissues to export excessive B from cells by using active transport, repair and antioxidative mechanisms. This restricted, energy-oriented arrangement suggests that inner stele cells rely on the surrounding cortex and epidermis for primary boron exclusion, while sustaining their own plastid and mitochondrial output to keep vascular transport functioning [45, 67].

Lastly, in trichoblasts (root-hair cells), severe boron stress shows a very focused reaction. GO analysis at 5 mM B impacts just one biological-process term “response to abiotic stimulus” with parallel to KEGG which is also a single pathway, “Protein processing in the endoplasmic reticulum,” driven by three up-regulated chaperone and folding-factor genes. This pattern suggests that, rather than launching broad metabolic re-programming, trichoblasts mainly activate an ER-stress/unfolded-protein response to preserve secretory-pathway function when excess boron interferes with the cell surface and wall [34, 41].

In summary, the single-cell transcriptomic analysis reveals that severe boron toxicity elicits a complex, cell type specific response in *Arabidopsis thaliana* roots. Each root cell type shows its own suite of defensive and adaptive gene expression changes. Moderate excess (3 mM) impacts as a broad “energy-first” reaction. cortex cells up-regulate oxidative phosphorylation, outer tissues boost ribosome biogenesis, and the stele enhances chloroplast photosynthetic machinery collection of all securing ATP and reductant to fuel detox processes. At severe excess (5 mM), each tissue layers on a different module. cortex couples its high ATP output to phenylpropanoid/flavonoid synthesis, peroxisomal ROS detox and a surge of ATP-driven transporters. The outer composite cluster maintains elevated translation however adds photosynthesis, oxidative phosphorylation and ion-pump activity to sustain active borate pump to outside. Columella cells focus on plasma and vacuolar-membrane transporters and UDP-sugar pathways for cell-wall sequestration. Stele simply enhances its plastid and respiratory electron pathways to keep vascular energy supply stable. Trichoblasts, rather than broad re-programming, it activates an endoplasmic-reticulum unfolded-protein response to protect secretory trafficking.

Together, these patterns reveal a coordinated strategy for energy mobilization followed by cell-type-specific specialization.

Outer layers pumps excessive boron, cortex reinforces and detoxifies themselves, the stele maintains transport power for the plant, and trichoblasts safeguard the protein folding. All together allowing the *Arabidopsis thaliana* root to tolerate severe boron toxicity.

6. CONCLUSION

We successfully identified 16 clusters of cells as conclusion of PCA analysis and grouped the closest similar differential gene expressions. Used marker genes to identify tissue specific cell types and as result 10 meaningful groups have been gathered from PCA analysis. From the expression profiles, we have observed the most significant upregulation with 258 different genes in outermost cell group (Lateral Root Cap/Epidermis/Quiescent Center/Columella) at 3mM boron toxicity. Further, we also observed that inner layer cells (cortex) represented significant upregulation in expression with 165 different genes at 5mM boron toxicity even though number of genes were 22 in the 3mM boron toxic environment.

The scientific revelations from this cell-level investigation highlight how different each type of root cell responds to severe boron influence. Under severe boron stress, the scRNA-seq technique revealed various transcriptome alterations in the several root layers and cell types, therefore indicating a complex, heterogeneous response that would be missed in whole-root investigations. Especially, the most responsive cell type changed with severe boron concentration. From previous study of Yılmaz et al,. (2023), at mild boron toxicity with levels 1mM and 2mM inner tissues like columella and endodermis shown greatest number of upregulated gene expression. On the other hand, under severe concentrations at 3mM and 5mM, outer root cap cells represented the largest transcriptional response. These findings show that root cap is the first defense or in other words, critical frontline tissue under severe boron toxic conditions while inner cell layers play more vital roe under milder boron toxic conditions. Therefore, instead of responding uniformly, the root uses a coordinated mosaic of cell-type-specific stress responses. Each layer of cells shows different strategies of defense and tolerance mechanism.

GO and KEGG analysis that performed revealed mechanisms and signals under severe boron toxic conditions. outer-layer cells (root cap/ epidermis) export excess boron by “sacrificing” themselves, through activation of ribosome-biogenesis and ion-pump modules, cortex reinforces its walls and detoxifies the cytoplasm by up-regulating oxidative phosphorylation, TCA/glycolysis, and phenylpropanoid/flavonoid biosynthesis pathways, the stele keeps long-distance transport by activating photosynthesis pathways and oxidative-phosphorylation pathways, and trichoblasts safeguard the protein quality by activation of protein-processing-in-endoplasmic-reticulum pathways.

This study provides a robust basis for transgenic and marker-assisted breeding programs designed to produce breeds that tolerate high-boron soils while maintaining or improving yields in boron-toxic conditions.

REFERENCES

[1] 10x Genomics. (2018). *How does cellranger aggr normalize for sequencing depth among multiple libraries?* 10X Genomics. https.//kb.10xgenomics.com/hc/en-us/articles/115004217543

[2] Ashburner, M., Ball, C. A., Blake, J. A., Botstein, D., Butler, H., Cherry, J. M., Davis, A. P., Dolinski, K., Dwight, S. S., Eppig, J. T., Harris, M. A., Hill, D. P., Issel-Tarver, L., Kasarskis, A., Lewis, S., Matese, J. C., Richardson, J. E., Ringwald, M., Rubin, G. M., & Sherlock, G. (2000). Gene Ontology. tool for the unification of biology. *Nature Genetics*, *25*(1), 25–29. https.//doi.org/10.1038/75556

[3] Bennett, T., van den Toorn, A., Sanchez-Perez, G. F., Campilho, A., Willemsen, V., Snel, B., & Scheres, B. (2010). SOMBRERO, BEARSKIN1, and BEARSKIN2 Regulate Root Cap Maturation inArabidopsis . *The Plant Cell*, *22*(3), 640–654. https.//doi.org/10.1105/tpc.109.072272

[4] Blaser-Grill, J., Knoppik, D., Amberger, A., & Goldbach, H. (1989). Influence of Boron on the Membrane Potential in Elodea densa and Helianthus annuus Roots and H Extrusion of Suspension Cultured Daucus carota Cells. *Plant Physiology*, *90*(1), 280–284. https.//doi.org/10.1104/pp.90.1.280

[5] Bolan, S., Hou, D., Wang, L., Hale, L., Egamberdieva, D., Tammeorg, P., Li, R., Wang, B., Xu, J., Wang, T., Sun, H., Padhye, L. P., Wang, H., Siddique, K. H. M., Rinklebe, J., Kirkham, M. B., & Bolan, N. (2023). The potential of biochar as a microbial carrier for agricultural and environmental applications. *Science of the Total Environment*, *886*, 163968. https.//doi.org/10.1016/j.scitotenv.2023.163968

[6] Bonke, M., Thitamadee, S., Mähönen, A. P., Hauser, M.-T., & Helariutta, Y. (2003). APL regulates vascular tissue identity in Arabidopsis. *Nature*, *426*(6963), 181–186. https.//doi.org/10.1038/nature02100

[7] Brady, S. M., Orlando, D. A., Lee, J.-Y., Wang, J. Y., Koch, J., DinnenyJ. R., Mace, D., Ohler, U., & Benfey, P. N. (2007). A High-Resolution Root Spatiotemporal Map Reveals Dominant Expression Patterns. *Science*, *318*(5851), 801–806. https.//doi.org/10.1126/science.1146265

[8] Bruex, A., Kainkaryam, R. M., Wieckowski, Y., Kang, Y. H., Bernhardt, C., Xia, Y., Zheng, X., Wang, J. Y., Lee, M. M., Benfey, P., Woolf, P. J., & Schiefelbein, J. (2012). A Gene Regulatory Network for Root Epidermis Cell Differentiation in Arabidopsis. *PLoS Genetics*, *8*(1), e1002446. https.//doi.org/10.1371/journal.pgen.1002446

[9] Butler, A., Hoffman, P., Smibert, P., Papalexi, E., & Satija, R. (2018). Integrating single-cell transcriptomic data across different conditions, technologies, and species. *Nature Biotechnology*, *36*(5), 411–420. https.//doi.org/10.1038/nbt.4096

[10] Ceyhun Kayıhan, Mehmet Öz, Füsun Eyidoğan, Meral Yücel, & Hüseyin Avni Öktem. (2017). *Physiological, Biochemical, and Transcriptomic Responses to Boron Toxicity in Leaf and Root Tissues of Contrasting Wheat Cultivars*. *35*(1), 97–109. https.//doi.org/10.1007/s11105-016-1008-9

[11] Chen, X., Ru, Y., Takahashi, H., Mikio Nakazono, Sergey Shabala, Smith, S. M., & Yu, M. (2023). Single-cell transcriptomic analysis of pea shoot development and cell-type-specific responses to boron

deficiency. *The Plant Journal*, *117*(1), 302–322. https.//doi.org/10.1111/tpj.16487

[12] Chen, Z., Bai, X., Zeng, B., Fan, C., Li, X., & Hu, B. (2023). Physiological and molecular mechanisms of Acacia melanoxylon stem in response to boron deficiency. *Frontiers in Plant Science*, *14*. https.//doi.org/10.3389/fpls.2023.1268835

[13] Cheng, C.-Y., Krishnakumar, V., Chan, A. P., Thibaud-Nissen, F., Schobel, S., & Town, C. D. (2017). Araport11. a complete reannotation of the*Arabidopsis thaliana* reference genome. *The Plant Journal*, *89*(4), 789–804. https.//doi.org/10.1111/tpj.13415

[14] Çöl, M., & Çöl, C. (2003). Environmental boron contamination in waters of Hisarcik area in the Kutahya Province of Turkey. *Food and Chemical Toxicology*, *41*(10), 1417–1420. https.//doi.org/10.1016/S0278-6915(03)00160-1

[15] Confraria, A., & Baena-González, E. (2016). Using Arabidopsis Protoplasts to Study Cellular Responses to Environmental Stress. *Methods in Molecular Biology (Clifton, N.J.)*, *1398*, 247–269. https.//doi.org/10.1007/978-1-4939-3356-3_20

[16] Denyer, T., Ma, X., Klesen, S., Scacchi, E., Nieselt, K., & Timmermans, M. C. P. (2019). Spatiotemporal Developmental Trajectories in the Arabidopsis Root Revealed Using High-Throughput Single-Cell RNA Sequencing. *Developmental Cell*, *48*(6), 840-852.e5. https.//doi.org/10.1016/j.devcel.2019.02.022

[17] Doğa Selin Kayıhan, Ceyhun Kayıhan, & Yelda Özden Çiftçi. (2016). Excess boron responsive regulations of antioxidative mechanism at physio-biochemical and molecular levels in *Arabidopsis thaliana*. *Plant Physiology and Biochemistry*, *109*, 337–345. https.//doi.org/10.1016/j.plaphy.2016.10.016

[18] Dordas, C., & Brown, P. H. (2005). Boron deficiency affects cell viability, phenolic leakage and oxidative burst in rose cell cultures. *Plant and Soil*, *268*(1), 293–301. https.//doi.org/10.1007/s11104-004-0309-1

[19] Duchefa Biochemie. (2025). *Cellulase R-10 | Duchefa Biochemie*. Duchefa-Biochemie.com. https.//www.duchefa-biochemie.com/product/details/number/c8001

[20] Froelich, D. R., Mullendore, D. L., Jensen, K. H., Ross-Elliott, T. J., Anstead, J. A., Thompson, G. A., Pélissier, H. C., & Knoblauch, M. (2011). Phloem Ultrastructure and Pressure Flow. Sieve-Element-Occlusion-Related Agglomerations Do Not Affect Translocation. *The Plant Cell*, *23*(12), 4428–4445. https.//doi.org/10.1105/tpc.111.093179

[21] Funakawa, H., & Miwa, K. (2015). Synthesis of borate cross-linked rhamnogalacturonan II. *Frontiers in Plant Science*, *6*. https.//doi.org/10.3389/fpls.2015.00223

[22] Gene Ontology Consortium. (2021). The Gene Ontology resource. enriching a GOld mine. *Nucleic Acids Research*, *49*(D1), D325–D334. https.//doi.org/10.1093/nar/gkaa1113

[23] González-Fontes, A., Herrera-Rodríguez, M. B., Martín-Rejano, E. M., Navarro-Gochicoa, M. T., Rexach, J., & Camacho-Cristóbal, J. J. (2016). Root Responses to Boron Deficiency Mediated by Ethylene. *Frontiers in Plant Science*, *6*. https.//doi.org/10.3389/fpls.2015.01103

[24] Guo, P., Qi, Y., Yang, L.-T., Ye, X., Jiang, H.-X., Huang, J.-H., & Chen, L. (2014). *cDNA-AFLP analysis reveals the adaptive responses of citrus to long-term boron-toxicity*. *14*(1). https.//doi.org/10.1186/s12870-014-0284-5

[25] Hao, Y., Hao, S., Andersen-Nissen, E., Mauck, W. M., Zheng, S., Butler, A., Lee, M. J., Wilk, A. J., Darby, C., Zager, M., Hoffman, P., Stoeckius, M., Papalexi, E., Mimitou, E. P., Jain, J., Srivastava, A., Stuart, T., Fleming, L. M., Yeung, B., & Rogers, A. J. (2021a). Integrated analysis of multimodal single-cell data. *Cell*, *184*(13). https.//doi.org/10.1016/j.cell.2021.04.048

[26] Hao, Y., Hao, S., Andersen-Nissen, E., Mauck, W. M., Zheng, S., Butler, A., Lee, M. J., Wilk, A. J., Darby, C., Zager, M., Hoffman, P., Stoeckius, M., Papalexi, E., Mimitou, E. P., Jain, J., Srivastava, A., Stuart, T., Fleming, L. M., Yeung, B., & Rogers, A. J. (2021b). Integrated analysis of multimodal single-cell data. *Cell*, *184*(13). https.//doi.org/10.1016/j.cell.2021.04.048

[27] Heumos, L., Schaar, A. C., Lance, C., Litinetskaya, A., Drost, F., Zappia, L., Lücken, M. D., Strobl, D. C., Henao, J., Curion, F., Schiller, H. B., & Theis, F. J. (2023). Best practices for single-cell analysis across modalities. *Nature Reviews Genetics*, 1–23. https.//doi.org/10.1038/s41576-023-00586-w

[28] Jiao, Y., Ran, M., Wu, J., & Li, J. (2025). Boron contributes to enhance antimony tolerance in rice (Oryza sativa L.) by activating antioxidant system, modifying the cell wall component and promoting cell wall deposition of Sb. *Journal of Environmental Management*, *374*, 124100. https.//doi.org/10.1016/j.jenvman.2025.124100

[29] José, L., Minguet, E. G., Sunil Kumar Singh, Edouard Pesquet, Vera-Sirera, F., Moreau-Courtois, C. L., Carbonell, J., Chory, J., & Tuominen, H. (2008). ACAULIS5 controls *Arabidopsis* xylem specification through the prevention of premature cell death. *Development*, *135*(15), 2573–2582. https.//doi.org/10.1242/dev.019349

[30] Kanehisa, M., Furumichi, M., Tanabe, M., Sato, Y., & Morishima, K. (2017). KEGG. new perspectives on genomes, pathways, diseases and drugs. *Nucleic Acids Research*, *45*(D1), D353–D361. https.//doi.org/10.1093/nar/gkw1092

[31] Karabal, E., Yücel, M., & Öktem, H. A. (2003). Antioxidant responses of tolerant and sensitive barley cultivars to boron toxicity. *Plant Science*, *164*(6), 925–933. https.//doi.org/10.1016/s0168-9452(03)00067-0

[32] KAYIHAN, C., AKSOY, E., & MUTLU, S. N. (2023). Boron toxicity induces sulfate transporters at transcriptional level in *Arabidopsis thaliana*. *Turkish Journal of Botany*, *47*(1), 1–22. https.//doi.org/10.55730/1300-008x.2740

[33] KAYIHAN, D. S., KAYIHAN, C., & ÇİFTÇİ, Y. Ö. (2019). Regulation of boron toxicity responses via glutathione-dependent detoxification pathways at biochemical and molecular levels in Arabidopsisthaliana. *TURKISH JOURNAL of BOTANY*, *43*(6), 749–757. https.//doi.org/10.3906/bot-1905-7

[34] KAYIHAN, D. S., KAYIHAN, C., & ÖZDEN ÇİFTÇİ, Y. (2019). Moderate level of toxic boron causes differential regulation of microRNAs related to jasmonate and ethylene metabolisms in *Arabidopsis thaliana*. *TURKISH JOURNAL of BOTANY*, *43*(2), 167–172. https.//doi.org/10.3906/bot-1810-10

[35] Ke, Y., Minne, M., Eekhout, T., & De Rybel, B. (2023). Single Cell RNA-Sequencing in Arabidopsis Root Tissues. *Methods in Molecular Biology (Clifton, N.J.)*, *2698*, 41–56. https.//doi.org/10.1007/978-1-0716-3354-0_4

[36] Khan, M. K., Pandey, A., Mehmet Hamurcu, Rajpal, V. R., Vyhnanek, T., Topal, A., Raina, S. N., & Sait Gezgin. (2023). Insight into the Boron Toxicity Stress-Responsive Genes in Boron-Tolerant Triticum dicoccum Shoots Using RNA Sequencing. *Agronomy*, *13*(3), 631–631. https.//doi.org/10.3390/agronomy13030631

[37] Kobayashi, M., Matoh, T., & Azuma, Ji. (1996). Two Chains of Rhamnogalacturonan II Are Cross-Linked by Borate-Diol Ester Bonds in Higher Plant Cell Walls. *Plant Physiology*, *110*(3), 1017–1020. https.//doi.org/10.1104/pp.110.3.1017

[38] Koornneef, M., & Meinke, D. (2010). The development of Arabidopsis as a model plant. *The Plant Journal*, *61*(6), 909–921. https.//doi.org/10.1111/j.1365-313x.2009.04086.x

[39] Krämer, U. (2015). Planting molecular functions in an ecological context with *Arabidopsis thaliana*. *ELife*, *4*(1), e06100. https.//doi.org/10.7554/eLife.06100

[40] Lee, M. M., & Schiefelbein, J. (2002). Cell Pattern in the Arabidopsis Root Epidermis Determined by Lateral Inhibition with Feedback. *The Plant Cell*, *14*(3), 611–618. https.//doi.org/10.1105/tpc.010434

[41] Liu, J., Yang, L., Luan, M., Wang, Y., Zhang, C., Zhang, B., Shi, J., Zhao, F.-G., Lan, W., & Luan, S. (2015). A vacuolar phosphate transporter essential for phosphate homeostasis in *Arabidopsis*. *Proceedings of the National Academy of Sciences*, *112*(47). https.//doi.org/10.1073/pnas.1514598112

[42] Loomis, W. D., & Durst, R. W. (1992). Chemistry and biology of boron. *BioFactors (Oxford, England)*, *3*(4), 229–239. https.//pubmed.ncbi.nlm.nih.gov/1605832/

[43] Martínez-Cuenca, M.-R., Martínez-Alcántara, B., Quiñones, A., Ruiz, M., Iglesias, D. J., Primo-Millo, E., & Forner-Giner, M. Á. (2015). Physiological and Molecular Responses to Excess Boron in Citrus macrophylla W. *PLOS ONE*, *10*(7), e0134372. https.//doi.org/10.1371/journal.pone.0134372

[44] Masucci, J. D., Rerie, W. G., Foreman, D. R., Zhang, M., Galway, M. E., Marks, M. D., & Schiefelbein, J. W. (1996). The homeobox gene GLABRA2 is required for position-dependent cell differentiation in the root epidermis of *Arabidopsis thaliana*. *Development*, *122*(4), 1253–1260. https.//doi.org/10.1242/dev.122.4.1253

[45] Miwa, K., Takano, J., Omori, H., Seki, M., & Fujiwara, T. (2007). Plants Tolerant of High Boron Levels. *Science*, *318*(5855), 1417. https.//doi.org/10.1126/science.1146634

[46] Murashige, T., & Skoog, F. (1962). A Revised Medium for Rapid Growth and Bio Assays with Tobacco

Tissue Cultures. *Physiologia Plantarum*, *15*(3), 473–497. https.//doi.org/10.1111/j.1399-3054.1962.tb08052.x

[47] Nielsen, F. H., & Eckhert, Curtiss D. (2020). Boron. *Advances in Nutrition*, *11*(2), 461–462. https.//doi.org/10.1093/advances/nmz110

[48] Nielsen, F., & Eckhert, C. (2019). Boron. *Advances in Nutrition (Bethesda, Md.)*, *11*. https.//doi.org/10.1093/advances/nmz110

[49] O'Neill, M. A. (2001). Requirement of Borate Cross-Linking of Cell Wall Rhamnogalacturonan II for Arabidopsis Growth. *Science*, *294*(5543), 846–849. https.//doi.org/10.1126/science.1062319

[50] Pang, P. P., & Meyerowitz, E. M. (1987). *Arabidopsis Thaliana*. A Model System for Plant Molecular Biology. *Nature Biotechnology*, *5*(11), 1177–1181. https.//doi.org/10.1038/nbt1187-1177

[51] Provart, N. J., Alonso, J., Assmann, S. M., Bergmann, D., Brady, S. M., Brkljacic, J., Browse, J., Chapple, C., Colot, V., Cutler, S., Dangl, J., Ehrhardt, D., Friesner, J. D., Frommer, W. B., Grotewold, E., Meyerowitz, E., Nemhauser, J., Nordborg, M., Pikaard, C., & Shanklin, J. (2015). 50 years of Arabidopsis research. highlights and future directions. *New Phytologist*, *209*(3), 921–944. https.//doi.org/10.1111/nph.13687

[52] Ralston, N. V. C., & Hunt, C. D. (2001). Diadenosine phosphates and S-adenosylmethionine. novel boron binding biomolecules detected by capillary electrophoresis. *Biochimica et Biophysica Acta (BBA) - General Subjects*, *1527*(1-2), 20–30. https.//doi.org/10.1016/s0304-4165(01)00130-1

[53] REID, R. J., HAYES, J. E., POST, A., STANGOULIS, J. C. R., & GRAHAM, R. D. (2004). A critical analysis of the causes of boron toxicity in plants. *Plant, Cell & Environment*, *27*(11), 1405–1414. https.//doi.org/10.1111/j.1365-3040.2004.01243.x

[54] Roppolo, D., De Rybel, B., Tendon, V. D., Pfister, A., Alassimone, J., Vermeer, J. E. M., Yamazaki, M., Stierhof, Y.-D., Beeckman, T., & Geldner, N. (2011). A novel protein family mediates Casparian strip formation in the endodermis. *Nature*, *473*(7347), 380–383. https.//doi.org/10.1038/nature10070

[55] Ryu, K. H., Huang, L., Kang, H. M., & Schiefelbein, J. (2019). Single-Cell RNA Sequencing Resolves Molecular Relationships Among Individual Plant Cells. *Plant Physiology*, *179*(4), 1444–1456. https.//doi.org/10.1104/pp.18.01482

[56] Salvi, E., Di Mambro, R., & Sabatini, S. (2020). Dissecting mechanisms in root growth from the transition zone perspective. *Journal of Experimental Botany*, *71*(8), 2390–2396. https.//doi.org/10.1093/jxb/eraa079

[57] Satija, R., Farrell, J. A., Gennert, D., Schier, A. F., & Regev, A. (2015). Spatial reconstruction of single-cell gene expression data. *Nature Biotechnology*, *33*(5), 495–502. https.//doi.org/10.1038/nbt.3192

[58] Shahan, R., Hsu, C.-W., Nolan, T. M., Cole, B. J., Taylor, I. W., Greenstreet, L., Zhang, S., Afanassiev, A., Vlot, A. H. C., Schiebinger, G., Benfey, P. N., & Ohler, U. (2022). A single-cell Arabidopsis root atlas

reveals developmental trajectories in wild-type and cell identity mutants. *Developmental Cell*, *57*(4), 543-560.e9. https.//doi.org/10.1016/j.devcel.2022.01.008

[59] Sigma Aldrich. (2025). NMR Chemical Shifts of Impurities. *Merck*, *1*(1). https.//www.sigmaaldrich.com/MX/en/technical-documents/technical-article/genomics/cloning-and-expression/blue-white-screening

[60] Stuart, T., Butler, A., Hoffman, P., Hafemeister, C., Papalexi, E., Mauck, W. M., Hao, Y., Stoeckius, M., Smibert, P., & Satija, R. (2019). Comprehensive Integration of Single-Cell Data. *Cell*, *177*(7), 1888-1902.e21. https.//doi.org/10.1016/j.cell.2019.05.031

[61] Subramanian, A., Tamayo, P., Mootha, V. K., Mukherjee, S., Ebert, B. L., Gillette, M. A., Paulovich, A., Pomeroy, S. L., Golub, T. R., Lander, E. S., & Mesirov, J. P. (2005). Gene Set Enrichment analysis. a knowledge-based Approach for Interpreting genome-wide Expression Profiles. *Proceedings of the National Academy of Sciences*, *102*(43), 15545–15550. https.//doi.org/10.1073/pnas.0506580102

[62] Takano, J., Wada, M., Ludewig, U., Schaaf, G., von Wirén, N., & Fujiwara, T. (2006). The Arabidopsis Major Intrinsic Protein NIP5;1 Is Essential for Efficient Boron Uptake and Plant Development under Boron Limitation. *The Plant Cell*, *18*(6), 1498–1509. https.//doi.org/10.1105/tpc.106.041640

[63] Taylor, N. G., Laurie, S., & Turner, S. R. (2000). Multiple Cellulose Synthase Catalytic Subunits Are Required for Cellulose Synthesis in Arabidopsis. *The Plant Cell*, *12*(12), 2529–2539. https.//doi.org/10.1105/tpc.12.12.2529

[64] The Arabidopsis Genome Initiative. (2000). Analysis of the Genome Sequence of the Flowering Plant *Arabidopsis Thaliana*. *Nature*, *408*(6814), 796–815. https.//doi.org/10.1038/35048692

[65] The Editors of Encyclopedia Britannica. (2017). boron | Properties, Uses, & Facts. In *Encyclopædia Britannica*. https.//www.britannica.com/science/boron-chemical-element

[66] Voxeur, A., & Fry, S. C. (2014). Glycosylinositol phosphorylceramides from Rosa cell cultures are boron-bridged in the plasma membrane and form complexes with rhamnogalacturonan II. *The Plant Journal*, *79*(1), 139–149. https.//doi.org/10.1111/tpj.12547

[67] Wang, G., Sandra Feuer DiTusa, Dong Ha Oh, Herrmann, A. D., Mendoza-Cózatl, D. G., O'Neill, M. A., Smith, A. P., & Maheshi Dassanayake. (2021). Cross species multi-omics reveals cell wall sequestration and elevated global transcript abundance as mechanisms of boron tolerance in plants. *New Phytologist*, *230*(5), 1985–2000. https.//doi.org/10.1111/nph.17295

[68] Wu, F.-H., Shen, S.-C., Lee, L.-Y., Lee, S.-H., Chan, M.-T., & Lin, C.-S. (2009). Tape-Arabidopsis Sandwich - a simpler Arabidopsis protoplast isolation method. *Plant Methods*, *5*(1). https.//doi.org/10.1186/1746-4811-5-16

[69] Yau, S. K., Nachit, M. M., Ryan, J., & Hamblin, J. (1995). Phenotypic variation in boron-toxicity tolerance at seedling stage in durum wheat (Triticum durum). *Euphytica*, *83*(3), 185–191.

https.//doi.org/10.1007/bf01678128

[70] Yılmaz, H., Kayıhan, C., Ünal, Halis Batuhan, Yaprak, O., & Aksoy, E. (2023). Singlecell transcriptional profiling in Arabidopsis root exposed to B toxicity at seedling stages. *BioRxiv*, 2023.03.09.531923. https.//doi.org/10.1101/2023.03.09.531923

[71] Yu, G., Wang, L.-G., Han, Y., & He, Q.-Y. (2012). clusterProfiler. an R Package for Comparing Biological Themes Among Gene Clusters. *OMICS. A Journal of Integrative Biology*, *16*(5), 284–287. https.//doi.org/10.1089/omi.2011.0118

[72] Zhang, T.-Q., Xu, Z.-G., Shang, G.-D., & Wang, J.-W. (2019). A Single-Cell RNA Sequencing Profiles the Developmental Landscape of Arabidopsis Root. *Molecular Plant*, *12*(5), 648–660. https.//doi.org/10.1016/j.molp.2019.04.004

[73] Zheng, G. X. Y., Terry, J. M., Belgrader, P., Ryvkin, P., Bent, Z. W., Wilson, R., Ziraldo, S. B., Wheeler, T. D., McDermott, G. P., Zhu, J., Gregory, M. T., Shuga, J., Montesclaros, L., Underwood, J. G., Masquelier, D. A., Nishimura, S. Y., Schnall-Levin, M., Wyatt, P. W., Hindson, C. M., & Bharadwaj, R. (2017). Massively parallel digital transcriptional profiling of single cells. *Nature Communications*, *8*(1). https.//doi.org/10.1038/ncomms14049

[74] Zhong, R., & Ye, Z.-H. (2014). Secondary Cell Walls. Biosynthesis, Patterned Deposition and Transcriptional Regulation. *Plant and Cell Physiology*, *56*(2), 195–214. https.//doi.org/10.1093/pcp/pcu140

[75] Zhu, Y., Cai, J., Hosmane, N. S., & Zhang, Y. (2022). Introduction. basic concept of boron and its physical and chemical properties. *Fundamentals and Applications of Boron Chemistry*, 1–57. https.//doi.org/10.1016/b978-0-12-822127-3.00003-x

[76] Muro, K., Kamiyo, J., Wang, S., Geldner, N., & Takano, J. (2023). Casparian strips prevent apoplastic diffusion of boric acid into root steles for excess B tolerance. Frontiers in Plant Science, 14. https.//doi.org/10.3389/fpls.2023.988419

[77] Miwa, K., & Fujiwara, T. (2010). Boron transport in plants. co-ordinated regulation of transporters. Annals of Botany, 105(7), 1103–1108. https.//doi.org/10.1093/aob/mcq044

[78] Yoshinari, A., & Takano, J. (2017). Insights into the Mechanisms Underlying Boron Homeostasis in Plants. Frontiers in Plant Science, 8. https.//doi.org/10.3389/fpls.2017.01951

[79] Jethva, J., Lichtenauer, S., Schmidt-Schippers, R., Steffen-Heins, A., Poschet, G., Wirtz, M., van Dongen, J. T., Eirich, J., Finkemeier, I., Bilger, W., Schwarzländer, M., & Sauter, M. (2023). Mitochondrial alternative NADH dehydrogenases NDA1 and NDA2 promote survival of reoxygenation stress in Arabidopsis by safeguarding photosynthesis and limiting ROS generation. The New Phytologist, 238(1), 96–112. https.//doi.org/10.1111/nph.18657

APPENDICES

APPENDIX 1: Gene Markers for Identification of Root Cells

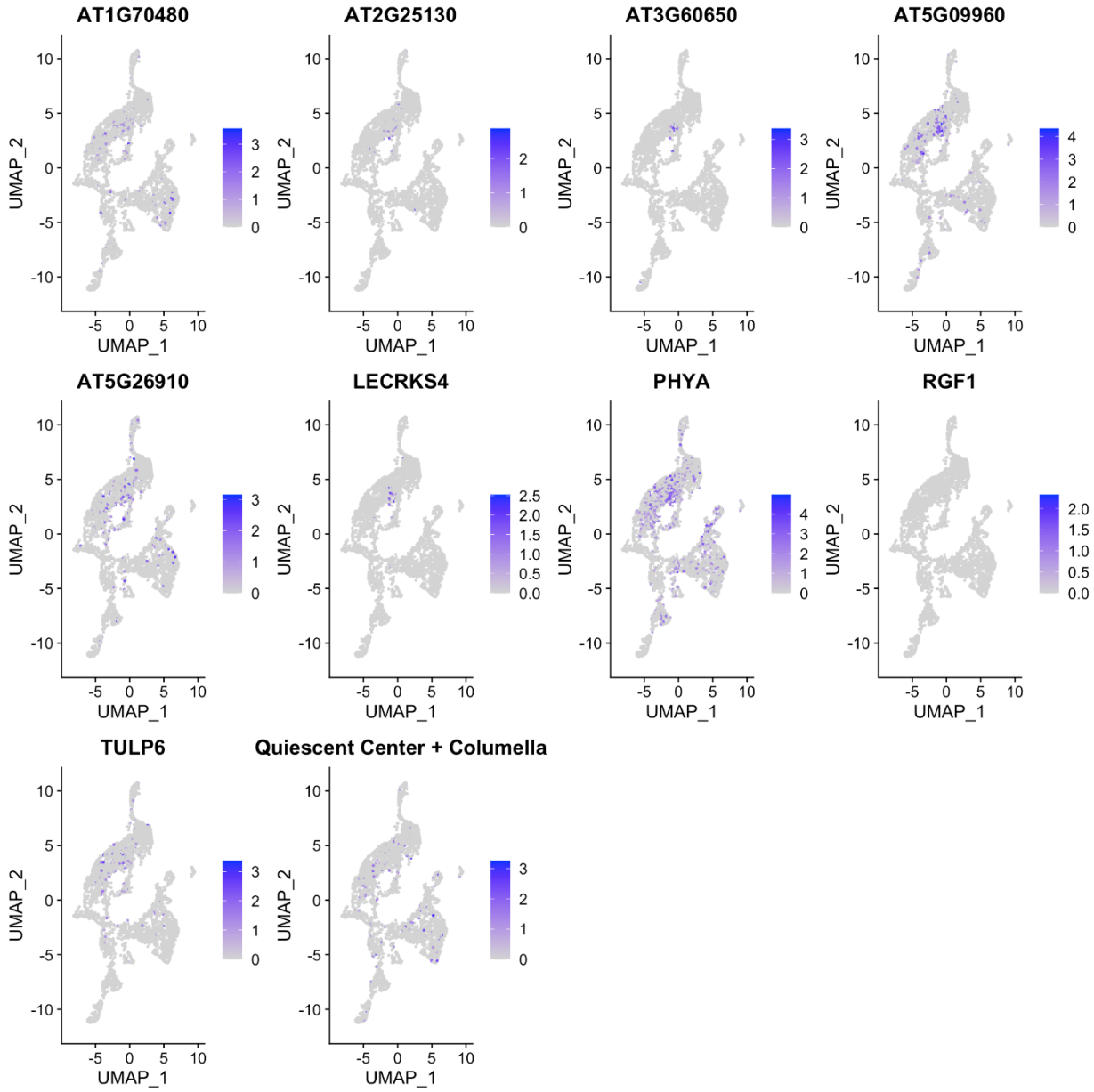

Appendix Figure 1.1. Part A. Quiscent Center + Columella Markers

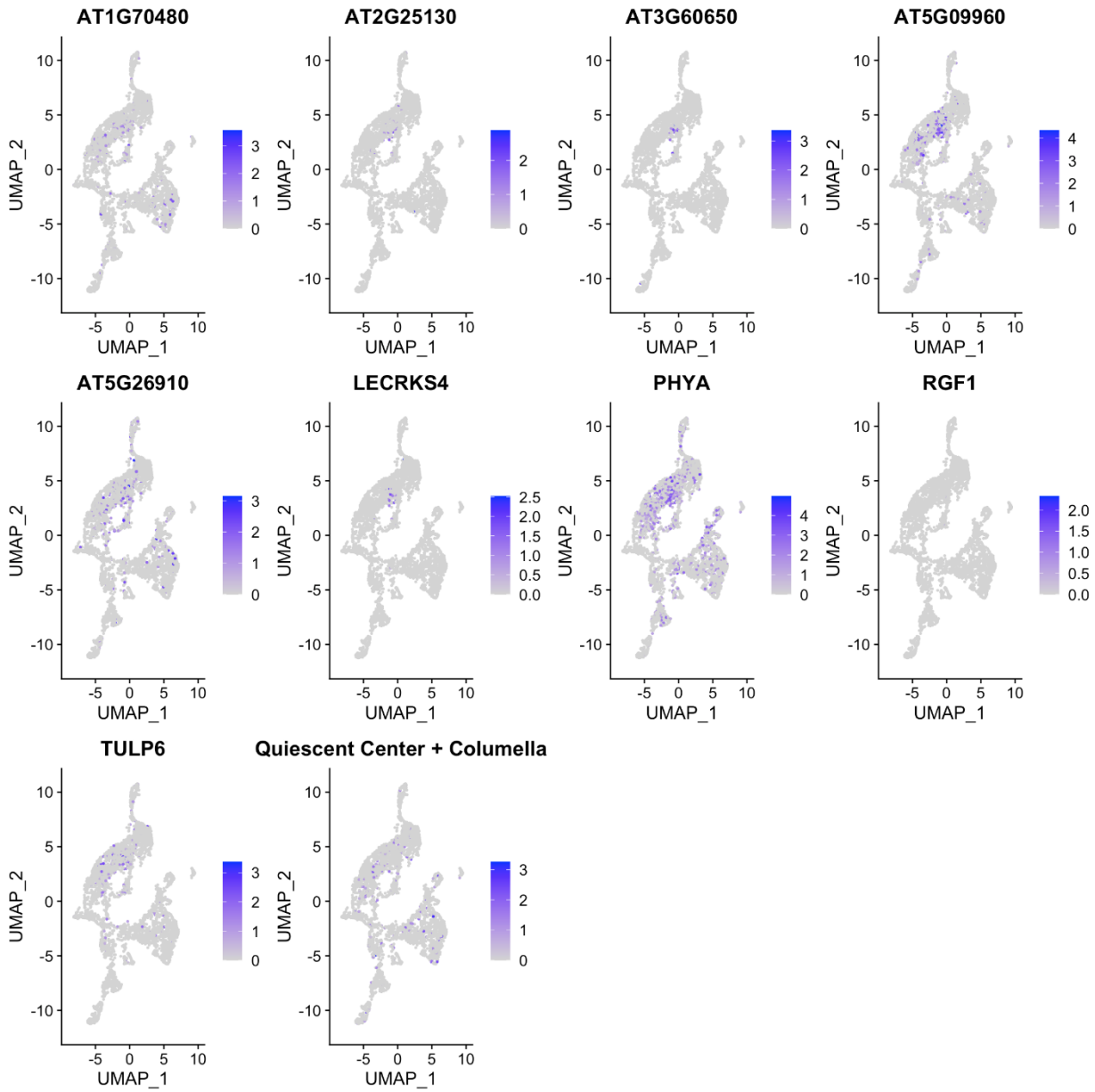

Appendix Figure 1.2. Part B. Atrichoblast Markers

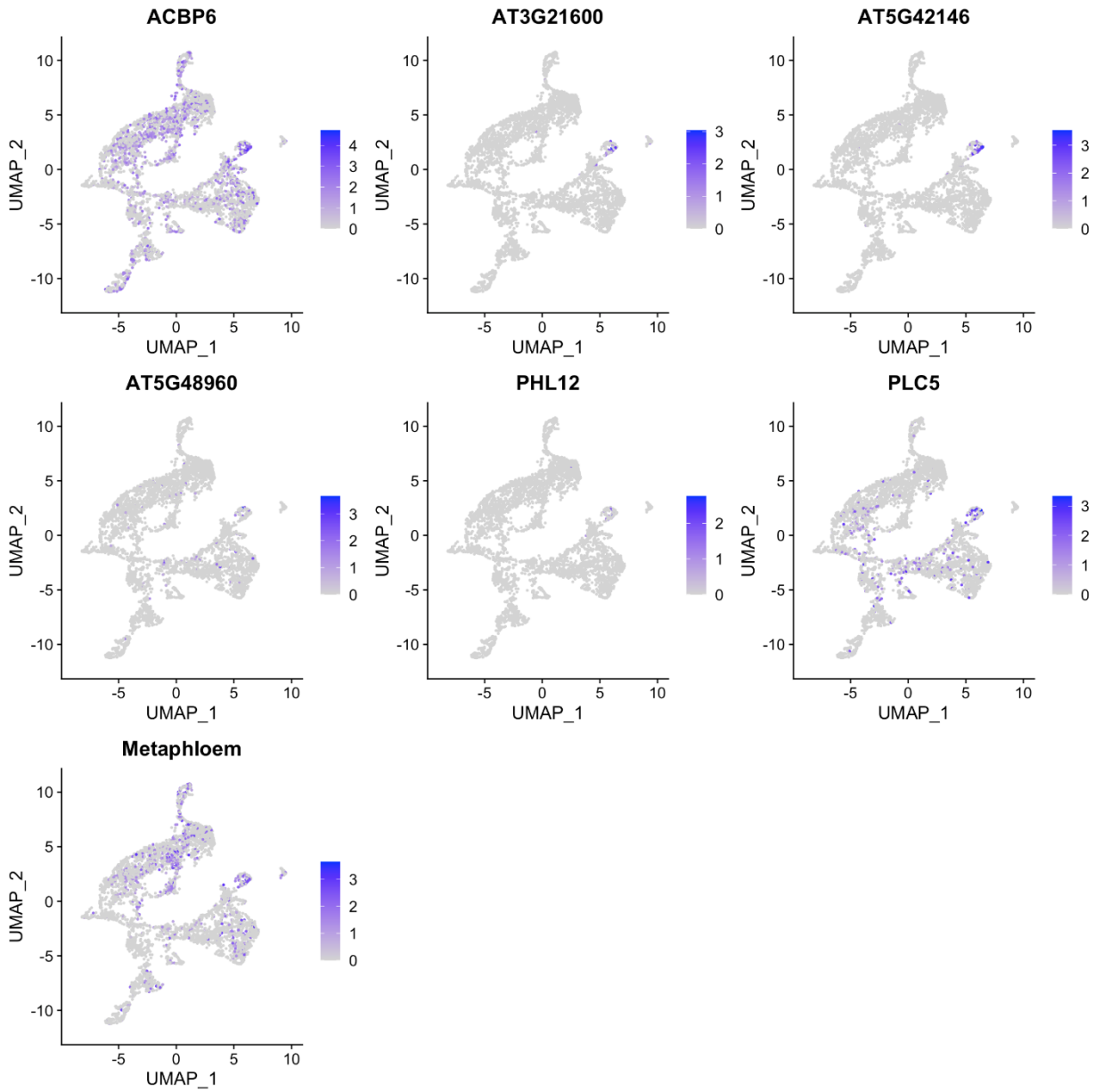

Appendix Figure 1.3. Part C. Metaphloem Markers

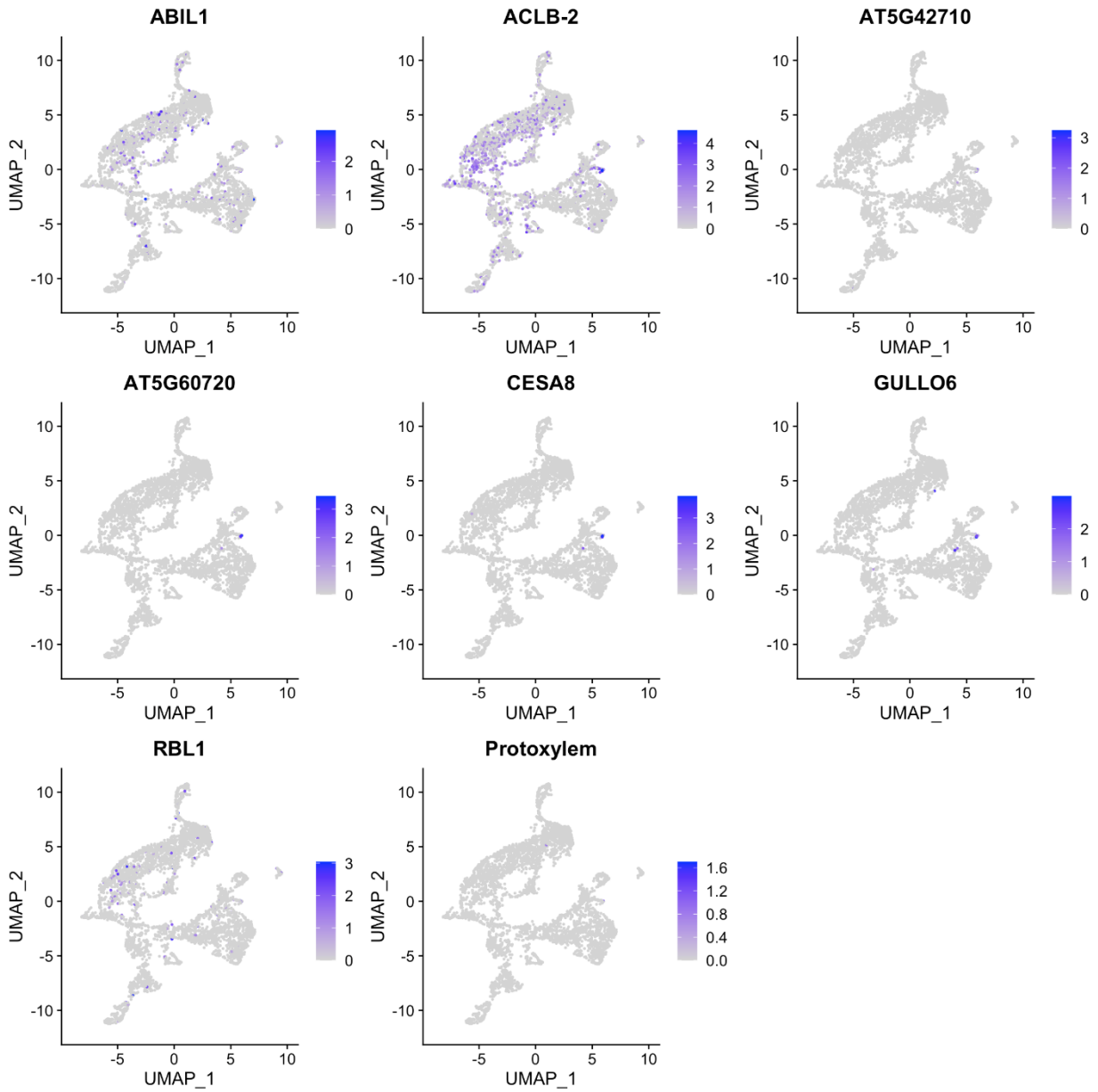

Appendix Figure 1.4. Part D. Protoxylem Markers

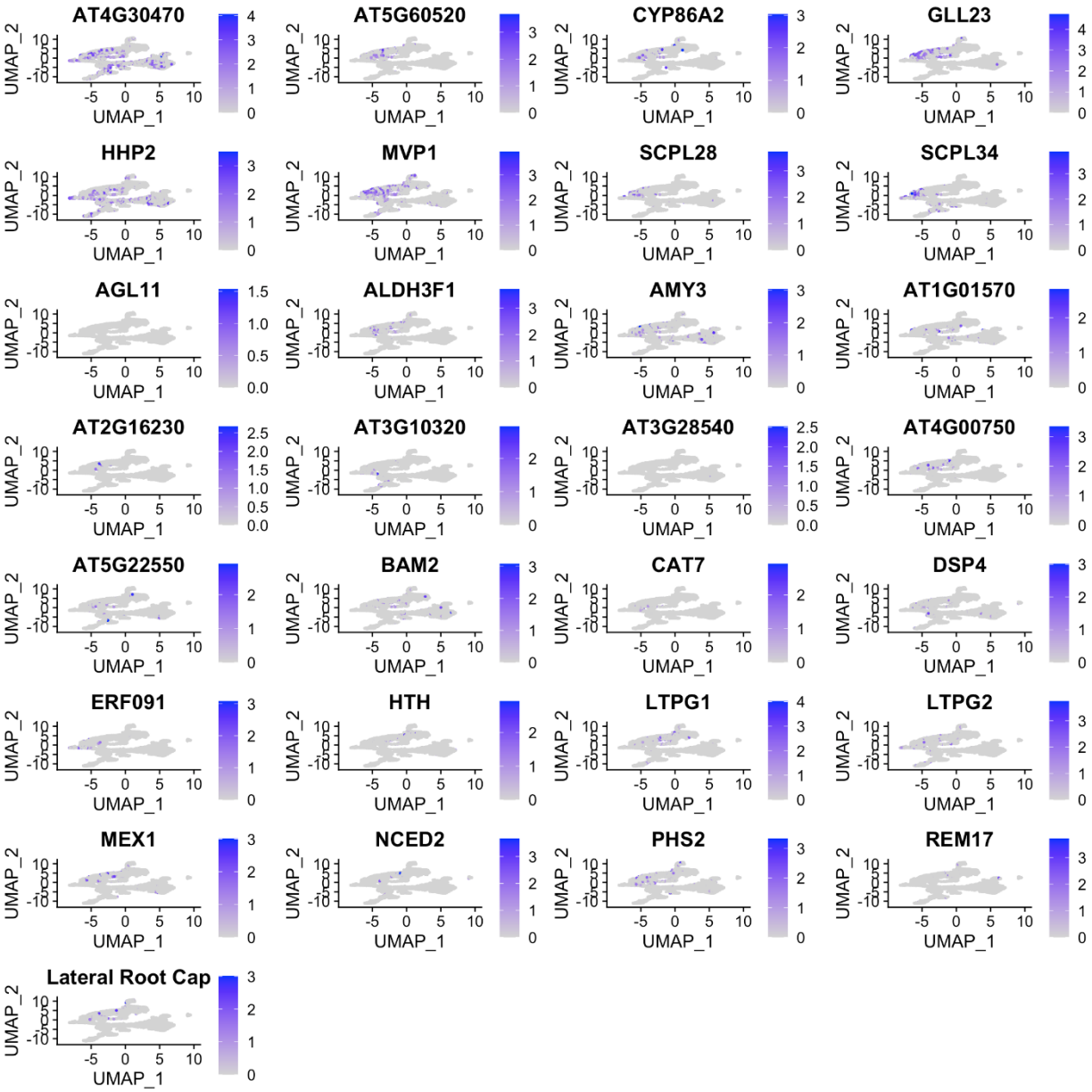

Appendix Figure 1.5. Part E. Lateral Root Cap Markers

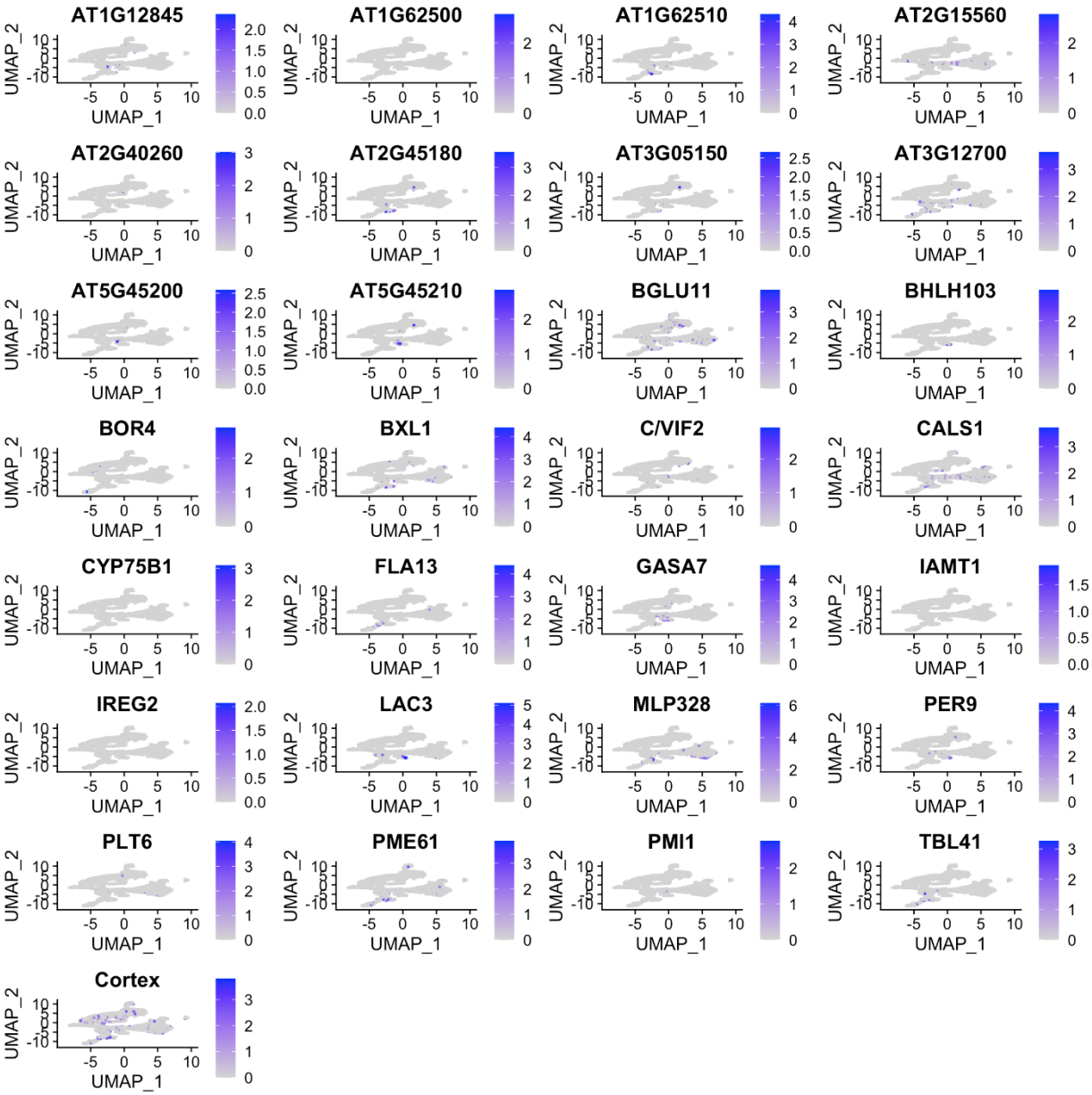

Appendix Figure 1.6. Part F. Cortex Markers

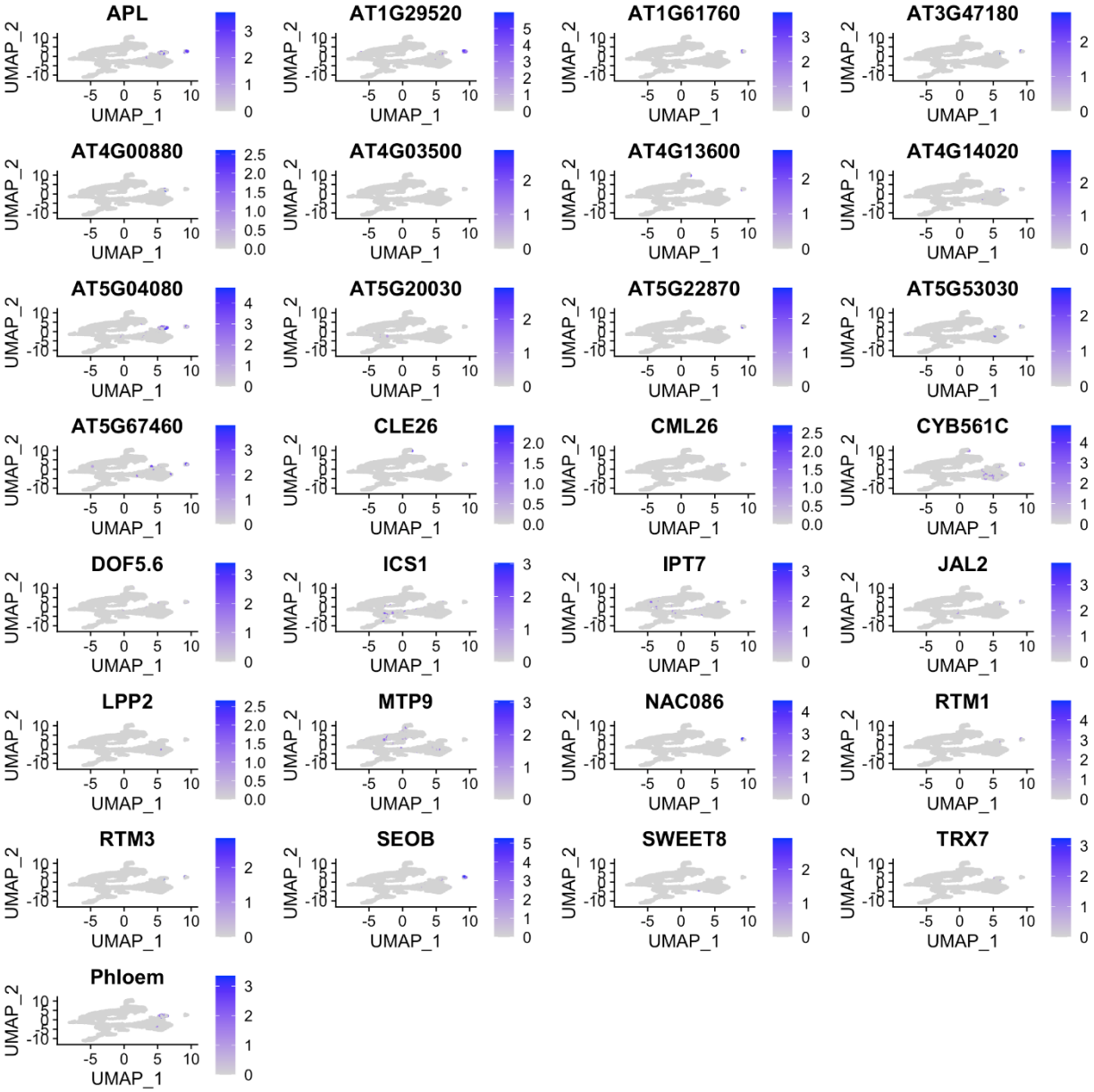

Appendix Figure 1.7. Part G. Phloem Markers

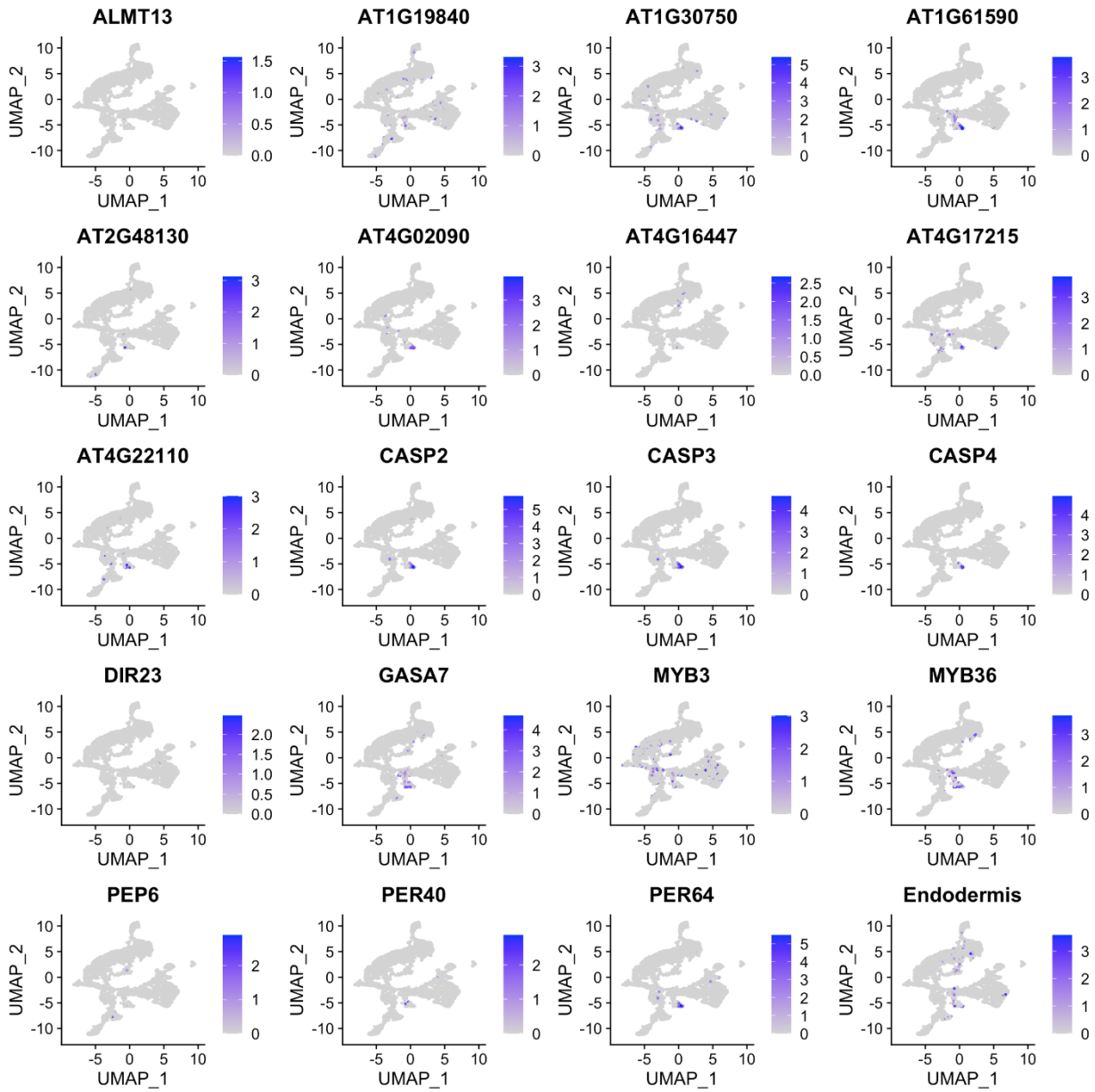

Appendix Figure 1.8. Part H. Endodermis Markers

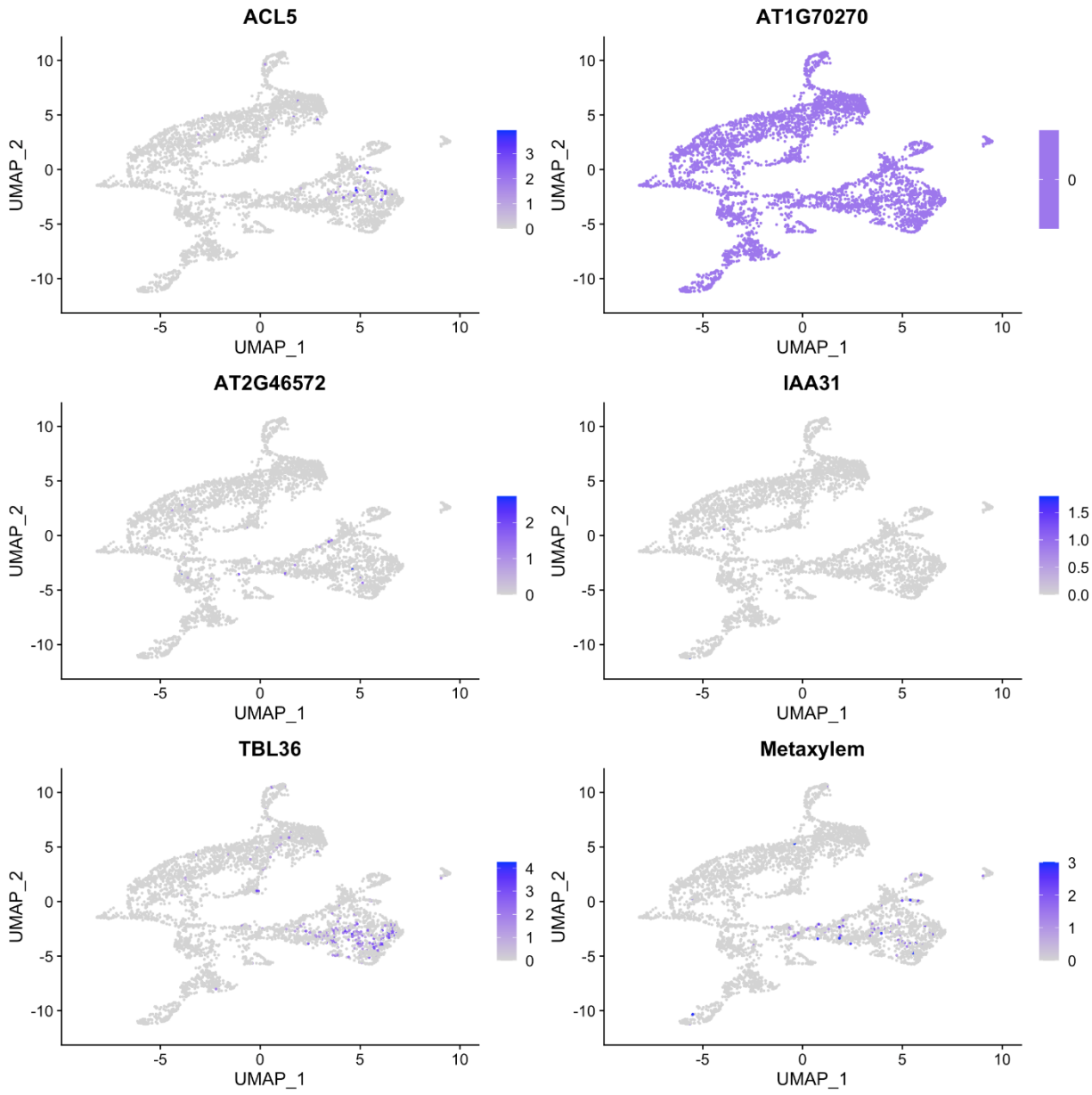

Appendix Figure 1.9. Part I. Metaxylem Markers

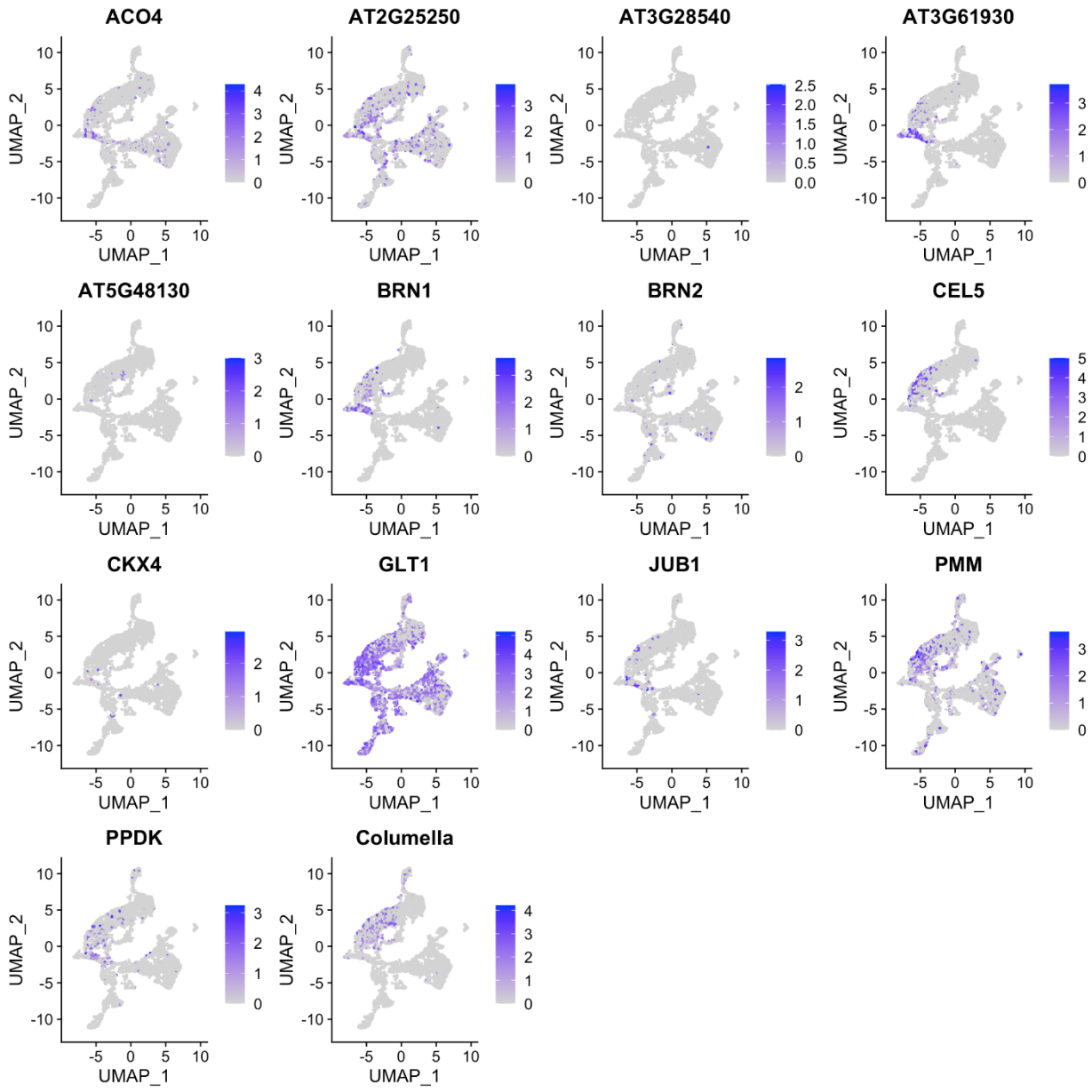

Appendix Figure 1.10. Part J. Columella Markers

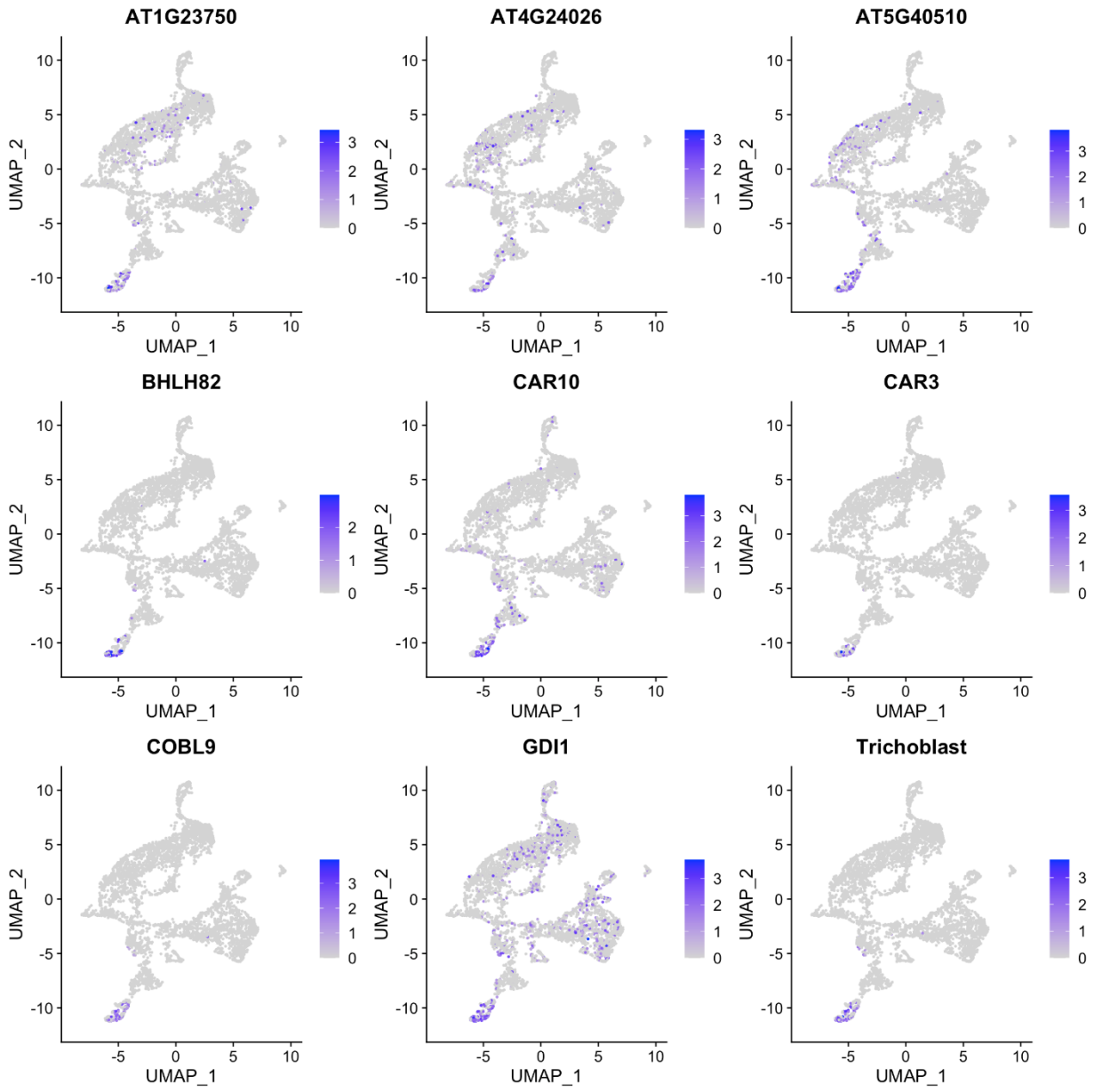

Appendix Figure 1.11. Part K. Trichoblast Markers

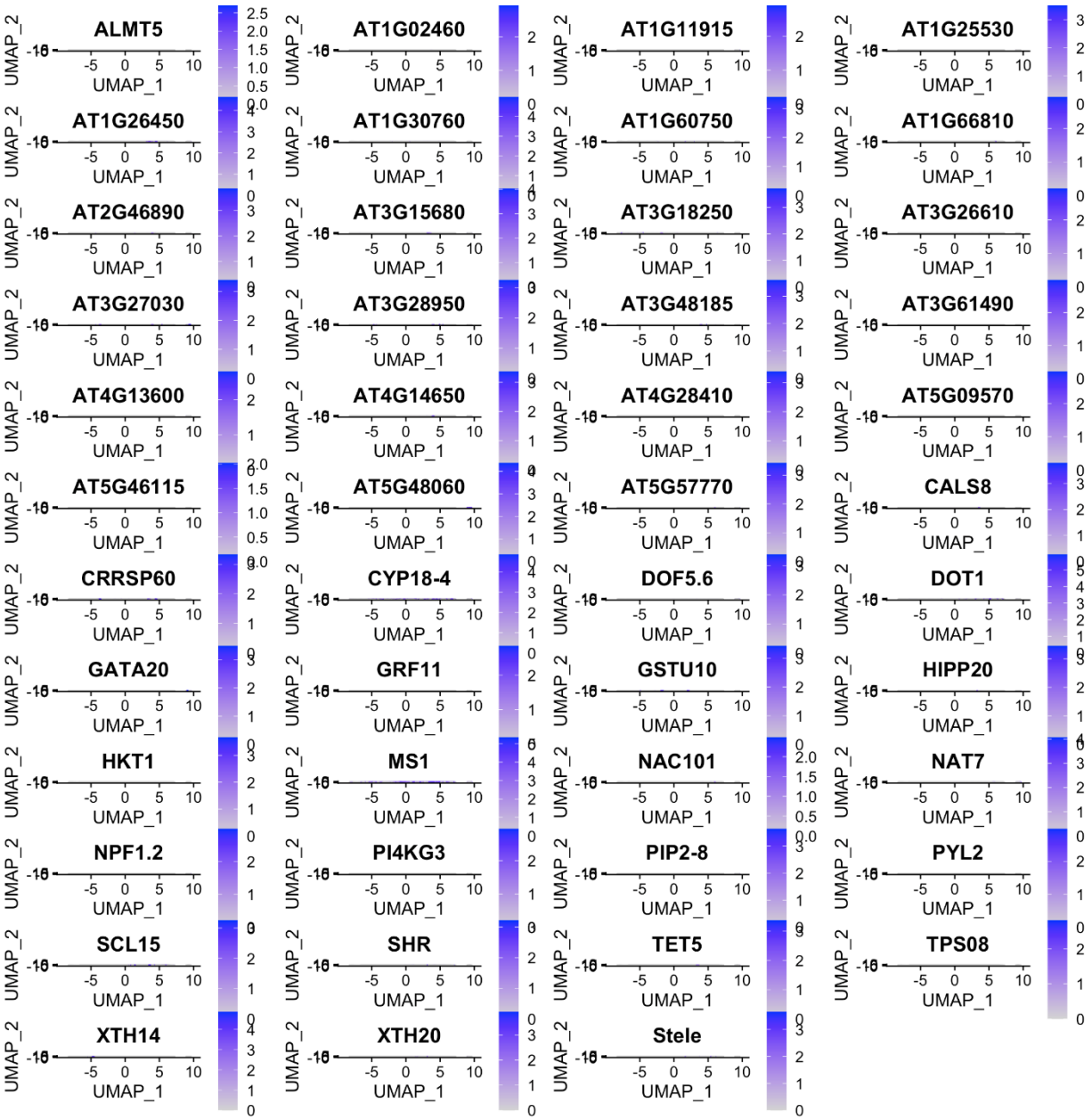

Appendix Figure 1.12. Part L. Stele Markers

APPENDIX 2: Marker Gene List and Respective Root Cell Region

Gene_Name	Preferential Expression in Root
GL2	Atrichoblast
AIR1B	Atrichoblast
ANL2	Atrichoblast
AT1G06120	Atrichoblast
AT1G10990	Atrichoblast
AT1G13730	Atrichoblast
AT1G19900	Atrichoblast
AT1G65481	Atrichoblast
AT3G08030	Atrichoblast
AT4G37160.1	Atrichoblast
AT5G66800	Atrichoblast
AT1G65310.2	Atrichoblast
FAR3	Atrichoblast
GPAT8	Atrichoblast
KAN1	Atrichoblast
KCS5	Atrichoblast
LTPG1	Atrichoblast
TPS22	Atrichoblast
WRKY44	Atrichoblast
XYL1	Atrichoblast
ACO4	Columella
AT2G25250	Columella
AT3G28540	Columella
AT3G61930	Columella
AT5G48130	Columella
BRN1	Columella
BRN2	Columella
CEL5	Columella
CKX4	Columella
AT1G17400.1	Columella
GLT1	Columella
JUB1	Columella
PMM	Columella
PPDK	Columella
SMB	Columella
AT1G12845	Cortex
AT1G62500	Cortex
AT1G62510	Cortex
AT2G15560	Cortex
AT2G40260	Cortex
AT2G45180	Cortex
AT3G05150	Cortex
AT3G12700	Cortex
AT5G45200	Cortex

AT5G45210	Cortex
BGLU11	Cortex
BHLH103	Cortex
BOR4	Cortex
BXL1	Cortex
C/VIF2	Cortex
CALS1	Cortex
CO2	Cortex
CYP75B1	Cortex
FLA13	Cortex
GASA7	Cortex
IAMT1	Cortex
IREG2	Cortex
LAC3	Cortex
MLP328	Cortex
PER9	Cortex
PLT6	Cortex
PME61	Cortex
PMI1	Cortex
TBL41	Cortex
XTH4	Cortex
AT3G56220	Cortex + Endodermis
TRI	Cortex + Endodermis
ALMT13	Endodermis
AT1G16390.1	Endodermis
AT1G19840	Endodermis
AT1G30750	Endodermis
AT1G61590	Endodermis
AT2G48130	Endodermis
AT4G02090	Endodermis
AT4G16447	Endodermis
AT4G17215	Endodermis
AT4G22110	Endodermis
AT5G245210	Endodermis
AT5G65790.1	Endodermis
CASP2	Endodermis
CASP3	Endodermis
CASP4	Endodermis
DIR23	Endodermis
GASA7	Endodermis
MYB3	Endodermis
MYB36	Endodermis
PEP6	Endodermis
PER40	Endodermis
PER64	Endodermis
SCR	Endodermis

AT4G30470	LRC
AT5G44440.2	LRC
AT5G60520	LRC
CYP86A2	LRC
GLL23	LRC
HHP2	LRC
MVP1	LRC
SCPL28	LRC
SCPL34	LRC
AT4G37160.1	LRC
AGL11	LRC
ALDH3F1	LRC
AMY3	LRC
AT1G01570	LRC
AT2G16230	LRC
AT2G33230.1	LRC
AT3G10320	LRC
AT3G28540	LRC
AT3G50310.1	LRC
AT4G00750	LRC
AT5G22550	LRC
BAM2	LRC
CAT7	LRC
DSP4	LRC
ERF091	LRC
HTH	LRC
LTPG1	LRC
LTPG2	LRC
MEX1	LRC
NCED2	LRC
PHS2	LRC
REM17	LRC
WER	LRC
ACBP6	Metaphloem
AT2G08610.1	Metaphloem
AT3G21600	Metaphloem
AT5G42146	Metaphloem
AT5G48960	Metaphloem
AT4G37180.2	Metaphloem
PHL12	Metaphloem
PLC5	Metaphloem
SUMO1	Metaphloem
ACL5	Metaxylem
AT4G08685.1	Metaxylem
AT1G12663.1	Metaxylem
AT1G23350.1	Metaxylem

AT1G70270	Metaxylem
AT1G28450.1	Metaxylem
AT2G46572	Metaxylem
IAA31	Metaxylem
SAH7	Metaxylem
TBL36	Metaxylem
VQ33	Metaxylem
LBD14	Pericycle_Initials
APL	Phloem
AT1G11570.3	Phloem
AT1G29520	Phloem
AT1G61760	Phloem
AT3G19550.1	Phloem
AT3G47180	Phloem
AT4G00880	Phloem
AT4G03500	Phloem
AT4G13600	Phloem
AT4G14020	Phloem
AT4G15690.1	Phloem
AT5G01370.1	Phloem
AT5G04080	Phloem
AT5G20030	Phloem
AT5G22870	Phloem
AT5G53030	Phloem
AT5G56600.1	Phloem
AT5G57130.1	Phloem
AT5G67460	Phloem
CLE26	Phloem
CML26	Phloem
CYB561C	Phloem
DOF5.6	Phloem
ICS1	Phloem
IPT7	Phloem
JAL2	Phloem
LPP2	Phloem
MTP9	Phloem
NAC086	Phloem
RTM1	Phloem
RTM3	Phloem
SEOB	Phloem
SWEET8	Phloem
TRX7	Phloem
UBC17	Phloem
ABIL1	Protoxylem
ACLB-2	Protoxylem
AT5G42710	Protoxylem

AT5G60720	Protoxylem
CESA8	Protoxylem
GULLO6	Protoxylem
RBL1	Protoxylem
AT3G25710.1	Protoxylem
AT1G71930.1	Protoxylem
ZHD3	Protoxylem
AT3G57550.2	Quiescent Center + Columella
AT1G70480	Quiescent Center + Columella
AT2G25130	Quiescent Center + Columella
AT3G20880	Quiescent Center + Columella
AT3G60650	Quiescent Center + Columella
AT5G09960	Quiescent Center + Columella
AT5G26910	Quiescent Center + Columella
ATLP-1	Quiescent Center + Columella
LECRKS4	Quiescent Center + Columella
PHYA	Quiescent Center + Columella
RGF1	Quiescent Center + Columella
TEL1	Quiescent Center + Columella
TULP6	Quiescent Center + Columella
WIP2	Quiescent Center + Columella
ALMT5	Stele
AT1G54330.1	Stele
AT3G17730.1	Stele
AT1G02460	Stele
AT1G11915	Stele
AT1G25530	Stele
AT1G26420.1	Stele
AT1G26450	Stele
AT1G26790	Stele
AT1G30760	Stele
AT1G31670	Stele
AT1G51640.1	Stele
AT1G60750	Stele
AT1G63910.1	Stele
AT1G66810	Stele
AT1G68810.1	Stele
AT1G73410.1	Stele
AT2G40490	Stele
AT2G43580.1	Stele
AT2G46890	Stele
AT3G15680	Stele
AT3G18250	Stele
AT3G26610	Stele
AT3G27030	Stele
AT3G28950	Stele

AT3G48185	Stele
AT3G61490	Stele
AT4G13600	Stele
AT4G14650	Stele
AT4G28410	Stele
AT5G09480.1	Stele
AT5G09570	Stele
AT5G46115	Stele
AT5G47635.1	Stele
AT5G48060	Stele
AT5G50610	Stele
AT5G57770	Stele
bZIP6	Stele
CALS8	Stele
AT2G27030.3	Stele
CRRSP60	Stele
CYP18-4	Stele
DOF5.6	Stele
DOT1	Stele
EPS1	Stele
GATA20	Stele
GRF11	Stele
GSTU10	Stele
HIPP20	Stele
HIPP31	Stele
HKT1	Stele
MS1	Stele
NAC101	Stele
NAT7	Stele
NPF1.2	Stele
PEAR1/DOF2.4	Stele
PI4KG3	Stele
PIP2-8	Stele
PYL2	Stele
SCL15	Stele
SHR	Stele
SHY2	Stele
TET5	Stele
TPS08	Stele
XPP	Stele
XTH14	Stele
XTH20	Stele
XTH21	Stele
ARA	Trichoblast
AT1G23750	Trichoblast
AT4G24026	Trichoblast

AT5G40510	Trichoblast
BHLH82	Trichoblast
CAR10	Trichoblast
CAR3	Trichoblast
COBL9	Trichoblast
EXT12	Trichoblast
GDI1	Trichoblast
LRL3	Trichoblast
PERK13	Trichoblast
RHD6	Trichoblast
RSL1	Trichoblast

Appendix Table 2.1. Table of Marker Genes for Identification for Cell Types of Root Cells of Clusters Based on Expressions from scRNA Results